Katholieke Universiteit Leuven

Faculteit Bio-Ingenieurswetenschappen

Hydrological characterisation of a catchment towards evaluating its water harvesting potential Tigray, Ethiopia

—

Hydrologische karakterisering van een stroomgebied ter begroting van het wateropvang potentieel in Tigray, Ethiopië

Promotoren:
Prof. Dr. Ir. J.A. Deckers
Prof. Dr. B. van Wesemael
Departement Aard- en Omgevingswetenschappen
Afdeling Bodem- en Waterbeheer

Masterproef voorgedragen tot het behalen van het diploma van Master of Science in de Bio-Ingenieurswetenschappen: Land- en Bosbeheer

Francesca Sorbie

Juni – 2012

“This dissertation is a document of examination that has not been corrected for possible mistakes after defence. In publications, one may only refer to this work with written permission of the promoter, whose name is mentioned on the title page.”

“Dit proefschrift is een examendocument dat na de verdediging niet meer werd gecorrigeerd voor eventueel vastgestelde fouten. In publicaties mag naar dit proefwerk verwezen worden mits schriftelijke toelating van de promotor, vermeld op de titelpagina.”

ACKNOWLEDGEMENTS

Writing this thesis was not a task accomplished in solitude, therefore I would like to express my sincere gratitude to everybody who has supported me during the past year.

First of all I would like to thank my promoter **Seppe Deckers**. Not only am I very thankful to have such an enthusiastic promoter with a rich background, who kept my motivation high from the beginning until the end, but also for helping solve any problems that were experienced (Sorbie *et al*., 2012 ☺). For his inspiration and valuable corrections of this thesis, and for always making time for a discussion: Tekasha Tekasha (shoulder to shoulder).

Bas van Wesemael, my co-promoter with his creative plan B's and his idea to do the measurements in real life circumstances (= in the rain ☺). I am very grateful for his contributions to this thesis and the support provided back in Belgium. The same goes for **Jean Poesen,** with his broad spectrum of knowledge and help in the field. Together they gave important input to this thesis.

Daniel Teka for being a helpful supervisor during discussions, for being there for me when I was sick and for all the jokes and laughs. **Gebeyehu** for the good conversations. Also the time we spent together in Belgium was memorable. **Ayalew** thank you for your homemade injera and buna from Ethiopia that I could taste once more in Belgium, in addition to sharing your interesting philosophical insights.

This study was conducted within the framework of the Institutional University Cooperation program between Mekelle University and the Flemish Universities. The scholarship funded by **VLIR-IRO** (Flemish Interuniversity Council - Interfaculty Council for Development) made this once in a lifetime experience possible, and I would like to thank all the people from the VLIR program who provided support before and after this amazing journey.

To **Arnaud, Sylvain, Anneleen, Laurens, Jessie, Maxime, Sander, Karel, Renske** and **Inge**, the Ferenji who made weekends in Mekelle truly delightful. To **Charlotte, Ruben** and **Ludwin**, the 'Bahir Dar-crew' who made our trip to Amhara Region an exceptional one: the Geode, Lake Tana, dorowat, shoulder shaking, … I will never forget these enjoyable times! An extra thank you goes to **Sylvain** for the beneficial data-exchange and communication back in Belgium not to forget the great photos.

To **Sammy,** for inviting us for a beautiful New Years day in his home and for being sincere and kind. **Germay** and **Medin,** for transporting us to and from Mayleba. To my **fieldworkers** in Mayleba, without them it would have been impossible to collect the amount of data I have at this moment.

Bereket, for the discussions on the transects. **Fortuna** & **Betelem,** for teaching Inge and myself Tigrinya and for taking care of us in your humble home. In general the hospitality of the Ethiopian people was heartwarming.

Water 2011: it was an exceptional opportunity to attend this congress during my stay in Ethiopia. It has made a great contribution to this thesis by inspiring me and, of course, due to the networking achieved during poster sessions and coffee breaks. A real eye opener to a broader view on the possibilities research and science can bring to life. A special thank you goes to **Seppe Deckers** and **Mark Vervenne** for the interesting bus trip during the post conference tour to and from Axum.

MU-IUC (WAREP) and **CUD,** for providing the initial concept of the thesis and its framework. **Jan Nyssen,** for the interesting tour of Mayleba. **SSSB**, for the opportunity to make a poster presentation. The **Department of Earth & Environmental Sciences** and the **Faculty of Science** for allowing me to use their facilities. **Lore Fondu,** for her help in the soil lab.

Mark Vervenne and **Leen Bogaert** for accommodating me in the Beguinage, it is a wonderful area of Leuven that I still find blissful and truly enjoy living in – it provided the ideal environment for writing this thesis. To my friends of "Huisje 43" **Karel, Astrid**, **Dorien**, **Liesbeth**, **Marjolein, Barbara, Annelies**, **Mario** and **Simon**. Not to forget **The Dancer** and our couch surfer **Victor**. What an amazing year!

A special appreciation goes to **Inge** who had to live with me for 3 months - in a hut! - and who accompanied me on our travels throughout Ethiopia. She was always there for me and made the times we spent together exceptional. Once back in Belgium she maintained the contacts between the 'Ethiopian-crew' to enable us to reflect on our journey and fieldwork which was incredibly valuable.

Last but not least I would like thank my **family and friends** for their encouragement and support in everything I have wanted to do *so far*, and of course for having a listening ear during my endless conversations. **Mumsie**, **Papsie**, **Charlie Farlie** and **Le Jaques**: "Did you know…?" You guys have to put up with me the most! Thank you for caring so much for me. I love you all to bits.

I have learnt a lot of important things during the course of this thesis, especially on-field in the highlands of Ethiopia. This was my first experience in a developing country, and a rather exceptional one it was. The challenges that faced me have made a valuable contribution to my perspective on life as it is.

Yekenyelle
Francesca Sorbie
May 2012, Leuven

ABSTRACT

Rainfall-runoff (P/R) relationships were investigated on 24 micro-plots (1 m²) in the highlands of Northern Ethiopia during the main rainy season of 2011. This study was conducted in order to develop a greater understanding of the hydrological behaviour of small catchments (5 - 20 km²) and come to more realistic estimates of their water harvesting potential.

The micro-plots were distributed over 8 experimental sites within the Mayleba catchment (17 km²), each site consisting of three replicate micro-plots. Cropland and grazing land were taken into account as well as three soil textures and three slope classes. Several characteristics of the individual micro-plots were recorded: rock fragment cover, random roughness, vegetation cover, vegetation height, soil texture and slope. Their influence on runoff production was assessed.

To describe the influence of these measured characteristics on the P/R relationships, runoff response, α, and precipitation threshold, P_T, were defined. Land use had the most significant impact on runoff response, whereas it was not much influenced by slope. However, the slope had the most significant impact on the precipitation threshold. The influence of random roughness was observed for both α and P_T.

Curve numbers were derived from the P/R data of the micro-plots to predict runoff. These were applied at sub-catchment level (0.4 km²) for verification. The application of these curve numbers to a larger area gave an overestimation of runoff. The estimations were however more accurate than when using curve numbers from literature. This indicates the advantage of determining area-specific curve numbers for further applications.

Realistic estimates of water harvesting potential can help improve water resource planning to prevent oversized reservoirs and provide the local population with water during dry periods.

Keywords: Northern Ethiopia, highlands, semi-arid, water harvesting, irrigation reservoirs, rainfall-runoff relationships, curve numbers, runoff response, precipitation threshold.

LIST OF ABBREVIATIONS

Alpha (α)	Runoff response to rainfall
AMC	Antecedent Moisture Condition
ARC	Antecedent Runoff Condition
CC	Canopy Cover
CD-ROM	Compact Disc Read-Only Memory
CL1	Cropland gentle slope
CL2	Cropland middle slope
CL3	Cropland steep slope
CN	Curve Number
CRS	Coordinate Reference System
CUD	Commission Universitaire pour le Développement
DEM	Digital Elevation Model
FAO	Food and Agriculture Organisation
FC	Field Capacity
G.C.	Gregorian Calendar
GIS	Geographical Information Systems
GL1	Grazing land gentle slope
GL2	Grazing land middle slope
GL3	Grazing land steep slope
GPS	Global Positioning System
I_a	Initial abstraction
KIS	Keep It Simple
L_c	Losses (depression storage, infiltration, interception, wetting, evaporation)
m.a.s.l.	Metres above sea level
MDG	Millennium Development Goal
MU-IUC	Mekelle University, Institutional University Cooperation
N	Net rainfall loss
NRCS	Natural Resources Conservation Service
P	Precipitation
P_T	Precipitation threshold
P/R	Rainfall-Runoff
PLSR	Partial Least Squares Regression
PWP	Permanent Wilting Point

Q	Runoff (in CN calculations)
R	Runoff
RC	Runoff Coefficient
REST	Relief Society of Tigray
RMSE	Root Mean Square Error
RR	Random Roughness
RUSLE	Revised Universal Soil Loss Equation
S	Storage parameter
SAT	Saturated soil water content
SEDEM	Sediment Delivery Model
SCS	Soil Conservation Service
SPAW	Soil, Plant, Air, Water
SSR	Soil Surface Roughness
SSSB	Soil Science Society of Belgium
SWC	Soil and Water Conservation
U2	Andelay, cropland, middle slope
USDA	United States Department of Agriculture
UTM	Universal Transverse Mercator
VLIR-IUC	Vlaamse Interuniversitaire Raad, Institutional University Cooperation
W2	Walka, cropland, middle slope
WAREP	Water Resource Planning
WATEM	Water and Tillage Erosion Model
WOCAT	World Overview of Conservation Approaches and Technologies
WRB	World Reference Base for Soil Resources

Extra: Ethiopian terms

Andelay	Brown coloured, medium textured soil, Leptosol
Bahakel	Light coloured, light textured soil, Cambisol
Belg	Small rainy season from March to May
Buna	Coffee
Dorowat	Spicy chicken dish
Ferenji	Foreigner
Kiremt	Main rainy season from June to September
Injera	Local food made from Teff, type of sour pancake

Leba	Thief
Maresha	Ox-drawn ard plough
May	Water
Tekasha	Shoulder
Walka	Dark coloured, heavy textured soil, Vertisol
Woreda	District
Yekenyelle	Thank you

LIST OF FIGURES

LIST OF TABLES

TABLE OF CONTENTS

Part I

1 INTRODUCTION

1.1 Problem statement

"When the well is dry, we learn the worth of water"
Benjamin Franklin

Water is an indispensible resource that must be used and managed carefully. Due to the growing world population there is increased pressure on water resources which is a serious concern. Water scarcity leads to tensions, conflicts between users, declining ground water tables and environmental degradation (UN-Water, 2007).

As the Ethiopian highlands are subject to frequent droughts, water harvesting systems have been installed for supplying the population with water during dry periods. One of the challenges for the 21st century is to optimise the management of available land and water resources. Quantifying and conserving available water resources is of importance for agricultural water use to secure food production and local sustainable development for the ever-growing population.

For water harvesting, a high runoff is desirable, but this can cause problems in the catchment due to the erosion prone hill slopes. This situation of land degradation is mainly caused by deforestation, low vegetation cover and overgrazing (Nyssen *et al*., 2004a). Soil and water conservation measures are applied to a vast extent in the area which result in a decrease of runoff and thus a lower water harvesting potential.

In this region many challenges are being addressed. This thesis research is framing within the project “Improving water resource planning at the scale of micro-dam catchments in Tigray, Northern Ethiopia: learning from success and failure”.

1.2 Objectives

1.2.1 Overall objectives

The overall objectives of this research are:

- To understand the hydrological behaviour of small catchments (5 - 20 km²), this to improve the design and spatial implementation of water harvesting systems and soil and water conservation measures.
- To come to realistic estimates of water supply, this in order to apply water resource planning more accurately and avoid oversized reservoirs.

1.2.2 Specific objectives

The specific objectives of this research are:

- To investigate the influence of land use, soil texture and slope on the rainfall-runoff relationships.
- To derive curve numbers based on the rainfall-runoff data at micro-plot level (1 m²).
- To verify the curve numbers at sub-catchment level (0.4 km²).

1.3 Research hypotheses

Hypothesis A. Variations of rainfall-runoff relationships within replicate micro-plots (1 m²) occur due to minor differences such as random roughness, stoniness and slope.

Hypothesis B. Slope and soil texture have a larger effect on the rainfall-runoff relationships than the antecedent moisture content (AMC).

Hypothesis C. Curve numbers, deduced from P/R data of micro-plots (1 m²), applied to a sub-catchment (0.4 km²) give an overestimation of runoff.

1.4 Action points

The main action points of this thesis were:

- Data collection in the Mayleba catchment:
    - Rainfall-Runoff (P/R) data during natural rainfall events
    - Characteristics of the installed micro-plots (1 m²)
    - Surveying soil characteristics at catchment level
- Data analysis:
    - Assess P/R relationships for the applied treatments on micro-plots
    - Derive curve numbers from micro-plot P/R data
    - Verify curve numbers at sub-catchment level

1.5 Structure of dissertation

This dissertation starts with the introduction in **Chapter 1** including problem statement and research hypotheses. As the study area is situated within Tigray, the literature review in **Chapter 2** focuses on this region of Ethiopia. It provides background information on the study area and elaborates on the concepts relevant to this research. **Chapter 3** discusses the methodology used for this research: the approach taken to progress toward the objectives. It describes which materials and methods were used in the experimental research and how the data was analysed. Research was conducted at three levels: micro-plot level (1m²), sub-catchment level (0.4 km²) and catchment level (17 km²). Using this methodology results were attained which are presented and discussed in **Chapter 4**. This chapter consists first of the 'modelling' using the data from the micro-plots and subsequently an upscaling to sub-catchment level for 'verification'. Also a 'generalisation' to catchment level is introduced. Finally in **Chapter 5** the general conclusions are formulated in response to the problem statement. This chapter also verifies the hypotheses formulated in the introduction and reveals recommendations for further research. In Figure 1.1 the structure of the dissertation is graphically presented.

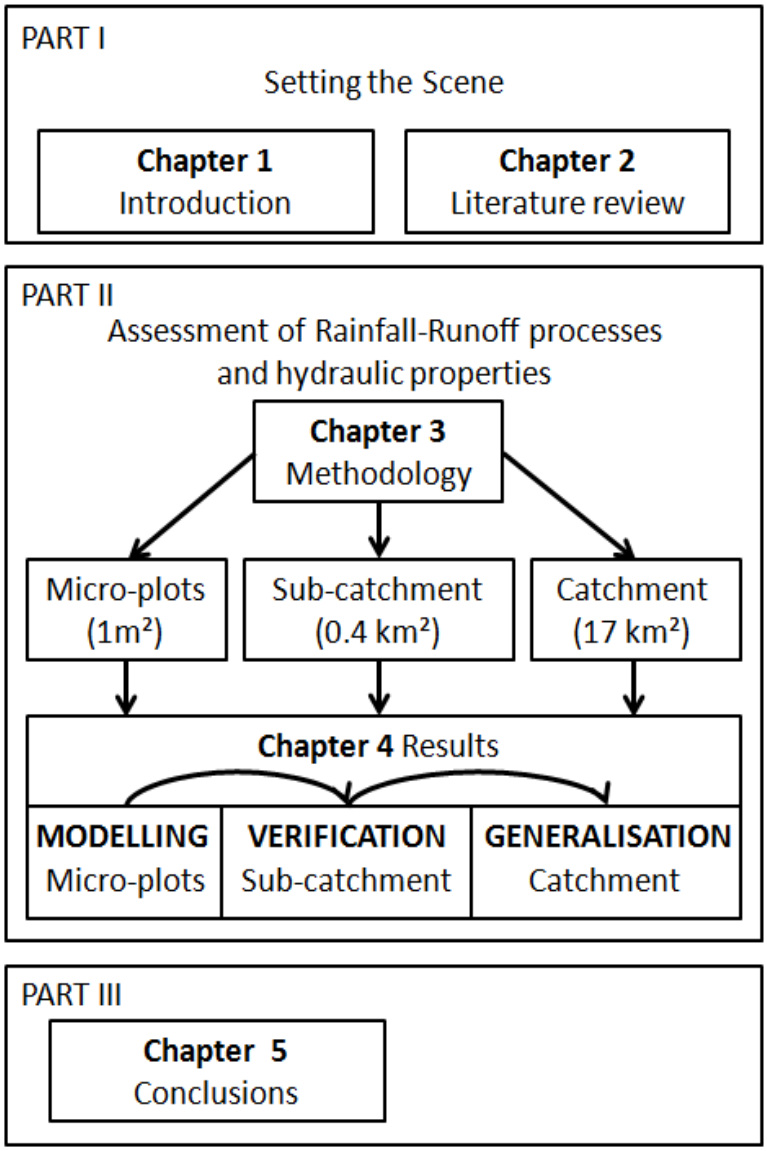

Figure 1.1 Structure of dissertation

2 LITERATURE REVIEW: THE STUDY AREA

The Federal Democratic Republic of Ethiopia (Figure 2.1 – middle) is located in the East of Africa (Figure 2.1 – left), often referred to as the 'Horn of Africa'. It lies between 3 and 15°N and 33 and 48°E with an area of 1.1 million km². This landlocked country borders six other countries: Djibouti, Eritrea, Kenya, Somalia, South Sudan and Sudan. There are an estimate of 93.8 million inhabitants, with a population growth rate of 3.179 %, this is the fifth fastest growth rate in the world (CIA, 2012; CSA, 2007).

It can be said that Ethiopia is a land of extremes. With the Northern part of the Rift Valley cutting through the entire country from North-East to South-West it implies many remarkable features. With an average altitude of 2,500 metres, Ethiopia's highest peak is the Ras Dashen (4,533 m.a.s.l.) and its lowest point is reached in the Danakil Depression (125 m below sea level). Due to the topographical differences the climate changes accordingly. Fekadu (1997) noted that the country can be divided into three climatic zones:

Kolla: Tropical zone: < 1,830 m.a.s.l. An average annual temperature of ± 27 °C with annual rainfall of ± 510 mm. The Danakil Depression is the hottest region in Ethiopia where the temperature can reach 50°C.

Woina dega: Subtropical zone: 1,830 to 2,440 m.a.s.l. An average annual temperature of ± 22 °C with annual rainfall between 510 and 1,530 mm. This zone includes the Ethiopian Highlands.

Dega: Cool zone: > 2,440 m.a.s.l. An average annual temperature of ± 16 °C with annual rainfall of ± 1,275 mm.

Rain-fed agriculture is the main economic activity in Ethiopia. This makes the country very vulnerable: it is dependent on a stable natural rainfall regime. Referring to the yield losses and famines in the 1980s, Ethiopia is often used as example for the catastrophes that can result from anthropogenic climate change (Conway *et al*., 2011).

Figure 2.1 Map of Africa -> Ethiopia -> Tigray Region (World Atlas, 2012; Edwards *et al*. 2011)

As this research was conducted in Tigray Region, the literature review will focus on this part of Ethiopia (Figure 2.1 - right).

2.1 Location

Tigray Region (Figure 2.2 - left) is located in the North of Ethiopia and is often considered the most degraded region of the country. It has an area of ± 50,000 km² with an average population density of 80 persons/km². In a statistical report of 2007 the population of Tigray was estimated at approximately 4.5 million inhabitants, with more than 80% of the human population in Tigray living in rural areas (CSA, 2007).

The Mayleba catchment (13° 41' N and 39° 15' E, Figure 2.2 - right) is the study area where the research was conducted. It is located in Central Tigray, 45 km West of Mekelle, Tigray's capital. More specifically it lies within the Dogu'a Tembien district, which has an area of ± 1,130 km² and Hagere Selam as main town (Nyssen *et al*., 2004b). The Mayleba catchment has a total area of ± 17 km², a perimeter of ± 18 km and an elevation range from ± 2300 to 2835 m.a.s.l. It has a micro-dam at the outlet which is located at ± 2,290 m.a.s.l. (Van de Wauw *et al*., 2008).

In the literature Mayleba is written in a number of ways, e.g. Mayleba, Mayleva, Mayleiba, Maileba. In Google Earth the micro-dam can be found as Mayleba, this is also the spelling that will be used throughout this dissertation. The translation of this Tigrinya word is water (*may*) thief (*leba*). The area of land that provides water for this dam is called the Mayleba catchment, often referred to simply as Mayleba, named after the micro-dam. It contains six villages: Raeset, Adi Koilo, Adiwerat, Alaesa and Medayeh (Van de Wauw, 2005).

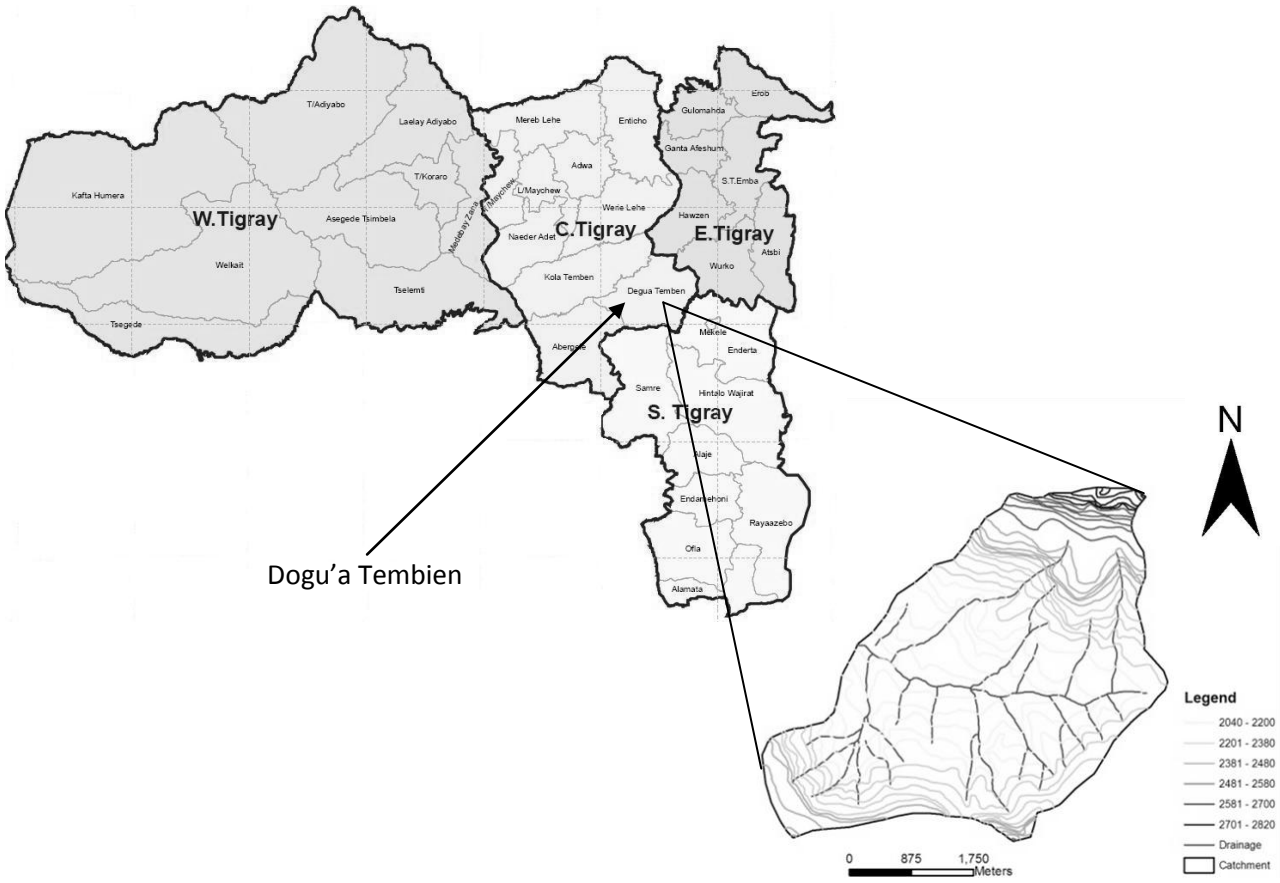

Figure 2.2 Situation of the Mayleba catchment within the Dogu'a Tembien district of the Tigray Region

2.2 Climate

The climate of Tigray is mainly semi-arid and is characterised by spatial and temporal rainfall variability. Average annual precipitation is 800 - 1000 mm in the West and the highlands in the South. In the East towards the Afar Region where the Danakil depression is located precipitation is limited to ± 400 mm (Edwards *et al*., 2011).

New_LocClim was used to present the local climatic conditions. New_LocClim is a software program with an extensive database that provides estimates of average climatic conditions at locations where no observations are available (FAO, 2010).

The rainfall pattern in the Dogu'a Tembien district is bimodal (Figure 2.3), with the main rains falling from June to September, also known as the *Kiremt* (> 80 % of total rainfall). From March to May there is a shorter, less marked rainfall called the *Belg*. Average yearly precipitation is in the order of 700 mm (Nyssen *et al*., 2007b). Daily potential evapotranspiration ranges from 3 mm in the rainy season to 5 mm in the dry season. The Dogu'a Tembien district has a mean temperature range between 18 and 20 °C (Figure 2.4).

The rainfall is very variable even at catchment scale. For the Northern Ethiopian Highlands this was investigated by Nyssen *et al*., 2005. The general orientation of the valley and the slope gradient (over longer distances) play an important role in the spatial distribution of annual rainfall. In the Mayleba catchment the Northern part receives relatively more rainfall and daily rainfall almost never falls before noon (Van de Wauw, 2005).

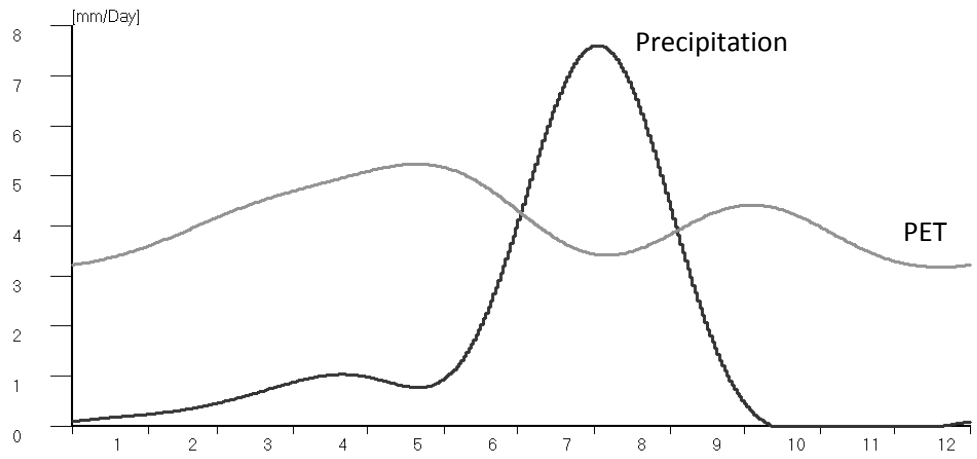

Figure 2.3 Daily average precipitation in mm and Potential Evapotranspiration (PET) in mm from the meteorological stations in the region of 13°41'N and 39°15'E, Tigray. Data from New_LocClim, (FAO, 2010).

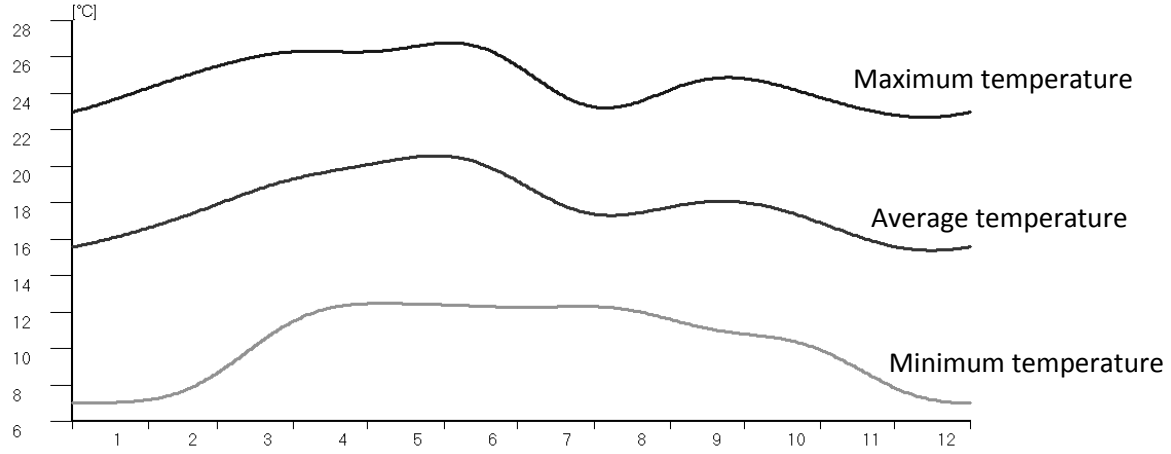

Figure 2.4 Daily mean temperatures in °C. Top curve: maximum-, middle curve: average- and bottom curve: minimum-temperature. Data from meteorological stations in the region of 13°41'N and 39°15'E, retrieved from New_LocClim, (FAO, 2010).

2.3 Geology

The geology of the Mekelle outlier (± 800 km²) consists of hard and soft Antalo limestone layers (± 400 m thick) overlain by Amba Aradam sandstone, both of Mesozoic age. Tertiary basalt flows covered these Mesozoic layers and are themselves separated from each other by silicified lacustrine deposits (Nyssen *et al.*, 2007).

As a result of Rift Valley tectonic uplifts (± 2500 m) and differential erosion a stepped landform can be observed. This reflects the sub horizontal structure of the geology.

The Mayleba catchment is located just outside the basalt dominated stepped uplands of the Geba catchment and is part of the Mekelle outlier (Figure 2.5). The South East corner is overlain by Agula Shale. The top of the table mountains consists mainly of Amba Aradam sandstone and the two series of Tertiary basalt lava flows. Silicified lacustrine deposit layers locally occur in between the basalt layers. Figure 2.6 shows the geological map of the study-area. The highest point of the catchment is located on a basalt ridge (2,835 m.a.s.l). In the South of the study area a dolerite sill outcrops, inducing an extra uplift in the higher lying sandstone and basalt. Another significant feature in the area is the landslides. They occur within the limestone but can also cause basaltic material to be displaced onto limestone areas, this is an important aspect to be taken into account for soil mapping (Bosellini *et al.*, 1997; Nyssen *et al.*, 2003; Van de Wauw, 2005).

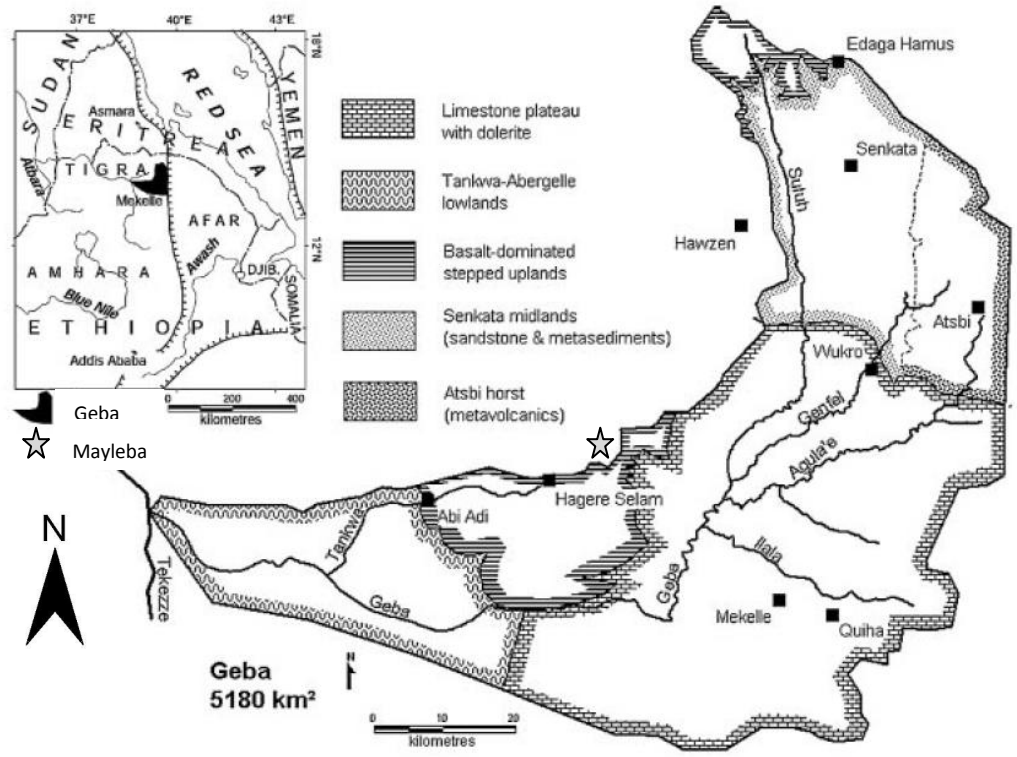

Figure 2.5 Location of Mayleba in relation to the Geba catchment (Nyssen *et al*., 2004b)

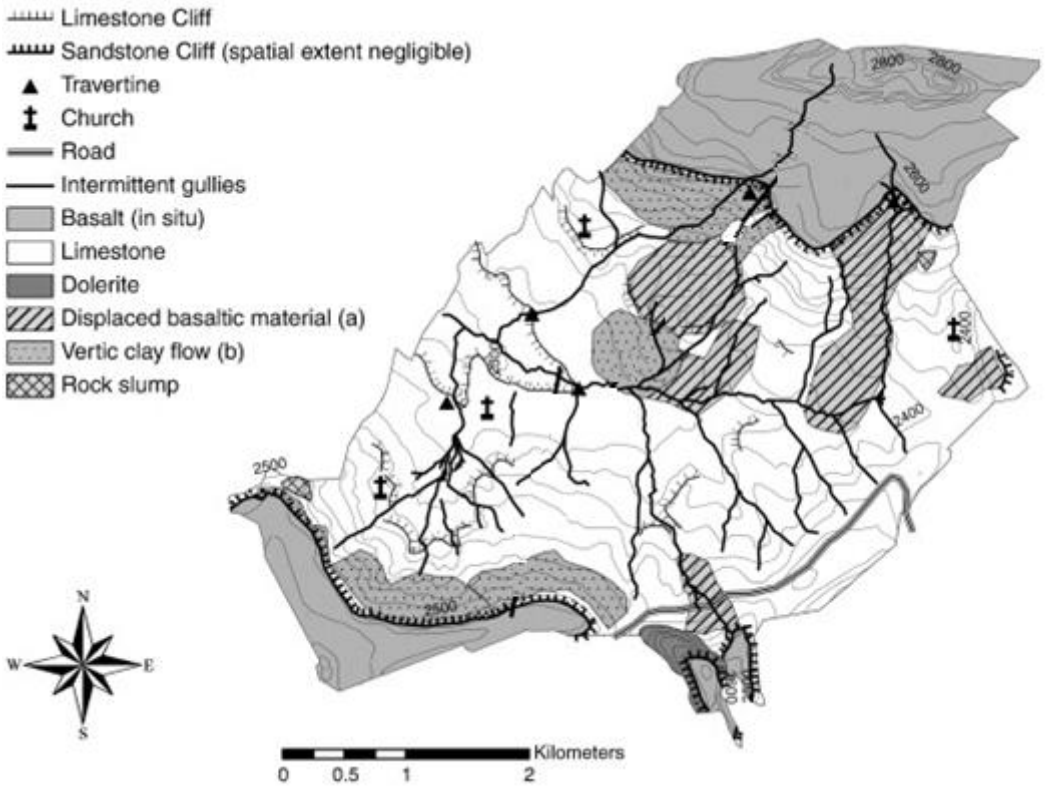

Figure 2.6 Geological and geomorphologic map of the Mayleba catchment (Van de Wauw *et al*., 2008)

2.4 Soil

The physical and chemical properties of a soil are decision-makers for the potential natural vegetation and crop choice or land use, but also for the soil erosion susceptibility. The occurrence of a certain soil depends on the prevalent geology and relief. Figure 2.7 shows the soils of the Mayleba catchment which was established by Van de Wauw *et al*., 2008. In the lower landscape areas Vertisols developed in basalt-derived parent materials. In the presence of basic cations, smectite clays may be formed.

In Mayleba some typical soils that develop on limestone are Calcaric Leptosols, Regosols in the slope positions and Cambisols in the flatter areas. On the footslopes Cumulic Calcaric Cambisols can be found and in the low landscape position Calcaric Vertisols are present. Due to increased runoff coarse material is deposited on top of the Vertisols. Regosols, Cambisols and Leptosols comprise 75% of the soil surface in Mayleba. (Van de Wauw *et al.*, 2008).

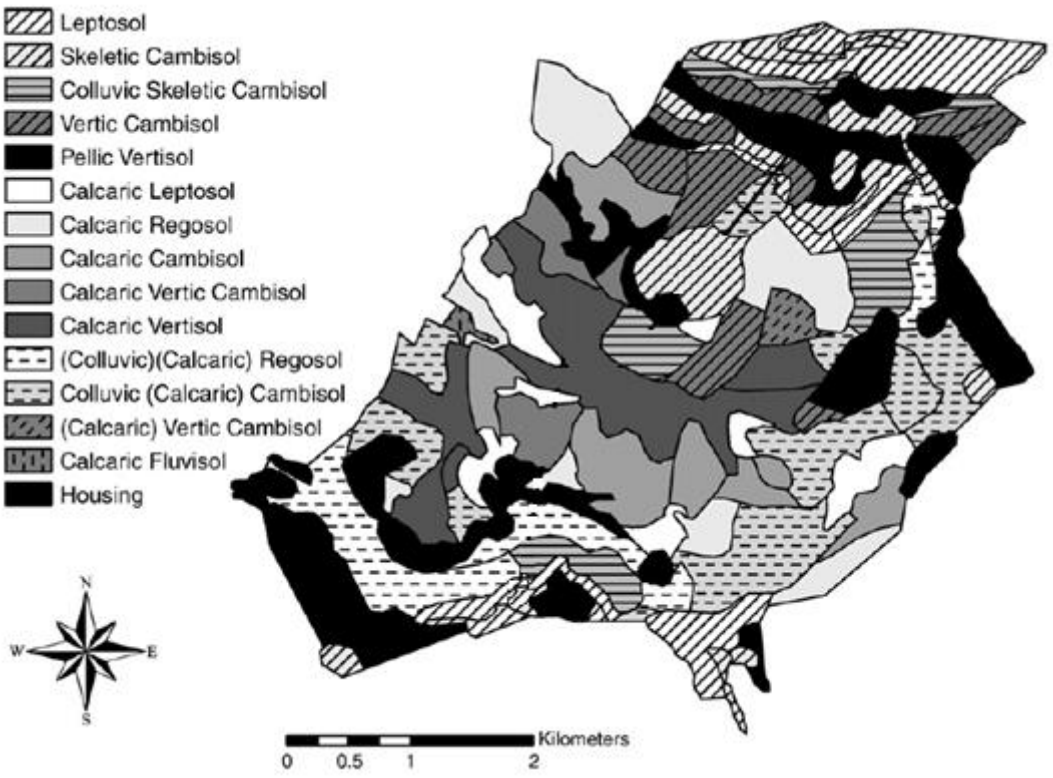

Figure 2.7 Soil map of the Mayleba catchment (Van de Wauw *et al*., 2008)

2.5 Land use

The dominant land use is small-scale rain-fed agriculture. The main crops cultivated are barley (*Hordeum vulgare*), wheat (*Triticum aestivum*) and teff (*Eragrostis teff*). Wheat and barley (a combination known as '*hamfets'*) are often sown together. Some varieties of pulses, such as lentils (*Lens culinaris*) and grass pea (*Lathyrus sativus*), have an important role in the crop rotation. These provide enrichment of nitrogen and mobilisation of fixed phosphorus. Almost all soils derived from basalt are cultivated. Soils derived from limestone are often only grazed (Nyssen *et al*., 2007).

It is noticeable that there is more cropland in the Northern part of the Mayleba catchment (Figure 2.8), this probably has to do with the displacement of basaltic material as a result of landslides. In view of the high numbers of livestock there is also a fair amount of grazing land, ± 30 % in the Mayleba catchment (Van de Wauw *et al*., 2008).

Due to growing livestock quantities and human population expansion not much of the natural vegetation remains. The forests around churches are protected for religious reasons and therefore the natural vegetation can only locally survive. *Acacia spp., Euphorbia abyssinica, Juniperus procera, Olea europea, Cordia Africana* and *Podocarpus gracilior* are some of the tree species that can still be found (Hagos *et al*., 2002). *Eucalyptus spp.* is commonly cultivated in the area as it is a fast growing tree that can be used for its wood. However, it only provides a minimal vegetation cover and it uses a large amount of the available water.

In some areas, usually located on steep and strongly degraded hill slopes, grazing and cropping are prohibited. These protected areas, called exclosures, aim at fighting land degradation by vegetation restoration (Descheemaeker *et al*., 2008).

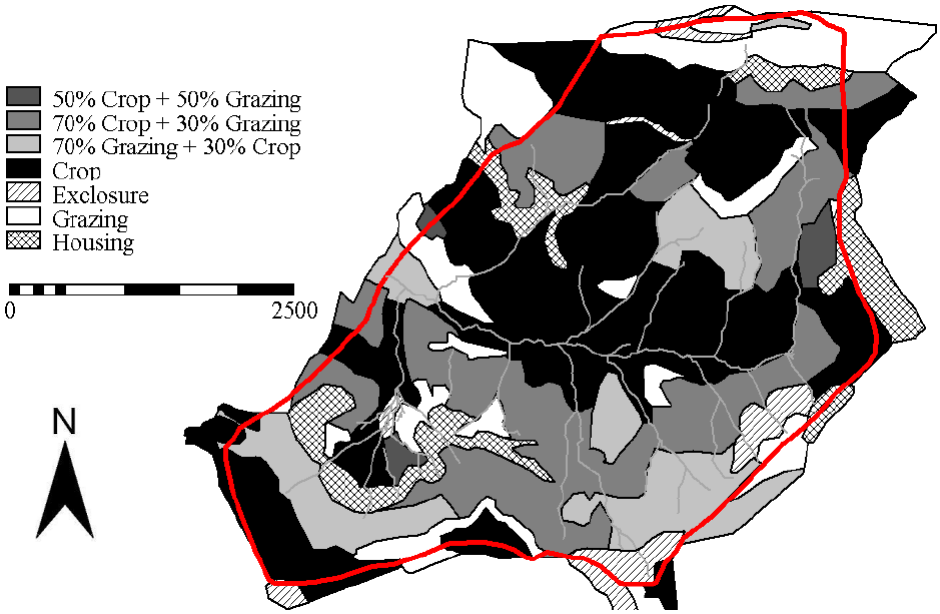

Figure 2.8 Land use map of Mayleba (Van de Wauw, 2005)

2.6 Soil erosion

Many areas in Tigray are subject to severe soil erosion due to prevalence of steep slopes, erosive rains and livestock- and population pressure. Rill and inter-rill erosion is combated with soil and water conservation (SWC) techniques which are applied throughout the region. Traditionally grass strips were maintained down slope of the field to capture the soil transported by runoff. These grass strips are often no longer present as they were ploughed for more cropping area. Stone bunds (Figure 2.9 - left) are commonly implemented in the landscape. According to a study, by Nyssen *et al*., (2007a), stone bunds can reduce soil loss by 68% after 3 to 20 years of age and slope gradients decrease 1 % every 3 years. Stone bunds, in addition, induce a higher moisture content on both sides of the bund. Trenches can also be found in the landscape (Figure 2.9 - right). These are made by removing soil and placing it down slope (or '*fanya juu*' – a term borrowed from Kiswahili, also used in WOCAT) of the trench. They capture loose soil in runoff, but are rapidly silted. These two SWC techniques, stone bunds and trenches, can easily be combined. The trench is then placed behind the stone bund (up-slope, also called '*fanya chini*') and the removed material can be used to fortify this bund. Another solution is the demarcation of exclosures, as mentioned above (Nyssen *et al*., 2007a).

Gully erosion has markedly scarred the landscape in Tigray. Some of the techniques used to counter the further incision of gullies are check dams, gabions and re-vegetation of the gully. Check dams are built in the gully from loose stones and are positioned at regular intervals. They decrease the erosive power of the runoff in the gully by slowing it down. Also part of the transported soil material is deposited behind these check dams. Gabions are piled stones fortified by a metal cage and have the

same function as check dams. Both structures have the risk of being bypassed due to the lateral expansion of the gully (Nyssen *et al*., 2004b). In the Mayleba catchment a sediment yield of 9.9 t ha^{-1} y^{-1} for cropland and 13.5 t ha^{-1} y^{-1} for rangeland was estimated by De Wit, 2003. This sediment ends up in the micro-dam.

Figure 2.9 Terraced landscape of the Mayleba catchment, due to stone bunds (left, July, 2011) and trenches (right, photo taken by Daniel Teka)

Figure 2.10 Check dam (left) and gabion (right) for gully erosion control in the Mayleba catchment, (August, 2011)

Tillage erosion also occurs, the ox-drawn ard ploughs (*maresha*) are used. Usually the farmer ploughs along the contour lines displacing more material downhill, this effect is larger for steeper hill slopes (Nyssen *et al*. 2000). Between two stone bund structures this effect can be noticed more easily. Down slope of a stone bund soil is constantly being removed and the less fertile substrate outcrops (Figure 2.11). Up slope of the subsequent stone bund the fertile soil is deposited. This fertility gradient between stone bund structures was discussed by Vancampenhout *et al*., 2006.

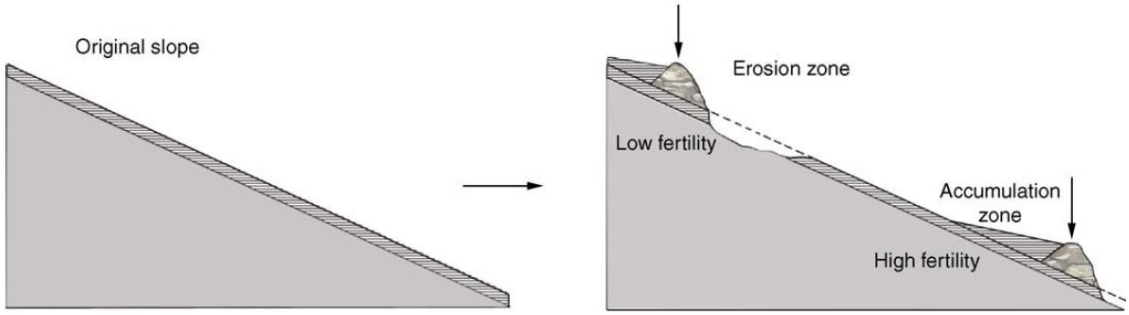

Figure 2.11 Illustration of the development of an erosion zone and an accumulation zone between two stone bunds (vertical arrows), from Vancampenhout *et al.*, 2006.

2.7 Hydrology

Tigray has many ephemeral rivers that are fed during the rainy season. The permanent rivers only have limited discharge during the dry season. The Tekeze-Atbara river basin of Tigray is a tributary of the Blue Nile. In this semi-arid climate the rainfall is very variable, both spatially and temporarily (Nyssen *et al.*, 2005). To accommodate this uncertainty many small-scale dams were built for irrigation.

The Mayleba micro-dam was built in 1997-1998 by REST. With a capacity of 0.98 million m³ it was designed to irrigate 50 ha of agricultural land. The life expectancy was at least 20 years. However, since 2002 the dam suffers from sedimentation and the outflow is hindered. In Figure 2.12 the irrigation channel behind the Mayleba micro-dam can be seen, it is no longer capable of operating (De Wit, 2003; Gebreyohannes *et al.*, 2012). According to Asmelash *et al.*, (2007) an area of approximately 15 ha is irrigated with water from this micro-dam. This irrigated area is mainly located directly behind the micro-dam. It is currently also used for livestock drinking.

Figure 2.12 An out of use irrigation channel, behind the Mayleba micro-dam (August, 2011)

Part II

3 METHODOLOGY

In this chapter the preliminary research, experimental setup, applied treatments and measurements are discussed. The data collected was later analysed through i.a. laboratory analysis, photo analysis and statistical analysis. These methods of analysis are elaborated upon in this paragraph.

3.1 Reconnaissance study

The specific choice of the Mayleba catchment was made in consultation of experts who have good knowledge of the area. The choice was mainly based on the fact that it meets the requirements of size (5 - 20 km²) and the presence of a micro-dam for water harvesting. Furthermore this area has been subject to a lot of project research in the recent past. The soil texture map from Van de Wauw (2005), that is available of the catchment, was of great value for the elaboration of this specific research.

A preliminary overview of the study area was vital before deciding on the location of the micro-plots and starting data collection. Maps and literature were consulted. Subsequently the catchment was visited. Via participatory reconnaissance with local farmers who have good knowledge of the soils, three major locally recognized soil types were differentiated: '*Walka*', '*Bahakel*' and '*Andelay*'. The three soil types stated are the local terms for respectively clay, silty clay loam and loam. According to Corbeels *et al*., 2000 these soil types are distinguished by farmers mainly based on their colour and texture. Walka is a black, heavy textured soil. Andelay is a brownish, medium textured soil. And Bahakel is a light coloured, light textured soil. In Table 3.1 the main characteristics of these local soil types are presented.

Table 3.1 The main characteristics of the local soil types, after Corbeels *et al*., 2000

	Soil type		
Characteristics	***Walka***	***Andelay***	***Bahakel***
Soil name (FAO classification)	Vertisols	Leptosols	Cambisols
Organic matter content	High	Low	Extremely low
Texture	Heavy	Medium	Light
Depth	Variable	Shallow	Shallow
Compaction	High	Low	Low
Colour	Black	Brown	White
Cracking	Severe	Slight	Slight
Drainage	Poorly drained	Well-drained	Well-drained
Moisture retention	High	Low	Low
Response to fertiliser	Moderate	Good	Good

3.2 Experimental Setup

The field work was conducted during the main rainy season (*Kiremt*) of 2011. The subsequent steps were: selecting an appropriate location for the micro-plots, installation and data collection on the micro-plots - discussed in paragraph 3.2.1. Carrying out sub-catchment surveying - discussed in paragraph 3.2.2. Locating sampling points along transects throughout the catchment and performing sampling - discussed in paragraph 3.2.3.

3.2.1 Micro-plots

Eight sites were selected for rainfall-runoff data collection (Figure 3.1), each site containing three replicate micro-plots (± 1 m²). These eight sites were selected to represent i) the different major land uses, ii) slopes and iii) soil textures in the catchment. Most sites were adjacent to experimental sites of other ongoing research (Gebeyehu Taye and Van Parijs Inge). This had many advantages such as the presence of guards to watch over the experimental equipment in the field. Also exchange of data was of interest, e.g. daily rainfall and soil moisture.

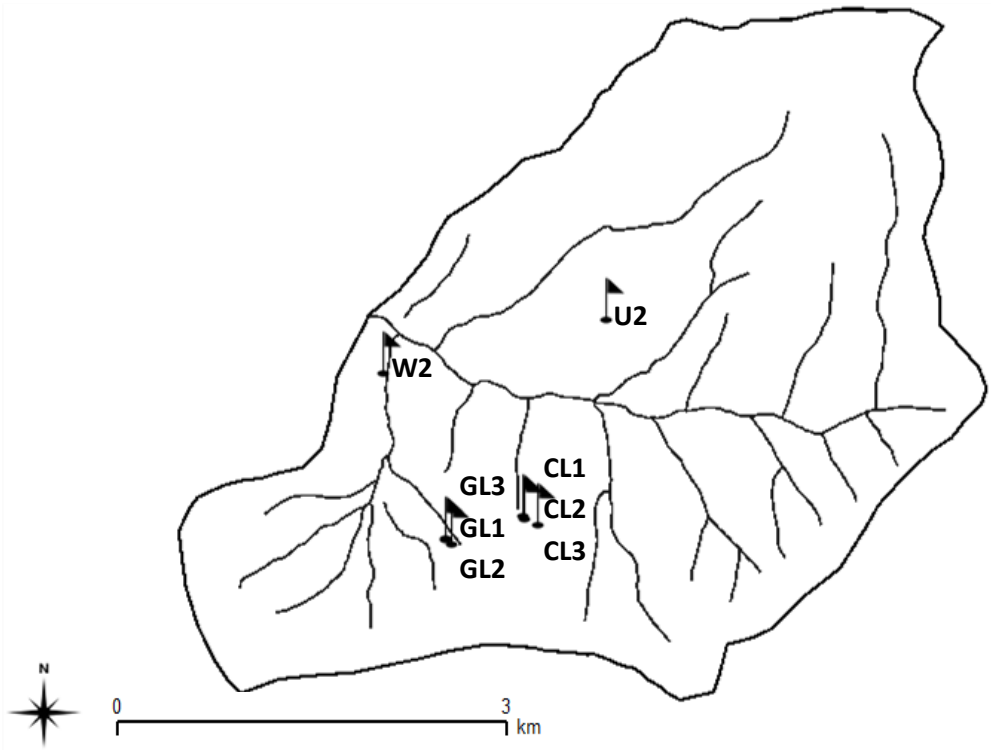

Figure 3.1 Location of the eight experimental sites, coordinates can be found on the CD-ROM (see Appendix)

In total, 24 micro-plots (8 sites each containing 3 replicate micro-plots) were examined. In Table 3.2 an overview can be found of the different treatments. Three sites were located on grazing land (GL), five sites on cropland (CL). The vegetation on cropland was always wheat (*Triticum aestivum*),

sometimes intercropped with barley (*Hordeum vulgare*). Each of the three grazing land sites was located on a different slope class, as were three of the cropland sites. The two other sites, both on cropland, were located on an intermediate slope, but with a different soil texture.

Table 3.2 Overview of the treatments of the micro-plots installed in the Mayleba catchment

	Land use	Texture	Slope	Replicate	Site code	Micro-plot code
To see effect of land use & slope	Cropland	Bahakel	1	A	CL1	CL1A
				B		CL1B
				C		CL1C
			2	A	CL2	CL2A
				B		CL2B
				C		CL2C
			3	A	CL3	CL3A
				B		CL3B
				C		CL3C
	Grazing land	Bahakel	1	A	GL1	GL1A
				B		GL1B
				C		GL1C
			2	A	GL2	GL2A
				B		GL2B
				C		GL2C
			3	A	GL3	GL3A
				B		GL3B
				C		GL3C
To see effect of soil texture	Cropland	Andelay	2	A	U2	U2A
				B		U2B
				C		U2C
		Walka	2	A	W2	W2A
				B		W2B
				C		W2C

Clarification of abbreviations: Each micro-plot has a code with structure **XYZ. X**: Type of land use and soil texture (CL: Cropland on Bahakel, GL: Grazing land on Bahakel, U: Cropland on Andelay, W: Cropland on Walka). **Y**: Slope classes (1: Gentle slope 0% - 8%, 2: Middle slope 8% - 15%, 3: Steep slope >15%). **Z**: Distinction between the 3 replicates (A: Most to the east, B: Middle plot, C: Most to the west)

3.2.1.1 Installation of the field experiments

The installation of each set of three replicate micro-plots started by finding a suitable location. This was based on soil texture and slope. Soil texture was assessed by finger tests and knowledge of local farmers. The slope, which is very variable at the micro-plot scale of 1 m², was assessed with the clinometer function of a geological compass. The design of a micro-plot can be seen in Figure 3.2. The micro-plots were installed perpendicular to the locally prevailing contour.

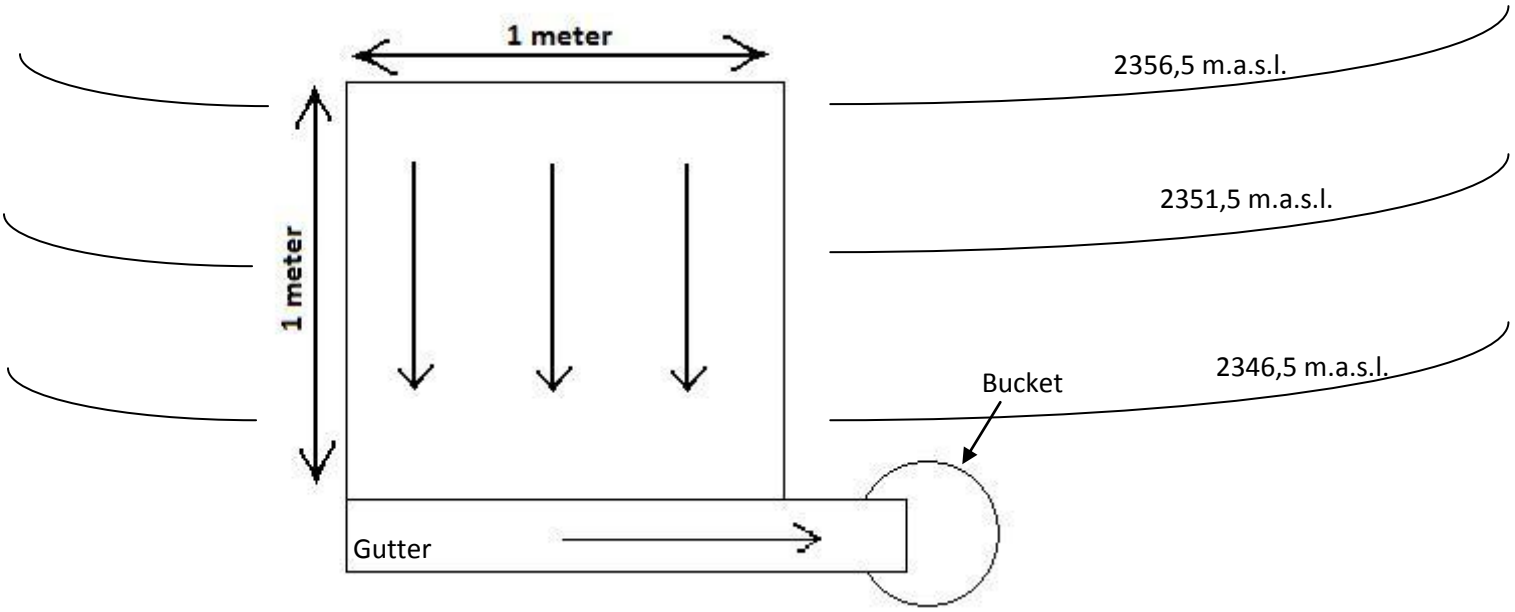

Figure 3.2 Design of a micro-plot (1 m x 1 m) with gutter for runoff collection and guidance into bucket, installed perpendicular to the locally prevalent contour lines.

To start the installation of each micro-plot first a hole was made in the ground which could enclose a 10 litre bucket. Then, a long slit was dug of ± 1.2 m for installing the gutter perpendicular to the slope direction. Each gutter included a gutter lip which was pushed into the soil as graphically shown in Figure 3.3.

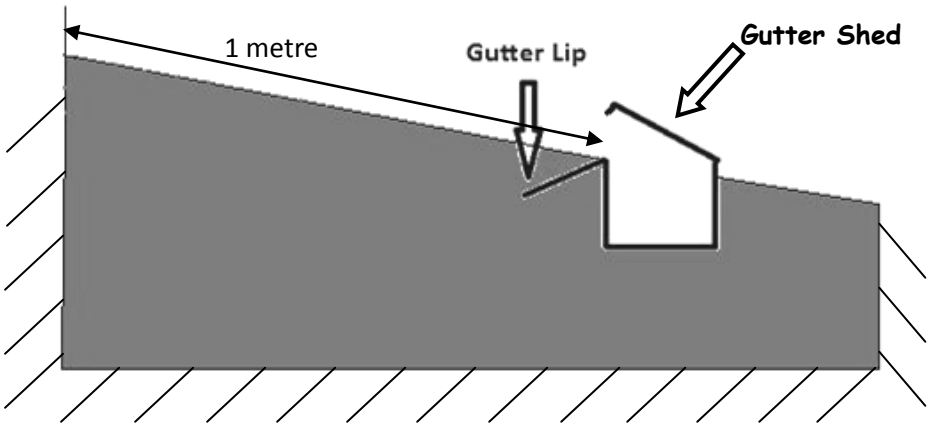

Figure 3.3 Vertical cross section of the gutter in the soil with indication of gutter lip and gutter shed

To complete the installation, three metal sheets were used to define the 1 m x 1 m area. The top metal sheet, parallel to the gutter, was extended to avoid run-on entering the micro-plot (Figure 3.4 - left). Also a trench was dug above each set of three replicate micro-plots to divert potential excessive runoff from above (Figure 3.4 - right).

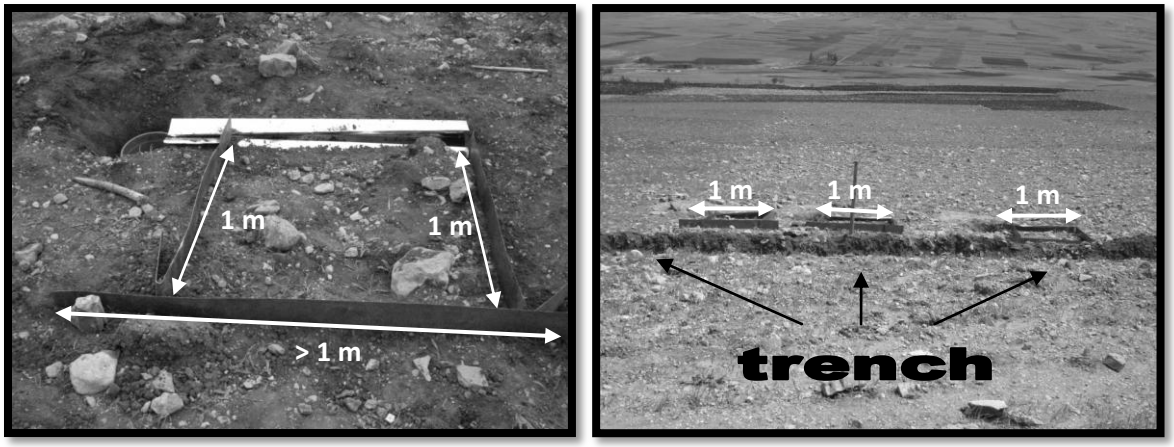

Figure 3.4 Runoff diversion via extended metal sheet (left) and trench (right), both photo's taken from an upslope, looking down slope, position, July 2011

During each rainfall event the bucket was covered with a geo membrane, fixed with stones to avoid it from blowing away by the wind, this prevented direct rainfall from entering the bucket.

In the proximity of each site a rain gauge was placed (Figure 3.5). This was important as the rainfall is variable throughout the catchment. Three weather stations are located in the catchment, each containing a data logging tipping bucket rain gauge, but this is not sufficient for the detail of rainfall intensity that is necessary at micro-plot level. For this reason simple rain gauges were used, with a precision of 1 mm rainfall and a maximum capacity of 40 mm.

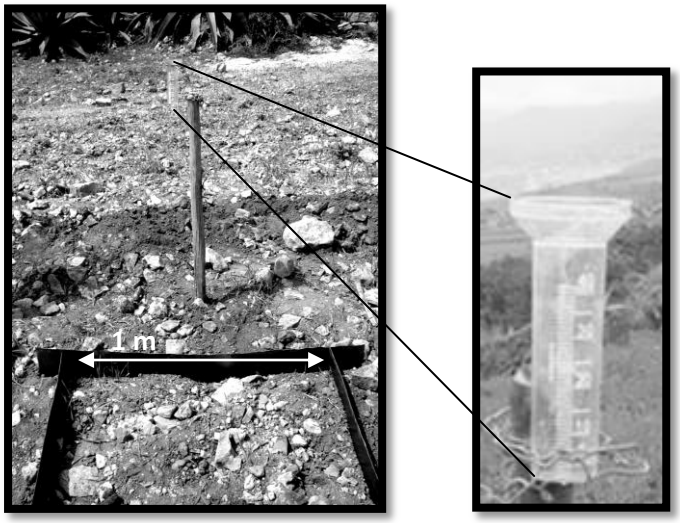

Figure 3.5 Rain gauge for rainfall intensity measurements per three minutes

3.2.1.2 The rainfall-runoff measurements for a set of three replicate micro-plots

At the start of each rainfall event the buckets were placed under the gutter outlet and protected by a geo membrane to avoid direct rainfall. The rain gauge was also put in place. Both bucket and rain gauge were placed in a horizontal position for accurate readings. Every three minutes the rainfall in the rain gauge was measured. The time at which ponding occurred in the micro-plots was recorded as well as the time from which runoff started. When runoff started it was collected in the bucket via the gutter. The depth of runoff in the bucket was measured every three minutes with a simple measuring tape (accuracy 1 mm). Measurements proceeded until runoff ceased.

Monitoring 24 micro-plots simultaneously during a rainfall event was a challenge. Fieldworkers were trained for this purpose. They were assigned in groups of two per monitoring site of three micro-plots for measuring rainfall and runoff every 3 minutes (Figure 3.6).

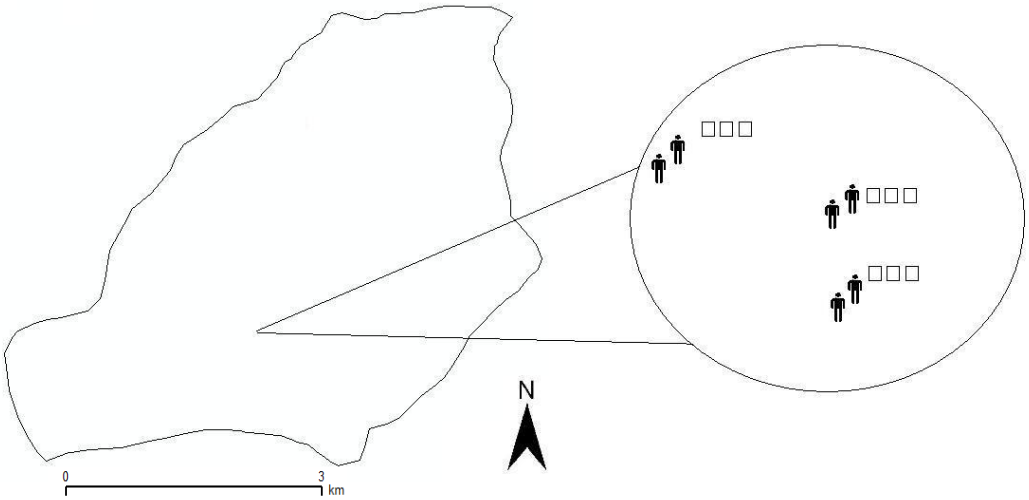

Figure 3.6 Each of the eight sites consisted of three micro-plots. Two workers per site were necessary due to intense data collection per three minutes. This sketch gives an example of three of the sites within the Mayleba catchment, each with two fieldworkers.

The first rainfall events were used for training the fieldworkers and also for sealing any occurring gaps. This was done to avoid loss of runoff and thus allow a more correct measurement. To correlate the depth of runoff measured in the buckets (in centimetres), to the corresponding volume of runoff (in liters), a volume-depth relation was established.

3.2.1.3 Measurements conducted on the plots and frequency

For each micro-plot several variables were recorded that can possibly explain the variations in runoff generation.

Daily rainfall

Not only was the rainfall recorded every 3 minutes, as described above, but also **daily rainfall** was measured nearby the plots on the adjacent experimental plots. This rainfall data was collected using non automatic rain gauges (Figure 3.7 - left) consisting of a metal container with a plastic tube to conduct water from the metal container to a secluded plastic container that was half buried in the ground. The reason for this diversion of the rainfall is to avoid evaporation of the rain and thus to acquire more accurate results. This daily rainfall data was used to calculate the cumulative rainfall amounts for this rainy season.

Instantaneous rainfall

At three locations within the catchment there are weather stations with automatic rain gauges of the aerodynamic tipping bucket type (Figure 3.7 - right), fitted with data logger devices that register the **instantaneous rainfall**. One of these rain gauges is situated near the three replicate micro-plots of site W2 (see Figure 3.1 for location). For this site the tipping bucket data was used instead of placing a manual rain gauge as used at the other sites.

Figure 3.7 Left - Non automatic rain gauge for measuring daily rainfall depths. Right – data logging tipping bucket rain gauge for rainfall intensities

Moisture

Moisture data was attained from the adjacent experimental sites of ongoing research by PhD student Gebeyehu Taye. Data logging theta probes were used for this purpose. These are soil moisture sensors that measure the volumetric soil moisture content, θv, by responding to changes in

the dielectric constant. Volumetric soil moisture content is the ratio between the volume of water present and the total volume of the sample. This is a dimensionless parameter, expressed either as a percentage (%Vol), or a ratio ($m^3.m^{-3}$). Data was viewed using DeltaLINK (version 2.6, 2011) software package from Delta T devices©.

$Area$

The **area** of each micro-plot was accurately calculated with simple measuring tapes (accuracy 1 mm). The four sides and diagonals of each micro-plot were measured and the cosines rule was applied (Figure 3.8). This was done to take into account that the corners are not always 90°. This is important for the calculations of runoff [l/m²] from each micro-plot.

The area of each micro-plot was calculated by the sum of the areas of its two triangles formed by their diagonal (Figure 3.8). Using the cosines rule (Figure 3.9) the area of both triangles was calculated. The sum of the areas is the area of the micro-plot. Both diagonals were measured so this could be performed twice. The average value was taken for further calculations.

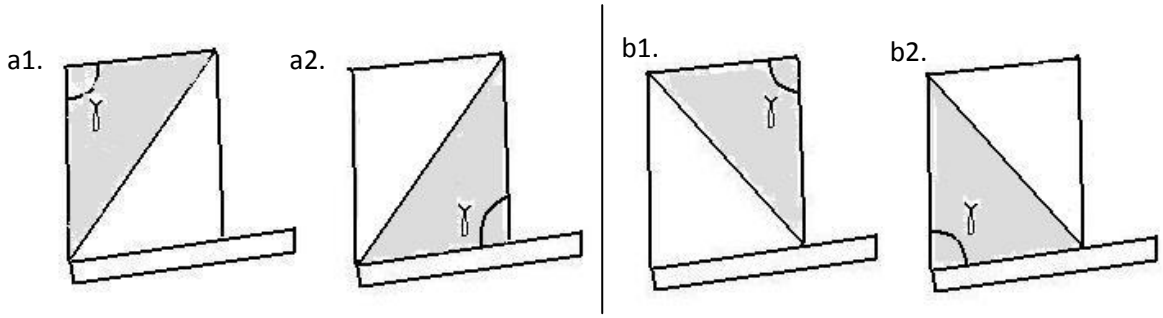

Figure 3.8 Calculation of the area micro-plots. The average area was calculated of (a1 + a2) and (b1 + b2)

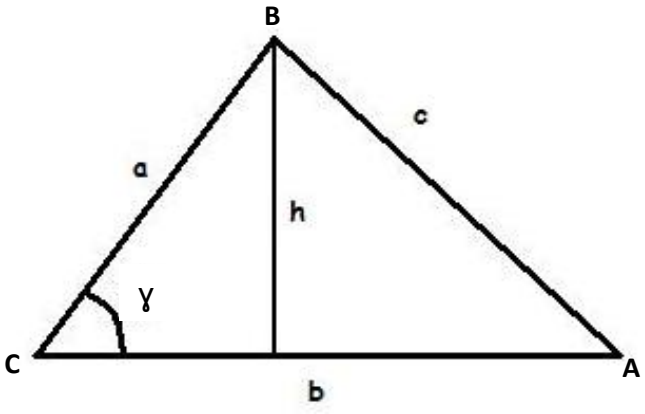

$$c^2 = b^2 + a^2 - 2ab\ \cos\ (\gamma)$$

$$Area\ \Delta ABC = \frac{b\ *\ h}{2}$$

$$h = a * \sin(\gamma)$$

Figure 3.9 Cosines rule applied for area measurements

Gaps – area exposed to direct rainfall

Any occurring **gaps** were also measured. A 'gap' is the area of gutter that was not fully covered by the gutter shed (Figure 3.3 and Figure 3.10), and thus exposed to direct rainfall. This is an important measurement for the abstraction of direct rainfall which would otherwise bias runoff measurements. The area was measured by looking perpendicular into the gutter (Figure 3.10). Some gutter sheds were bent upwards (Figure 3.10 - right) to avoid rainfall running from the gutter shed into the gutter which would lead to errors in runoff measurements that are less easy to quantify.

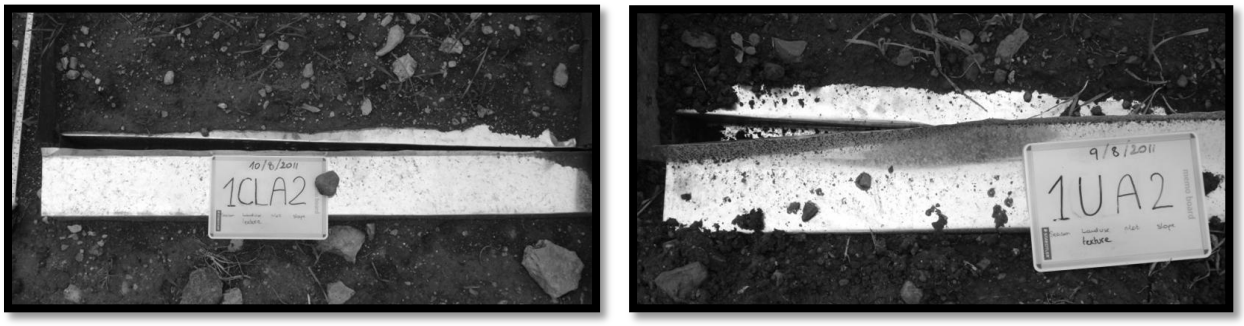

Figure 3.10 Example of gutter sheds that do not fully cover the gutter. Rainfall can directly enter the gutter and this can lead to errors in runoff measurements. Right: gutter was purposely bent to divert rainfall from running into the gutter

Slope

The **slope** was measured at each micro-plot with a clinometer that was integrated into a geological compass. This clinometer was placed on a flat object, levelled and the degrees were recorded. The slope in degrees was converted to percentage slope by taking the tangent {tan(degrees clinometer) = percent slope}. In some of the micro-plots slope was variable, an average value was taken.

Classification of slopes:

- Gentle slope: 0 - 8%
- Middle slope: 8 – 15%
- steep slope: > 15%

Figure 3.11 Slope measurement on flat object to smooth out the micro-relief

Soil surface roughness

The **soil surface roughness** was estimated for the cropland sites. This land use is ploughed before sowing. After ploughing, the micro-relief or roughness is likely to change significantly during the rainy season as a result of e.g. rain impact, runoff and wind. This soil surface roughness was measured using a similar approach to the pin method (García *et al*., 2008). Within the micro-plot a graded metal bar was placed orthogonal to the contour lines (which was also orthogonal to the plough marks). Using a measuring tape the distance from the metal bar to the soil was measured (Figure 3.12). This was done at a regular interval of 50 mm. The metal bar was 1 m long. This was initially done each week and towards the end of the rainy season every two weeks. The ruler was placed at the same position within the micro-plot each recording. Infiltration rates, surface runoff and erosion are a function of this roughness (van Wesemael *et al*., 1996). The data was analysed using the statistical index random roughness (RR). This is the standard error of individual elevations. Usually oriented roughness such as tillage marks and land slope are eliminate from this index. In this study they are not eliminated as they are of interest when considering the rainfall-runoff processes. This index was plotted against the cumulative rainfall.

Figure 3.12 Example of the measurement of soil surface roughness

Properties of the vegetation

Several varying properties of the vegetation were measured during the rainy season:

- Vegetation **height** on cropland sites using a simple measuring tape, initially two times every week and later in the rainy season weekly.
- The vegetation **cover** was monitored twice a week at the beginning of the rainy season and towards the end of the rainy season at least once a week. This was done by taking digital pictures and later analysing them using the pixel-analyzing software SigmaScan Pro® to determine the percentage of canopy cover. The digital photographs were taken using a Sony Cyber-shot digital camera with a resolution of 7.2 megapixels. SigmaScan Pro® is an automated

image analysis program. To calculate the canopy cover using this software the SigmaScan Macro 'Turf Analysis 1-2.BAS' (Karcher *et al*., 2005) was implemented. Photo's were rotated and cropped to select the area on the picture located within the 1 m² micro-plot. Appropriate hue and saturation thresholds were selected so the green canopy cover was marked (red) (add figure with canopy cover in red) and the soil not. Batch analysis was performed on each set of photos with identical threshold values. For each run the amount of pixels in every picture was recalculated, this is necessary as the photo's have been cropped individually and thus do not have the same amount of pixels. The canopy cover was calculated as the number of red pixels divided by the total number of pixels per picture and is expressed as a percentage. As the crop ages at the end of its growing period it turns more brown/yellow, this is lowers the percentage of vegetation cover calculated by Sigma Scan Pro®.

- **Weeding** practices are very variable. Generally weeds are destroyed during the preparation of the seedbed by **ploughing**. For wheat usually the soil is ploughed two times. Ox-drawn ard ploughs are used for this purpose. Weeding by hand is usually carried out two times during one growing period.
- A **seed rate** between 50 and 100 kg/ha is observed in the catchment, this amount is depending on the fertility of the soil. A larger seed rate is applied to a more fertile soil.
- If a **fertiliser** is applied, commonly 100 kg of Diammonium Phosphate (DAP) and 50 kg of Urea is used. These values are recommended by the Ministry of Agriculture. According to Corbeels *et al*. (2000) only 12% of farming households use mineral fertilisers. Manure and crop residues are also sometimes applied as nutrient inputs.

The use of these varying properties is to check their influence on the runoff coefficients throughout the growing season.

Rock fragment cover

The rock fragment cover is an important characteristic as it can influence the water movement and the nutrient status of the soil (van Wesemael *et al*., 2002). They also reflect the origin of the soil and the management of the soil depends on the abundance of rock fragments (FAO, 2006).

The **rock fragment cover** (%) of each micro-plot was analysed in three different ways:

- Using an early stage, low crop cover photograph of each micro-plot and analysing it using the same image analysis method as for the vegetation cover: '*photo method*'.

- By placing a grid on over the micro-plot with interval of 10 cm x 10 cm and at each intersection recording if there is a stone or not, subsequently the percentage of stone cover can be easily calculated: '*point method*'
- By using a graded metal bar of 1 m which is placed randomly in the micro-plot. The amount of centimetres stone can be added and expressed as a percentage of the graded metal bar. This was done three times on each micro-plot *'transect method'* (Poesen *et al*., 1998).
- Additional method: the proportion of stones in each micro-plot was visually estimated based on Figure 3.13. The abundance of rock fragments was compared with this chart and the corresponding percentage was used. This visual estimate is a very fast method but may be rather subjective for an inexperienced eye. Here it is used to cross check the values attained by the other methods.

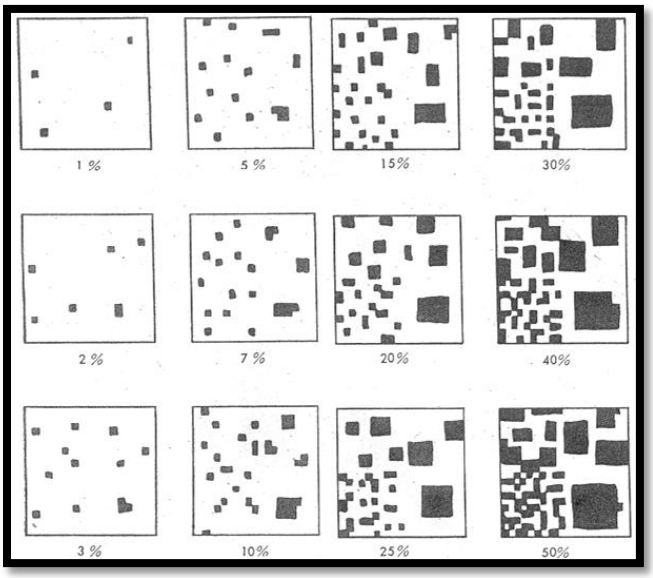

Figure 3.13 Chart for estimating proportions of coarse fragments and mottles, used to estimate the rock fragment cover on each micro-plot, (FAO, 2006)

The threshold diameter for a rock fragment was taken at ± 5 mm. The summarised methods were compared to see if there was a great variation between them, and the rock fragment percentages were investigated to see if there was an influence on the runoff coefficients.

Soil texture

The **soil texture** map of the Mayleba catchment, developed by Van de Wauw (2005), is not detailed enough to be used as a reference for the 1 m² micro-plots. Therefore the soil texture of each micro-plot was analysed. This was done by taking soil samples at each micro-plot, which gave three replicate soil samples per site. In the soil analysis laboratory at the Catholic University of Leuven (KULeuven) they were analysed. This was done with the Beckman Coulter LSI3 320, Laser diffraction particle size analyzer using multi wavelength.

The sample load was as little as 1 mg of soil. To retrieve a representative milligram of soil, preliminary preparation was necessary. First the soil sample was dried for 24 h in an oven at 65 °C and sieved (2 mm mesh). The soil sample was then ground using a pestle and mortar. Using a riffle box (Figure 3.14) the soil was divided into two compartments several times until there was only a small amount (± 1 mg) left. This 1 mg was placed in a test-tube with some demineralised water to suspend the soil sample. The test-tube was then placed on a hot plate at approximately 250°C until the mixture was boiling. This mixture was then used for the laser diffraction particle size analyser. No pre-treatment was performed as the chemicals are harmful for the analyser. When loading the sample into the analyser it passed a sieve with 0.5 mm mesh, the retained particles larger than 2 mm were removed by hand. What was left in the sieve (< 2 mm) was washed into the analyser with demineralised water and the sample was analysed.

Figure 3.14 Riffle box, used for unambiguous division of a soil sample into two compartments

Loizeau *et al.*, 1994 evaluated laser diffractometry. They found that the Coulter LS-100 underestimated the clay content of their samples relative to the classic sedimentation method: the underestimation increased with increasing clay content. Beuselinck *et al.*, 1998 looked further into this inconsistency and saw that it was only affecting the clay content, not the other soil texture size classes. This is interesting as the soils analysed here have a relatively high clay content.

The result of this analysis is a list of particle sizes classes with the corresponding frequency of occurrence, expressed as a percentage. These fractions can be grouped into sand, silt and clay classes. For this research the fractions were grouped as following (USDA, 2003):

Sand 63 µm – 2000 µm

Silt 2 µm – 63 µm

Clay < 2 µm

The soil texture was also determined using a **sedimentation method** (or decantation, Verachtert *et al.,* 2011). First the sample was prepared by removing carbonates with hydrochloric acid (HCl) and washed with demineralised water. A peptising agent (mixture of sodiumoxalate and sodiumcarbonate) was added to disperse the soil particles, the mixture was boiled and cooled. A wet sieving was performed to abstract the sand fraction (> 0.063 mm). The fraction that passed the sieve was collected in a 1 L column and complemented with demineralised water. At specific time intervals and at a specific depth samples were taken at room temperature. These samples were dried and weighed. This method is based on Stokes' law: the larger particles will settle first, and later the smaller particles.

$$v_s = \frac{2}{9}.g.r^2.\frac{\rho_s - \rho_w}{\eta}$$

v_s = the particles setting velocity (m/s)

g = gravitational acceleration (9.81 m/s²)

r = radius of the particle

ρ_s = mass density of the particles

ρ_w = mass density of the fluid (in function of the temperature)

η = viscosity

The soil texture was also determined by **finger test identification**, the scheme in Table 3.3 shows how this was done. This was a field exercise which is used to compare with the laser analysis and sedimentation results.

Table 3.3 Key to soil textural classes, used for field assessment of soil texture (FAO, 2006)

				~% clay
1	Not possible to roll a wire of about 7 mm in diameter (about the diameter of a pencil)			
1.1	not dirty, not floury, no fine material in the finger rills:	sand	S	< 5
	• if grain sizes are mixed:	unsorted sand	US	< 5
	• if most grains are very coarse (> 0.6 mm):	very coarse and coarse sand	CS	< 5
	• if most grains are of medium size (0.2–0.6 mm):	medium sand	MS	< 5
	• if most grains are of fine size (< 0.2 mm) but still grainy:	fine sand	FS	< 5
	• if most grains are of very fine size (< 0.12 mm), tending to be floury:	very fine sand	VFS	< 5
1.2	not floury, grainy, scarcely fine material in the finger rills, weakly shapeable, adheres slightly to the fingers:	loamy sand	LS	< 12
1.3	similar to 1.2 but moderately floury:	sandy loam	SL (clay-poor)	< 10
2	Possible to roll a wire of about 3–7 mm in diameter (about half the diameter of a pencil) but breaks when trying to form the wire to a ring of about 2–3 cm in diameter, moderately cohesive, adheres to the fingers			
2.1	very floury and not cohesive			
	• some grains to feel:	silt loam	SiL (clay-poor)	< 10
	• no grains to feel:	silt	Si	< 12
2.2	moderately cohesive, adheres to the fingers, has a rough and ripped surface after squeezing between fingers and			
	• very grainy and not sticky:	sandy loam	SL (clay-rich)	10–25
	• moderate sand grains:	loam	L	8–27
	• not grainy but distinctly floury and somewhat sticky:	silt loam	SiL (clay-rich)	10–27
2.3	rough and moderate shiny surface after squeezing between fingers and is sticky and grainy to very grainy:	sandy clay loam	SCL	20–35
3	Possible to roll a wire of about 3 mm in diameter (less than half the diameter of a pencil) and to form the wire to a ring of about 2–3 cm in diameter, cohesive, sticky, gnashes between teeth, has a moderately shiny to shiny surface after squeezing between fingers			
3.1	very grainy:	sandy clay	SC	35–55
3.2	some grains to see and to feel, gnashes between teeth			
	• moderate plasticity, moderately shiny surfaces:	clay loam	CL	25–40
	• high plasticity, shiny surfaces:	clay	C	40–60
3.3	no grains to see and to feel, does not gnash between teeth			
	• low plasticity:	silty clay loam	SiCL	25–40
	• high plasticity, moderately shiny surfaces:	silty clay	SiC	40–60
	• high plasticity, shiny surfaces:	heavy clay	HC	> 60

Note: Field texture determination may depend on clay mineralogical composition. The above key works mainly for soils having illite, chlorite and/or vermiculite composition. Smectite clays are more plastic, and kaolinitic clays are stickier. Thus, clay content can be overestimated for the former, and underestimated for the latter.

Coordinates

The **coordinates** of the micro-plots were obtained using a Trimble® GeoXT™ 2005 series GPS Receiver, which has great spatial accuracy. An accuracy of up to 50 cm can be achieved after post-processing with Trimble DeltaPhase technology. Using the installed TerraSync™ software, designed for fast and efficient field GIS data collection, coordinates were collected in the field. These coordinates were registered using the Adindan UTM zone 37 N coordinate reference system (CRS). The data collected with this GPS receiver was later combined with Quantum GIS 1.5.0 (Geographical Information System). These coordinates are presented in the micro-plot layout map (Figure 3.1).

3.2.2 Sub-catchment

The Mayleba catchment comprises several sub-catchments. A selection of these are equipped with automatic or manual runoff gauges. These are part of the experimental setup of an ongoing study by PhD student Daniel Teka. The manually obtained discharge data of a sub-catchment (MLRMT5) was provided for further consideration, see Figure 3.15. This data was used for a verification of the micro-plot results, as will be discussed in paragraph 3.3.

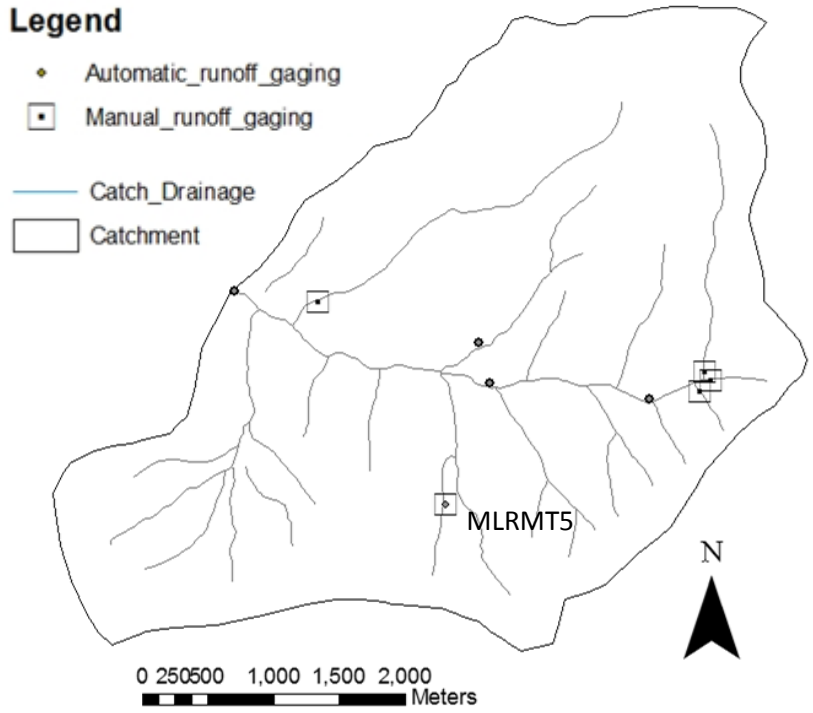

Figure 3.15 Location of the automatic and manual runoff gauges for recording discharge data of several sub-catchments in the Mayleba catchment

3.2.3 Catchment

To characterise the soils in the Mayleba catchment for their hydrologic properties the following field work was conducted.

11 parallel transects with a 45° NE-SW orientation were selected to cover the catchment. A total of 205 points were located along these transects, with 200 metres between each point along each transect and 300 metres between parallel transect lines (Figure 3.16). These points were divided into groups according to their soil texture. The soil texture classification map from Van de Wauw *et al*. (2008) was used for this purpose. This map contains four classes of soil texture: heavy clay, clay_silty clay, silty clay loam and loam_clay loam. These four groups of points in the catchment were each randomly shuffled using the open source software R (version 2.9.2). The top four sample points were chosen from each group. In total there were 16 sampling points, four sampling points of each of the four soil textures.

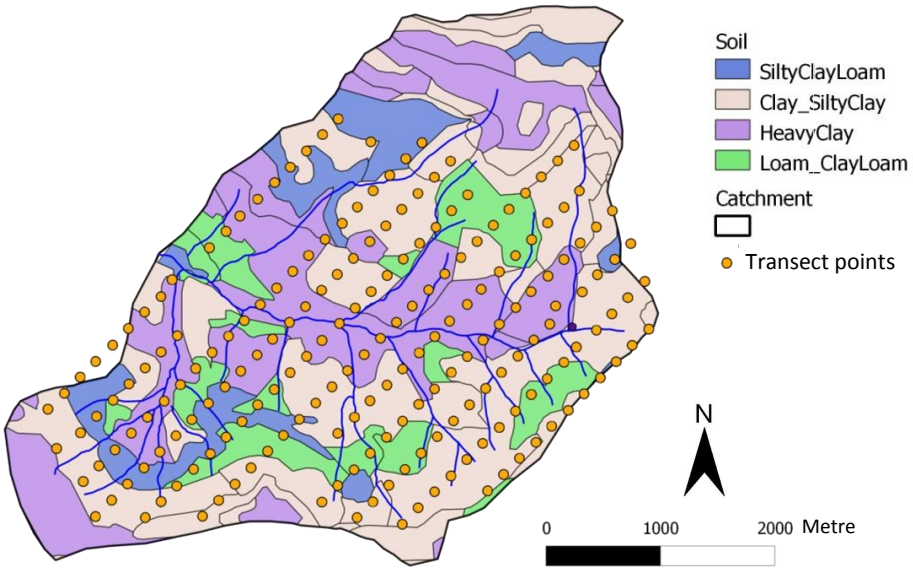

Figure 3.16 Transect points located in the Mayleba catchment. 300 metres between parallel transect lines, 200 metres between each point along each transect

At each sample point four undisturbed core samples of 100 cm^3 were taken using Kopecky rings (Eijkelkamp Agrisearch equipment). Sufficient disturbed sample and soil peds were also collected. These were taken for the following analyses in the soil laboratory of Mekelle University:

One Kopecky ring was taken for the determination of saturated soil water content and field capacity. The disturbed sample was used to determine the permanent wilting point.

- The **saturated soil water content** (SAT) was determined by protecting the core sample with a cotton cloth and saturating it on a sand plate. The samples were weighed at saturation point and again after drying at 105°C for 24 h. These weights are subtracted from each other and divided by the dry weight of the soil, multiplied by 100 to obtain the saturation.
- **Field capacity** (FC) was determined by placing the saturated core sample under 1/3 atmospheric pressure (0.33 bar) in pressure barrels. Once the sample reached equilibrium it was weighed again. The field capacity is the amount of soil moisture held in the soil after 0.33 bar has been applied and the soil moisture has come to equilibrium. The dry weight is subtracted from this equilibrium weight and calculations proceeded the same as for SAT.
- The **permanent wilting point** (PWP) was analysed with peds of soil that were put under 15 bar of pressure. The pressure was applied until equilibrium had been reached. The calculations proceeded the same as for SAT and FC.

SAT, FC and PWP were also estimated using the soil water characteristic equations developed by Saxton and Rawls (2006). A program has been developed for this purpose: SPAW Hydrology interface, Soil water characteristics, hydraulic properties calculator (version 6.02.74). It estimates the water holding capacities based on soil texture, organic matter, gravel content, salinity, and compaction. These values for SAT, FC and PWP (volumetric moisture content) are compared with the values attained from the laboratory analyses (gravimetric moisture content). A conversion between volumetric and gravimetric moisture content is possible using the bulk density of the soil and the bulk density of water.

The other Kopecky rings were used for bulk density analysis. This is determined by drying the core samples (24h at 105°C) and weighing the core samples. As a Kopecky ring has a precise volume of 100 cm³ the following simple calculation can be made, results are in [g/cm³]:

$$Bulk\ density = \frac{(oven\ dry\ core\ sample - kopecky\ ring\ weight)\ g}{100\ cm^3}$$

The rest of the soil that was taken from the sample point was used to analyse the texture by means of finger test identification and the Coulter laser particle distribution analysis method as discussed above. Also the land use and vegetation were observed. The outcome of these analyses were used to correlate with the soil texture map of Van de Wauw (2005).

At each point on the 11 transects the hydrological condition and condition of the soil and water conservation measures was recorded by M.Sc student Sylvain Trigalet, in August 2011. They were classed as Average/good or Worse/NA(no SWC). The above discussed Trimble GPS was used to locate these points.

3.3 Data processing

3.3.1 Micro-plots

Rainfall-runoff relationships

It is commonly assumed that the amount of runoff produced is a percentage of the rainfall depth, this percentage is called the runoff coefficient (RC) (Critchley, 1991):

$$Runoff\ [mm]\ =\ RC\ x\ Rainfall\ depth\ [mm]$$

For each rainfall-runoff (P/R) event the runoff coefficient was calculated. This is defined as the ratio of the total runoff depth to the total rainfall depth during one rainfall event (after Descheemaeker *et al*., 2006). Also the seasonal RC was calculated by dividing the cumulative runoff by the cumulative rainfall from all P/R events recorded during the rainy season of 2011.

The rainfall-runoff (P/R) data recorded throughout the rainy season of 2011 on the micro-plots was also analysed using regression analysis (Descheemaeker *et al*., 2006). An example is given in Figure 3.17. Per experimental site the regression was performed to establish P/R relationships for the different treatments. The runoff data from the three replicate plots was averaged (n = 3). From this regression the gradient (α) and precipitation threshold (P_T) were determined to use as descriptive values per experimental site. This gradient (α) gives an idea of the degree of runoff depth increase with increasing rainfall depth, after the precipitation threshold is exceeded.

To explore the influence of the vegetation cover on P/R relationships the P/R data was divided into two vegetation periods: < 30 % cover and > 30 % cover. This is an important cover percentage in conservation tillage. This is defined as any tillage/planting system which leaves at least 30 % of the field surface covered with crop residue after planting has been completed. Erosion is reduced by at least 50 % compared to bare soil if 30 % of the surface is covered with residue (Lal, 1997; Poesen *et al*., 1994). From these regressions the gradient (α) and precipitation threshold (P_T) were determined to use as descriptive values for both vegetation periods.

The influence of moisture on the P/R relationship was also investigated. This was done by grouping the P/R data into three classes according to their antecedent moisture content (Table 3.4).

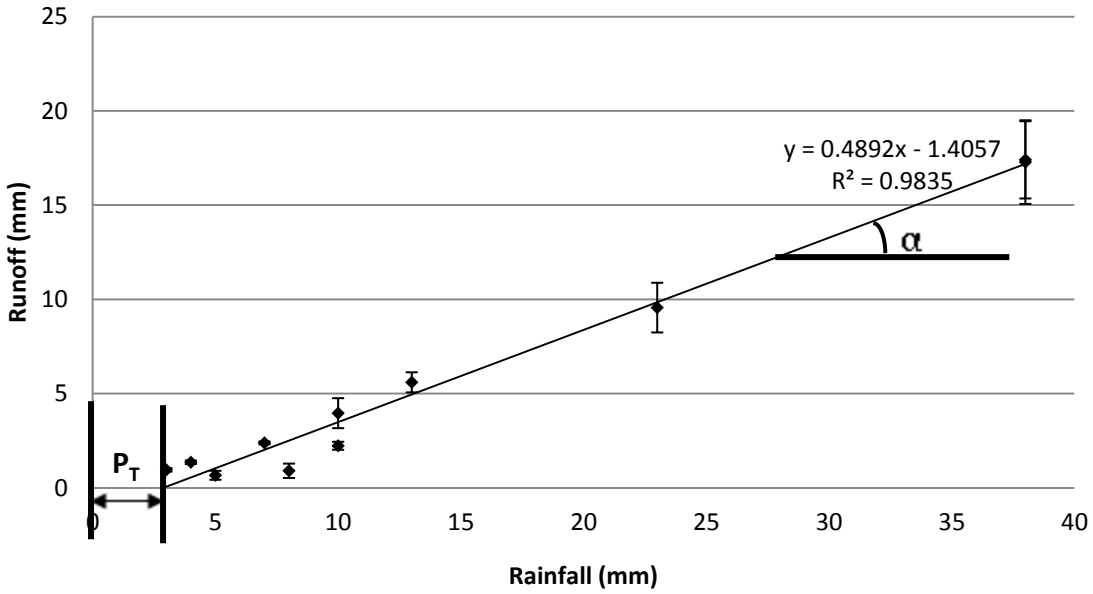

Figure 3.17 Illustration of regression of rainfall (mm) and runoff (mm) data. Trend line shows the gradient: α, and the intercept on the x-axis: P_T. Error bars show standard deviation (n = 3)

Table 3.4 Antecedent moisture condition (AMC) classes, based on the total rainfall in the previous five days

	Total rainfall in the 5 previous days (mm)	
AMC class	Dormant season	Growing season
I	< 12.5 mm	< 35 mm
II	12.5 - 27.5 mm	35 – 52.5 mm
III	> 27.5 mm	> 52.5 mm

Statistical analysis

Descriptive statistics were applied to describe the main features of the P/R data. These included both quantitative and visual methods such as calculation of mean, standard deviation, plotting of box- and whisker diagrams and correlation and regression analysis. The non-parametric Kruskal-Wallis test was used to check the significance of differences between treatments. These statistics were performed with SPSS 16.0 (SPSS Inc., 2007).

Partial least squares regression (PLSR) analysis was performed to check the influence of the measured characteristics of the micro-plots on the runoff production, α, and precipitation threshold, P_T. This method models a response variable by constructing new predictor variables, known as components. PLSR is one of the least restrictive multivariate extensions of the multiple linear regression model (Helland *et al.,* 1991). Analysis was performed in open source software R, version 2.14.2.

Runoff Curve Number

The runoff curve numbers (CN's) were calculated from the rainfall-runoff data recorded on the micro-plots. The Add-in, 'Solver', in Excel from Microsoft Office (2007) was used to facilitate this procedure (more information on the Solver can be found on the CD-ROM, see Appendix). The curve number method was created by the USDA-SCS (United States Department of Agriculture, Soil Conservation Service, currently called the Natural Resources Conservation Service, NRCS) which uses following equations (USDA-SCS, 1972; Hawkins *et al*., 2010):

$I_a = \lambda S$ (1)

If $P < I_a \rightarrow Q = 0$ (2)

If $P > I_a \rightarrow Q = \frac{(P-I_a)^2}{P-I_a+S}$ (3)

$CN = \frac{25\,400}{254+S}$ (4)

I_a is the initial abstraction [mm], **λ** is the initial abstraction ratio (= I_a/S) and often set to 0.20. **S** is a dimensionless storage parameter, **P** is precipitation [mm], **Q** is runoff [mm], and **CN** is the curve number.

In this study the initial abstraction ratio, λ = 0.05 is used. This value was obtained by Descheemaeker *et al*., 2008 from a study conducted near Hagere Selam, some 9 km from the Mayleba catchment. Also studies by Hawkins *et al*., 2002 found that a λ value of 0.05 provides a better fit. This mainly has an effect on calculations using lower rainfall depths or lower curve numbers.

To take the antecedent moisture condition (AMC) into account the rainfall during the previous 5 days is considered and three classes are defined (Table 3.4). This approach has been generalised by the ARC or Antecedent Runoff Condition, which is now applied by NRCS.

3.3.2 Sub-catchment

The boundary of the sub-catchment was defined using a digital elevation model (DEM raster GIS layer). Hec_GeoHMS (version 5.0) hydrological modelling software was used for this purpose. The obtained polygon was overlain with the soil texture map and land use map of Van de Wauw (2005).

The CN's deduced from the P/R measurements on the micro-plots are used to predict the runoff for the sub-catchment. The different units of the sub-catchment are derived by overlaying the sub-catchment polygon with the soil texture map and land use map of Van de Wauw (2005) as mentioned above. This was done using the 'Intersect' and 'Union' geo-processing tools in Quantum GIS (1.5.0). The predicted runoff is compared to the observed runoff for the same rainfall events. This is a verification step to check if the deduced CN's from micro-plot level are capable of predicting the runoff of a larger area.

To compare the observed runoff with the predicted runoff the root mean squared error (RMSE) was calculated. The formula used for this purpose is following:

$$RMSE = \sqrt{\sum_{i=1}^{n} \frac{1}{n} (Qobs - Qpred)_i^2}$$

Where **Qobs** is the observed runoff, **Qpred** the predicted runoff and **n** is the amount of observations

3.3.3 Catchment

By combining the data recorded at catchment scale with the findings from the sub-catchment and micro-plots, an up-scaling to catchment level is attempted. This was done by making classes based on the soil texture, land use, rainfall-runoff relationships, CN's, water holding capacities and hydrological condition. This is interesting to gain a broad idea of the hydrological characteristics of the catchment and progress towards a generalisation at catchment level.

Kriging was applied to make maps based on observations along the transect points. Kriging is a geostatistical tool that interpolates values from a random field in order to make values for unobserved locations based on observed data nearby (Govers *et al.*, 2011).

4 RESULTS AND DISCUSSION

4.1 Micro-plots

4.1.1 Characteristics

Area, gaps, slope

In Table 4.4 a summary of the micro-plot characteristics can be seen with the corresponding codes. The calculated area of each micro-plot and the size of the gaps are listed here ('gaps' are areas exposed to direct rainfall, used for runoff volume correction). The slope (%) is also in this table.

Soil surface roughness (SSR)

The random roughness (RR) was measured from ploughing until the end of the rainy season and plotted against the cumulative rainfall from the beginning of the main rainy season. In Figure 4.1 it can be seen that the decline of the RR is very fast during the first rainfall events after ploughing. These data are from the three different slopes on cropland sites with Bahakel (silty clay loam) soil. After ± 80 mm of rainfall the RR becomes more constant. There are still some variations where the RR slightly increases or decreases. This may be a result of placing the metal bar at a slightly different position within the micro-plot and/or due to vegetation growth. Towards the end of the season the vegetation cover was denser and taller which made the measurement of the RR more difficult. No clear trend can be seen between the different slope classes Figure 4.1. In micro-plots with high rock fragment cover (such as CL3 with many large rocks) the rock fragments were avoided when placing the metal bar for RR measurements, therefore it is not reliable to draw any conclusions for the possible effect of rock fragments on the RR development. Soils covered by rock fragments do not usually follow the frequently assumed exponential decrease of RR (van Wesemael *et al*., 1996).

In Figure 4.2 there is no clear trend found for RR. This data is from sites U2 and W2, these are cropland sites on resp. Andelay (loam, large fraction of small rock fragments) and Walka (silty clay, low rock fragment cover). For these sites the measurements of RR started later, approximately 20 days after ploughing had been completed. As can be seen, a cumulative rainfall of 280 mm was already reached at the time of the first measurements. Most likely this was too late to capture the main decrease in random roughness.

An indication value of RR was chosen to describe the effect on rainfall-runoff relationships. This value was taken at 280 mm cumulative rainfall, as there is data for this point and the RR is relatively constant throughout the rest of the rainy season after this point. This indication value is shown in

Table 4.4. It is expected that a higher RR will increase infiltration and postpone the runoff initiation due to increased ponding (Descheemaeker *et al*., 2006).

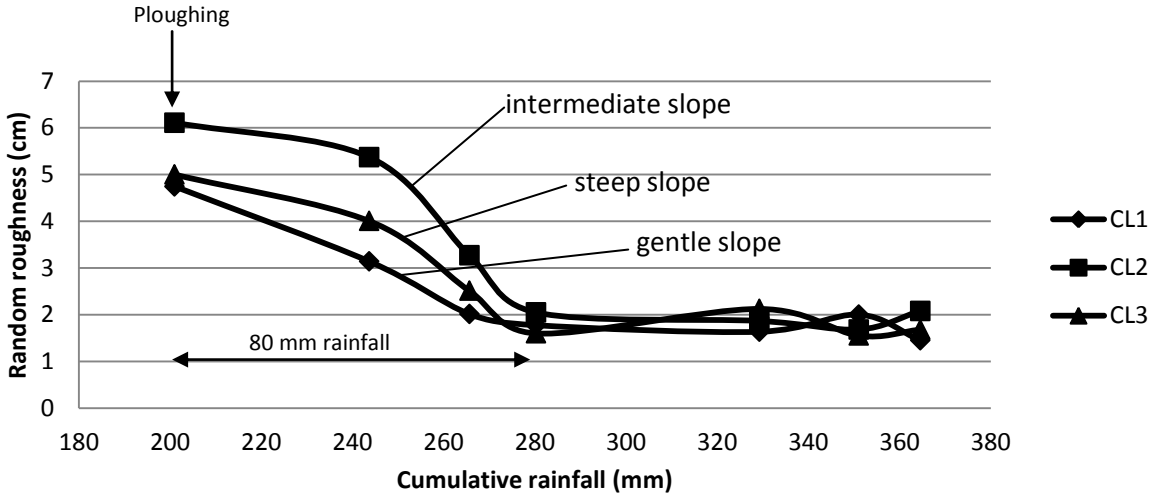

Figure 4.1 Random roughness of experimental sites on Bahakel (silty clay loam) soil, land use cropland, for three different slopes. CL1: gentle slope, CL2: intermediate slopes, CL3: steep slope.

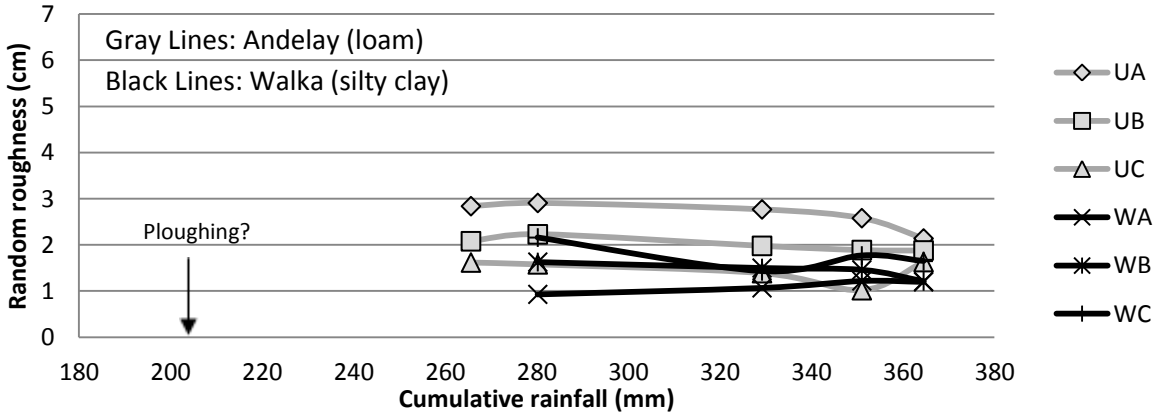

Figure 4.2 Random Roughness for the three replicates (A, B and C) of both Walka (W, silty clay) and Andelay (U, loam). Land use: cropland. Slope class: intermediate. Axes are set to same values as those in Figure 4.1.

Vegetation height

On the five cropland sites the vegetation height of wheat (sometimes intercropped with barley) was measured from 10 August to 16 September 2011 (Figure 4.3). The planting date of the cropland sites were similar, all sown towards the end of the second decade of July. It seems that the crops had not yet reached their maximum height during the last measurements on 16 September as the curves are still increasing and not yet levelling off or declining. The Walka (silty clay) experimental site has the tallest wheat plants, this is also the more fertile soil compared to the other experimental sites. It has a higher clay content and thus better water holding capacities. It also holds nutrients better (Ismail *et al*., 2007). Based on its darker colour it is also likely have a higher organic matter content. Further, It

can be noticed that the vegetation height of the cropland steep slope (CL3) site is taller than the two other slopes on the same soil (see dotted lines in Figure 4.3). Also the cropland middle slope (U2) has a high vegetation cover, its soil texture is lighter than the CL1, CL2 and CL3 sites and it is derived from displaced basaltic material. The other experimental sites were developed on limestone. The CL3 and U2 sites also have the highest rock fragment cover, this could be correlated with vegetation height, due to the positive effects of rock fragments on the water balance (van Wesemael *et al*., 2002). On the grazing land sites grass was present, this grass was always short, between 4 and 6 cm.

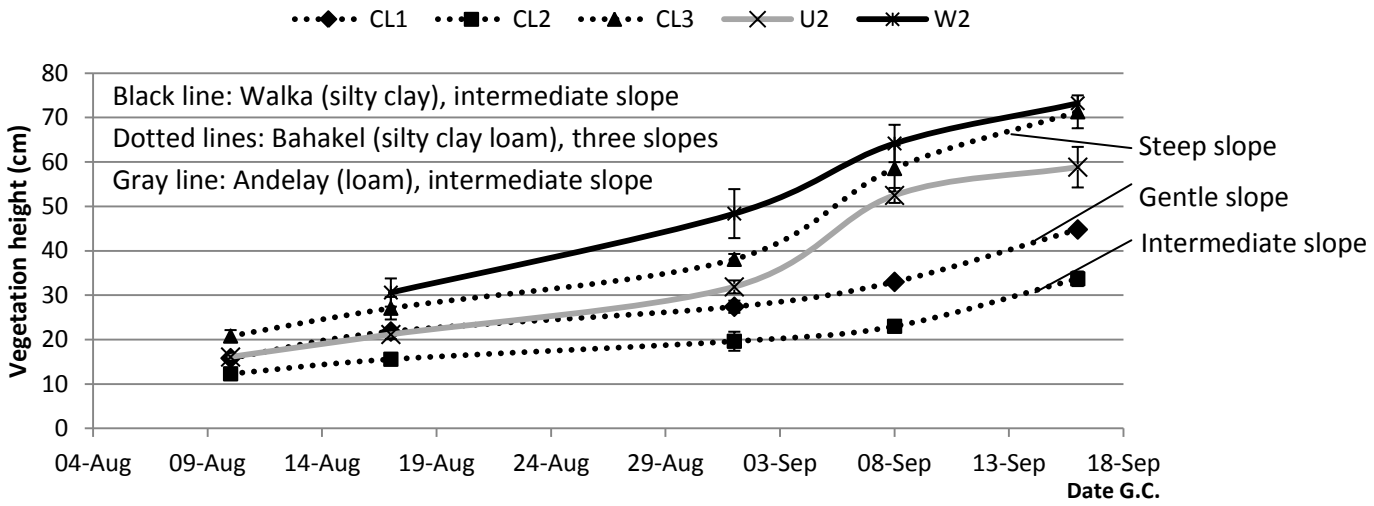

Figure 4.3 Vegetation height (cm) for the five cropland sites, in function of time.
Measured during the main rainy season of 2011. Error bars show standard deviation (n = 3). CL: Cropland on Bahakel, U: Cropland on Andelay, W: Cropland on Walka. Slope class 1: Gentle slope, 2: Middle slope, 3: Steep slope.

Photo's of the CL2B (cropland, intermediate slope, replicate B) micro-plot are shown in Figure 4.5. The photo on the right is a view on the vegetation height. It is taken from a perspective across the field, close to the ground. The photo on the left is a photo taken from the top-down perspective, used for vegetation cover calculation.

Vegetation cover

In Figure 4.4 the expansion of the vegetation cover, expressed in percentage, can be seen for all the experimental sites from 20 July until 16 September 2011. The vegetation cover on grazing land is more constant than that on cropland. By the end of the growing period the cropland had a higher vegetation cover than the grazing land. This is an important factor concerning erosion, more important than the vegetation height. A constant vegetation cover is desirable, preferably higher than 30% cover. This 30% threshold is attained by the grazing land steep slope site (GL3) but not by the two other slopes on grazing land. From mid August onwards the cropland sites surpass the 30% threshold.

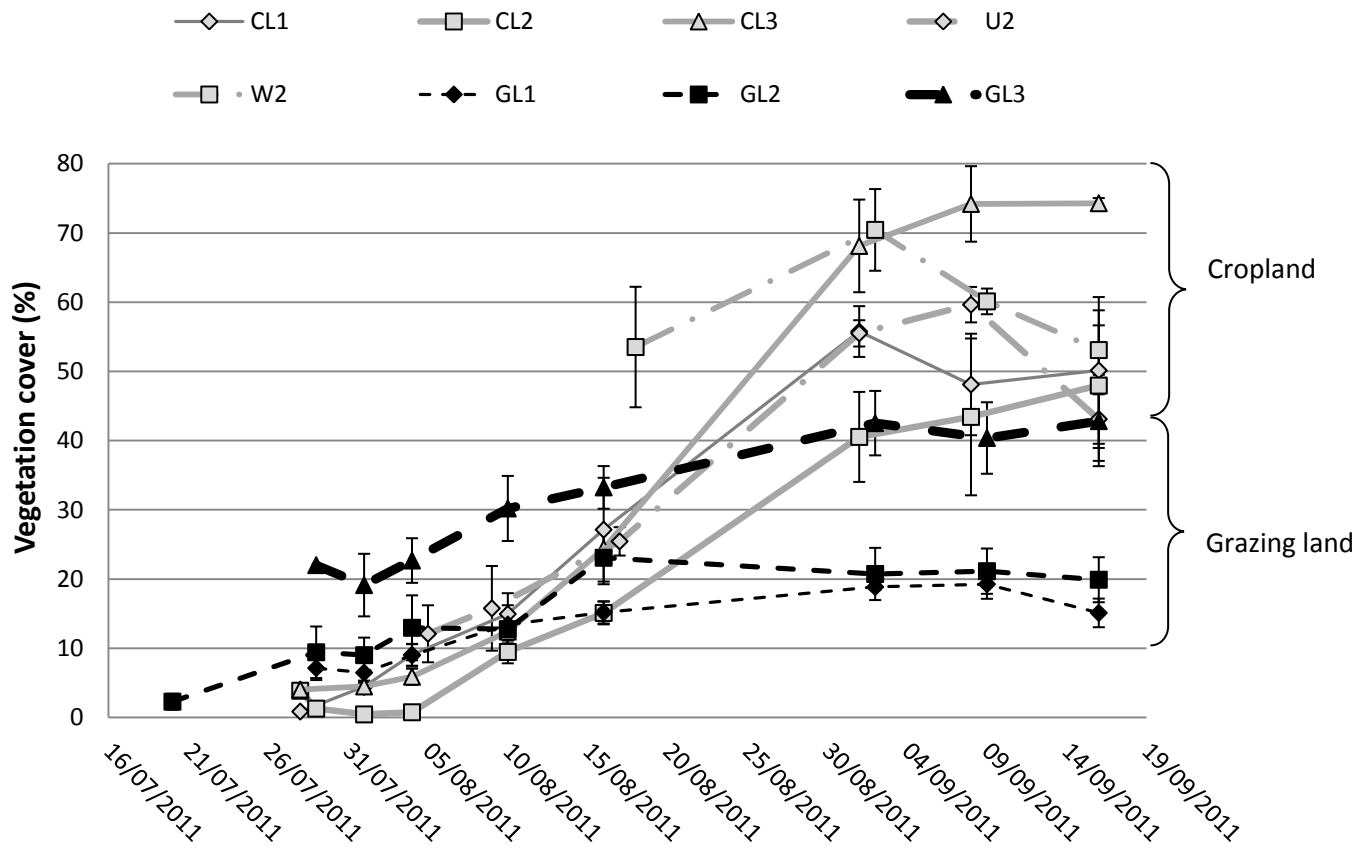

Figure 4.4 Vegetation cover in % for the eight experimental sites during the main rainy season of 2011, black dashed lines indicate grazing land, gray line (full and dash-dot) indicate cropland. Error bars show standard deviation (n = 3).
CL: Cropland on Bahakel, GL: Grazing land on Bahakel, U: Cropland on Andelay, W: Cropland on Walka. Slope class 1: Gentle slope, 2: Middle slope, 3: Steep slope.

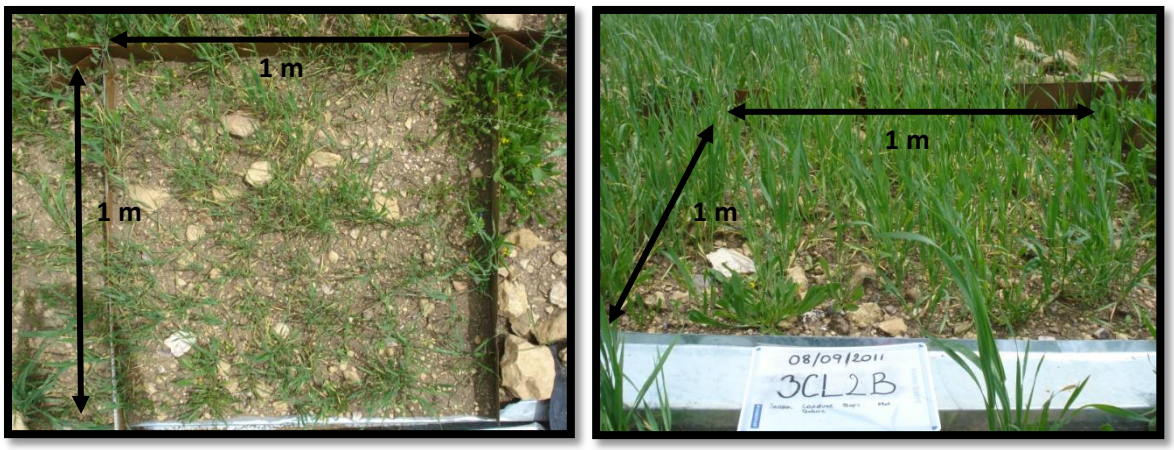

Figure 4.5 Photo's of micro-plot CL2B (cropland, Bahakel soil, intermediate slope, replicate B). Left is an example of a photo used for vegetation cover calculation. Right is the same micro-plot but taken from a different angle to show the vegetation height. Both photo's taken on 8 September 2011

Rock fragment cover

The rock fragment cover percentage could not be obtained from the photographs in the same manner the vegetation cover was obtained using SigmaScan Pro®. The rock fragment cover was largely covered by a thin layer of soil which gave it the same colour as the soil (see example in Figure 4.6). This hindered the analysis, based on saturation and hue differences, and it was not achievable to clearly distinguish the stones from the soil accurately.

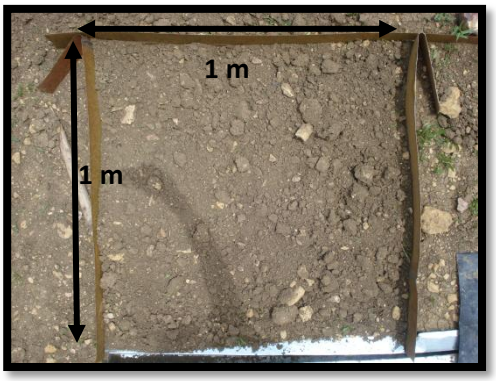

Figure 4.6 Example of a photograph used for image-analysis to determine the rock fragment cover. The rock fragment was not distinguishable from the soil using this image analysis technique based on saturation and hue. Thus the rock fragment cover estimation using the 'photo-method' was not possible.

The results of the point-method and transect-method used to estimate the rock fragment cover are shown in Table 4.1. It can be seen that the transect-method consistently gives a lower estimation of rock fragment cover than the point-method. An average of 7% lower cover estimation was observed. Further, the rock fragment cover was also estimated using the chart in Figure 3.13, these results are also presented in Table 4.1, in the last column. Results of these three methods and the averages are shown in Figure 4.7.

In literature the rock fragment cover shows various positive and negative effects. They can positively affect the biomass production by holding the soil moisture during moderate water stress. They can preserve the surface roughness and depending on the rainfall intensity they can lower runoff. These effects depend on the percentage of rock fragments present and the size of the rock fragments. At micro-plot scale of 1 m² the rock fragment cover has a positive effect on erosion control. The 30% threshold can be applied to this rock fragment cover (Poesen *et al*., 1994; van Wesemael *et al*., 2002). Only the CL3 and U2 experimental sites are in the 30% range of rock fragment cover. CL3 is characterised with large rock fragments and U2 by cobbles. The average rock fragment cover percentage of these three methods was used in the further analysis, also presented in Table 4.4.

Table 4.1 Summary of rock fragment cover percentages measured with the point-method and the line-transect method. The visual estimations are in the last column.

Site	Method	Replicate A	Replicate B	Replicate C	Average	STDEV	Difference between methods	Visual Estimate
CL1	point-method	14%	6%	11%	**10%**	4	4%	**6%**
	transect-method	5%	5%	8%	**6%**	2		
CL2	point-method	22%	26%	24%	**24%**	2	8%	**22%**
	transect-method	13%	18%	19%	**16%**	3		
CL3	point-method	43%	34%	37%	**38%**	5	4%	**42%**
	transect-method	41%	27%	35%	**34%**	7		
GL1	point-method	22%	34%	18%	**24%**	8	10%	**15%**
	transect-method	11%	12%	19%	**14%**	5		
GL2	point-method	34%	20%	27%	**27%**	7	8%	**17%**
	transect-method	21%	18%	18%	**19%**	2		
GL3	point-method	24%	28%	35%	**29%**	5	14%	**22%**
	transect-method	13%	18%	15%	**15%**	2		
U2	point-method	28%	36%	34%	**33%**	4	5%	**25%**
	transect-method	21%	30%	33%	**28%**	6		
W2	point-method	8%	7%	6%	**7%**	1	2%	**3%**
	transect-method	6%	4%	5%	**5%**	1		
Average of the differences							7%	

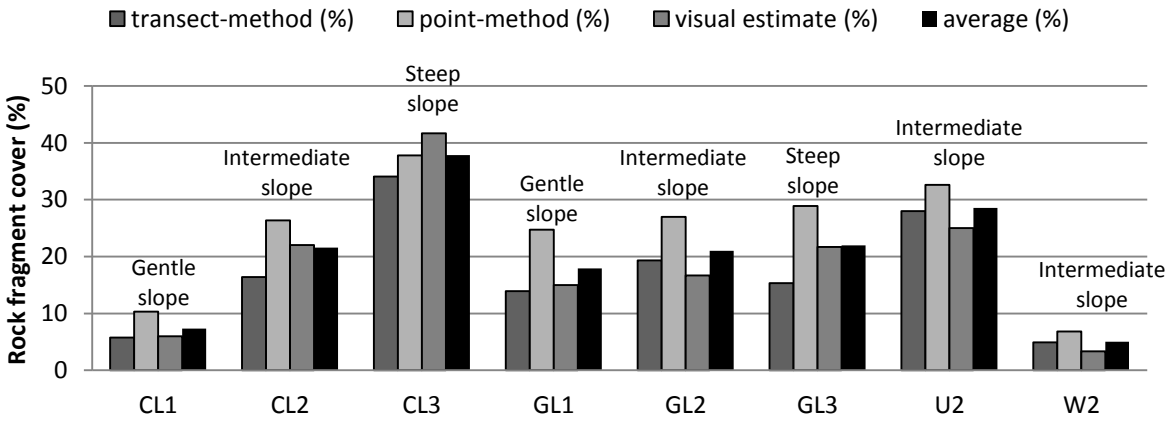

Figure 4.7 Histogram of the rock fragment cover percentages retrieved from the three methods used. Also the average of the three methods is presented in the histogram.
CL: Cropland on Bahakel (silty clay loam), GL: Grazing land on Bahakel (silty clay loam), U: Cropland on Andelay (loam), W: Cropland on Walka (silty clay). 1: Gentle slope, 2: Middle slope, 3: Steep slope

Soil texture

The soil texture was determined on the eight experimental sites using the laser diffractometry method, the sedimentation method and the finger test identification method.

According to the soil texture map of Van de Wauw (2005) the three grazing land sites are on a silty clay loam soil texture, as are three of the cropland sites. The other two experimental sites are on a loam/clay loam and a heavy clay soil texture (Table 4.2).

Table 4.2 Soil texture, parent material and soil of the eight sites according to Van de Wauw, 2005.
CL: Cropland on Bahakel, GL: Grazing land on Bahakel, U: Cropland on Andelay, W: Cropland on Walka. 1: Gentle slope, 2: Middle slope, 3: Steep slope

Site	Soil texture	Parent material	Soil
GL1, GL2, GL3	Silty Clay Loam	Limestone	(Colluvic) (Calcaric) Regosol
CL1, CL2, CL3	Silty Clay Loam	Limestone	Calcaric Cambisol
U2	Loam/Clay Loam	Basalt	Leptosol
W2	Heavy Clay	Limestone	Calcaric Vertisol

Using the laser diffractometry method for soil texture analysis, each soil sample from the eight sites returned the same soil texture: silty loam. Three replicate soil samples were taken at each site. As mentioned in the methodology, Loizeau *et al*. (1994) and Beuselinck *et al*. (1998) evaluated the laser diffractometry method and found that it underestimated the clay content. It must be noted that the samples were not subject to any pre-treatment to disperse the particles, to remove organic matter nor to remove carbonates. However, the soils developed on limestone have a high $CaCO_3$-content which could bias the analysis. The cementation of particles by $CaCO_3$ and presence of small weathered limestone particles are amongst the reasons for the obtained result. The samples were boiled in demineralised water, but this may not have been sufficient to disperse the particles. The pre-treatment was not possible as the necessary chemicals could damage the analyser.

Using the sedimentation method the samples were pre-treated with hydrochloric acid (HCl) to remove carbonates. A peptising agent was added to disperse all particles. Organic matter was not removed. The U2 experimental site (cropland, loam, intermediate slope) did not contain any carbonates as it did not react with HCl. These soils are derived from the displaced basaltic material mentioned in Figure 2.6. The other sites contained a high content of carbonates, these soils are derived from limestone. The sedimentation method however shows very little variation in soil texture between sites. All samples returned a silty loam soil texture. As the organic matter was not removed with H_2O_2, this could have biased the texture measurement due to the aggregation of silty organic material particles with clay particles forming larger micro-aggregates.

The results of the finger test identification method correlated best with the soil texture map of Van de Wauw (2005) and the opinion of the local farmers (Table 4.2). This method is fast and inexpensive, only some water is necessary to wet the soil. The more experienced in this method, the more detailed the soil texture can be determined. Notice that smectite clays can feel more plastic and give overestimations of clay content (FAO, 2006). Results are presented in Table 4.3. Noticeable was that the steeper slopes had a more sandy feel. Clay particles are carried away more easily than sand and the finer particles are deposited on lower, more gentle slopes. The more sandy feel can also be explained by the cementation of particles by $CaCO_3$ and small weathered limestone particles. Also,

the samples were always taken from the top soil which is usually has a lighter soil texture (Van de Wauw, 2005).

The variations of soil texture in these results are small, all the observed soil textures are situated centrally in the soil texture triangle. Van de Wauw (2005) recorded much higher clay percentages in the Mayleba catchment using the pipette and sieve-method (n.n., 2004). All previously mentioned pre-treatments were applied before analysis, including the removal of organic matter. For further analysis the soil texture as listed in Table 4.3 is used.

According to the local farmers the soil types at the eight sites were Bahakel, Andelay and Walka (Table 3.1, Table 4.3). The colour of the Bahakel soil at the grazing land sites (GL1, GL2 and GL3) was more yellow than the brown colour of the same soil at the cropland sites (CL1, CL2 and CL3). The Walka soil was dark brown, and the Andelay soil was gray (Figure 4.8). If the observations are compared with the characteristics of the soil types listed in Table 3.1 some differences can be noticed in colour and soil texture. In this case, the Andelay soil has a lighter soil texture than the Bahakel soil and a lighter colour than the Bahakel soil on cropland. The other characteristics correspond well between the observations made and the local farmers' information.

Table 4.3 Soil texture of the eight experimental sites, determined by finger test identification. The soil type according to local farmers is listed in the last column.
CL: Cropland on Bahakel, GL: Grazing land on Bahakel, U: Cropland on Andelay, W: Cropland on Walka. 1: Gentle slope, 2: Middle slope, 3: Steep slope

Site	Soil texture	Local soil type
CL1	Silty Clay Loam	Bahakel
CL2	Sandy Clay Loam	Bahakel
CL3	Sandy Clay Loam	Bahakel
GL1	Silty Clay Loam	Bahakel
GL2	Silty Clay Loam	Bahakel
GL3	Sandy Clay Loam	Bahakel
U2	Loam	Andelay
W2	Silty Clay	Walka

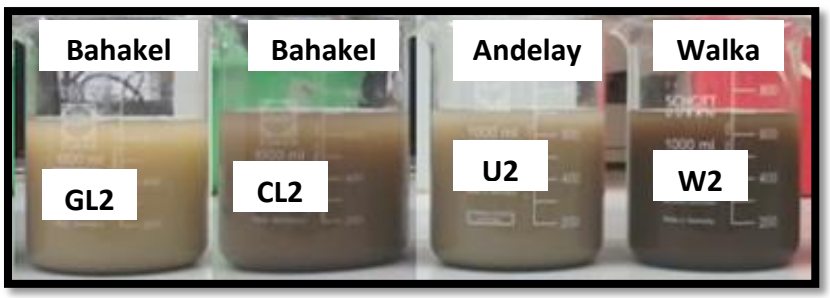

Figure 4.8 Colour of the soil texture after carbonate removal and dispersion.
CL: Cropland on Bahakel, GL: Grazing land on Bahakel, U: Cropland on Andelay, W: Cropland on Walka. 1: Gentle slope, 2: Middle slope, 3: Steep slope.

Table 4.4 Summary of the micro-plot characteristics

	Land use	Slope class	Replicate	Site code	Micro-plot code	Area (m²)	Gaps[1] (cm²)	Slope (%)	Indicator RR (%)[2]	Veg. height max. (cm)	Veg. cover max. (%)	Rock fragment cover (%)	Soil texture
To see effect of land use & slope	Cropland	1	A	CL1	CL1A	0.9512	5	6.1	2.02	45.0	59.9	14	Silty clay loam
			B		CL1B	0.8859	64	4.4	1.58	44.4	56.7	6	Silty clay loam
			C		CL1C	0.9485	44	4.4	1.73	45.0	51.7	11	Silty clay loam
		2	A	CL2	CL2A	1.0034	225	12.8	1.56	31.8	47.1	29	Sandy clay loam
			B		CL2B	0.9948	322	14.9	1.96	34.7	38.3	26	Sandy clay loam
			C		CL2C	1.006	223	13.2	2.63	34.6	59.7	24	Sandy clay loam
		3	A	CL3	CL3A	0.8723	0	17.6	1.72	74.6	80.5	43	Sandy clay loam
			B		CL3B	0.9461	52	21.7	0.96	72.0	73.8	34	Sandy clay loam
			C		CL3C	0.8275	50	17.6	2.13	67.3	73.9	37	Sandy clay loam
	Grazing land	1	A	GL1	GL1A	0.8763	0	5.7	/	4	19.8	22	Silty clay loam
			B		GL1B	0.9568	0	7.9	/	4	18.8	34	Silty clay loam
			C		GL1C	0.8861	0	6.1	/	4	21.1	18	Silty clay loam
		2	A	GL2	GL2A	0.9882	547	13.2	/	5	24.2	34	Silty clay loam
			B		GL2B	0.9526	233	13.2	/	5	23.2	20	Silty clay loam
			C		GL2C	0.9561	303	12.3	/	5	19.2	27	Silty clay loam
		3	A	GL3	GL3A	0.9247	0	22.2	/	6	47.2	24	Sandy clay loam
			B		GL3B	0.9743	0	16.3	/	6	39.8	28	Sandy clay loam
			C		GL3C	0.8517	45	15.8	/	6	44.0	35	Sandy clay loam
To see effect of soil texture	Cropland	2	A	U2	U2A	0.8609	84	8.7	2.91	55.9	58.6	28	Loam
			B		U2B	0.8573	0	8.7	2.23	56.5	62.6	36	Loam
			C		U2C	0.9433	0	13.2	1.58	64.1	57.8	34	Loam
		2	A	W2	W2A	0.9263	0	14.9	0.93	77.3	65.4	8	Silty clay
			B		W2B	0.9169	0	7.9	1.63	73.5	76.9	7	Silty clay
			C		W2C	0.9039	0	14.9	2.16	68.9	69.0	6	Silty clay

Clarification of abbreviations: Each micro-plot has a code with structure **XYZ. X**: Type of land use and soil texture (CL: Cropland on Bahakel, GL: Grazing land on Bahakel, U: Cropland on Andelay, W: Cropland on Walka). **Y**: Slope classes (1: Gentle slope 0% - 8%, 2: Middle slope 8% - 15%, 3: Steep slope >15%). **Z**: Distinction between the 3 replicates (A: Most to the east, B: Middle plot, C: Most to the west)

[1] area exposed to direct rainfall

[2] Random Roughness (RR), not measured on grazing land

4.1.2 Rainfall-Runoff relationships

Volume-depth relation

To correlate the depth of runoff measured in the buckets (in centimetres), to the corresponding volume of runoff (in liters), a volume-depth relation was established (Figure 4.9). The bucket was not a cylinder, but a cone shape, therefore this relation is parabolic.

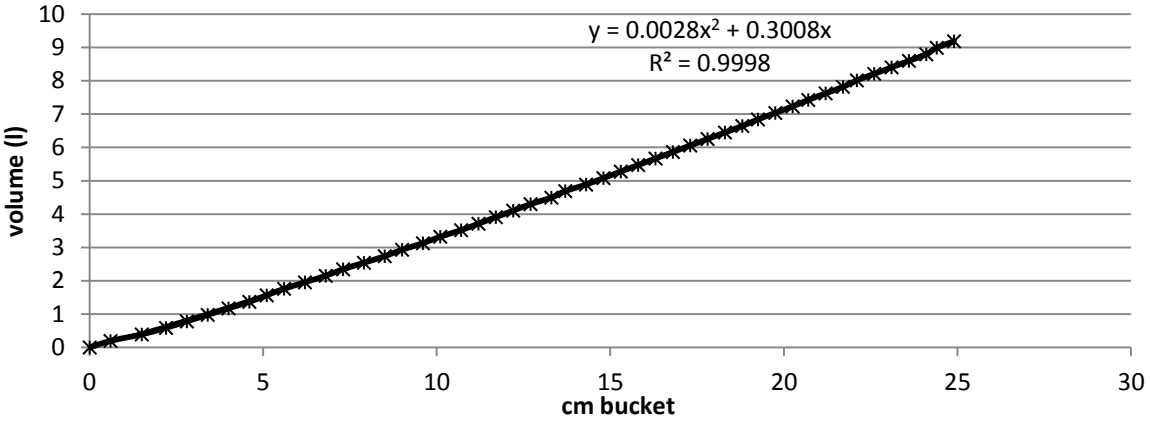

Figure 4.9 volume-depth relation of runoff measured in the buckets (in centimetres), to the corresponding volume of runoff (in litres)

The volume of rainfall that directly entered the gutter through the gaps was subtracted from the collected runoff volume in the bucket. This volume was then divided by the exact area of each micro-plot [l/m²]. As 1 l/m² = 1 mm, the rainfall in mm can be compared to the runoff in mm. The micro-plot areas and gap areas of each micro-plot are listed in Table 4.4.

Rainfall

The daily and cumulative rainfall measured in the Mayleba catchment from 08/05/11 to 25/09/11 can be seen in Figure 4.10. A frequency analysis was performed by Descheemaeker *et al*. (2009) in RAINBOW (Raes *et al*., 2006) using 20 years of annual rainfall data from Hagere Selam. The total rainfall during the main rainy season (*Kiremt*) from June 2011 to September 2011 was ± 460 mm. If 80% of the yearly rainfall is expected to fall during this rainy season then this rainy season can be classified as an abnormally dry year. Remarkable is the occurrence of an extreme rainfall event of > 60 mm/day on 30 July (Figure 4.10).

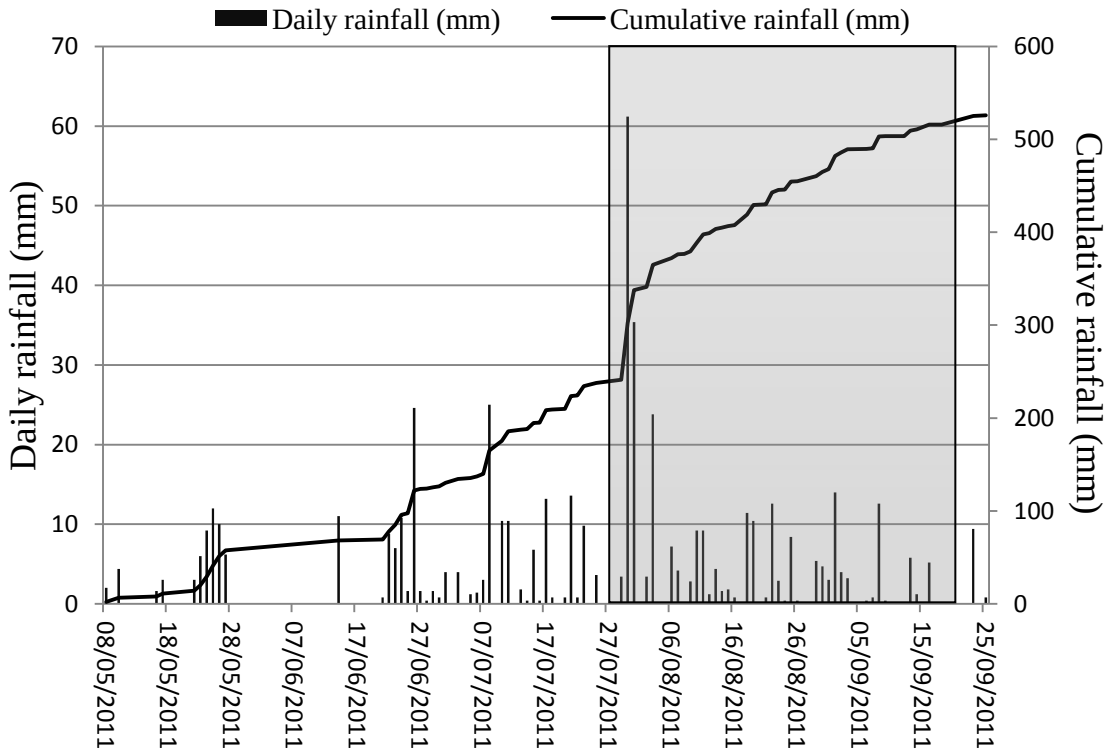

Figure 4.10 Daily rainfall (mm) measured in the Mayleba catchment from 08/05/11 to 25/09/11. The gray zone is the indication of the period that rainfall-runoff data was collected for this study.

Instantaneous Rainfall-Runoff Relationships

The rainfall and runoff was measured every three minutes during most rainfall events from 28 July to 23 September. It was expected that the rainfall- and runoff-intensities could be plotted in time and that graphs similar to the one in Figure 4.11 could be attained. The 'net rainfall' (**N**) is the amount of rainfall that produces runoff. The 'rainfall losses' ($\mathbf{L_c}$) are due to depression storage and infiltration. Also interception, wetting losses and evaporation are potential losses. The initial abstraction is indicated with '$\mathbf{I_a}$'.

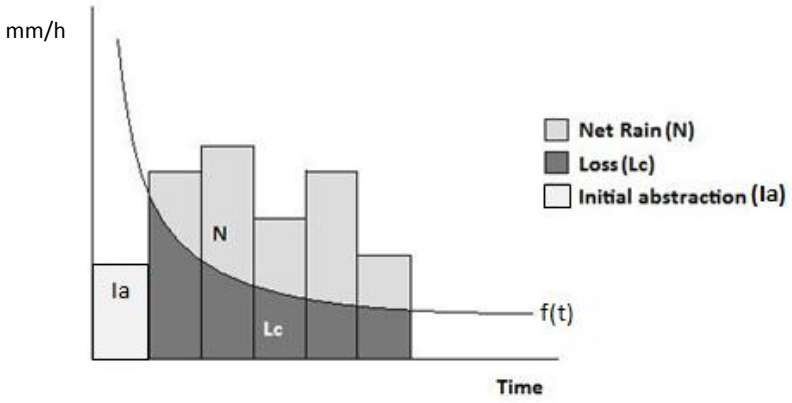

Figure 4.11 Rainfall-runoff model, the net rainfall is the amount of rainfall that produces runoff, the rainfall loss is the fraction of rainfall that did not produce runoff due to losses such as infiltration and depression storage. The curve between net rainfall and rainfall loss is the infiltration rate (mm/h).

When plotting the observations in function of time the result was not as evident as anticipated (see example in Figure 4.12). Such plots were made for a selection of long lasting rainfall events with high total rainfall. The rainfall-runoff event in example Figure 4.12 had a total rainfall depth of 34 mm and a rainfall duration of 2h21min. The rainfall intensity is very variable (0 mm/h to 40 mm/h) and not intense enough to support a constant infiltration rate. Also the error on rainfall and runoff depth over an interval of 3 min is extrapolated to [mm/h] by multiplying by 20, this multiplies the error. Therefore it was not possible to derive the final infiltration rate from such data. When the data was grouped over 9 minutes, 12 minutes or 15 minutes to attain more constant rainfall intensities there was still no clear trend observed.

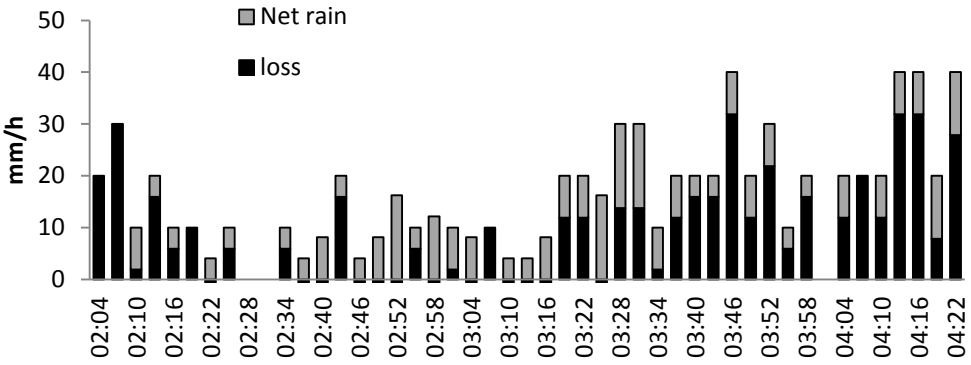

Figure 4.12 Example of rainfall-runoff relationship for a P/R event on CL3 (cropland, steep slope) site 30 July from 2:01 PM to 4:22 PM, total rainfall 34 mm.

Due to the high variability in instantaneous P/R data, the event P/R data was used for further analysis using the regression method. This is the total rainfall depth during a rainfall event and the corresponding total produced runoff (Descheemaeker *et al.*, 2006).

Rainfall-Runoff data per treatment

All event P/R data that produced > 0.5 mm runoff was grouped and regression analysis was performed per experimental site. An example for the GL1 site (grazing land, gentle slope, silty clay loam soil texture) can be seen in Figure 4.13. All the data and graphs of the other experimental sites can be found on the CD-ROM (for copyright reasons available upon request). Contents of the CD-ROM are listed in the Appendix.

The gradients, α, and the precipitation thresholds, P_T, of the regressions of the eight experimental sites are assembled in Table 4.5, Figure 4.14 and Figure 4.15. A higher alpha implies a higher runoff response to rainfall. The number of observations is very low for the U2 site (n = 12), also there are two outliers recorded from micro-plot replicate U2A (visualised with box- and whisker-plot). As indicated by a large error bar.

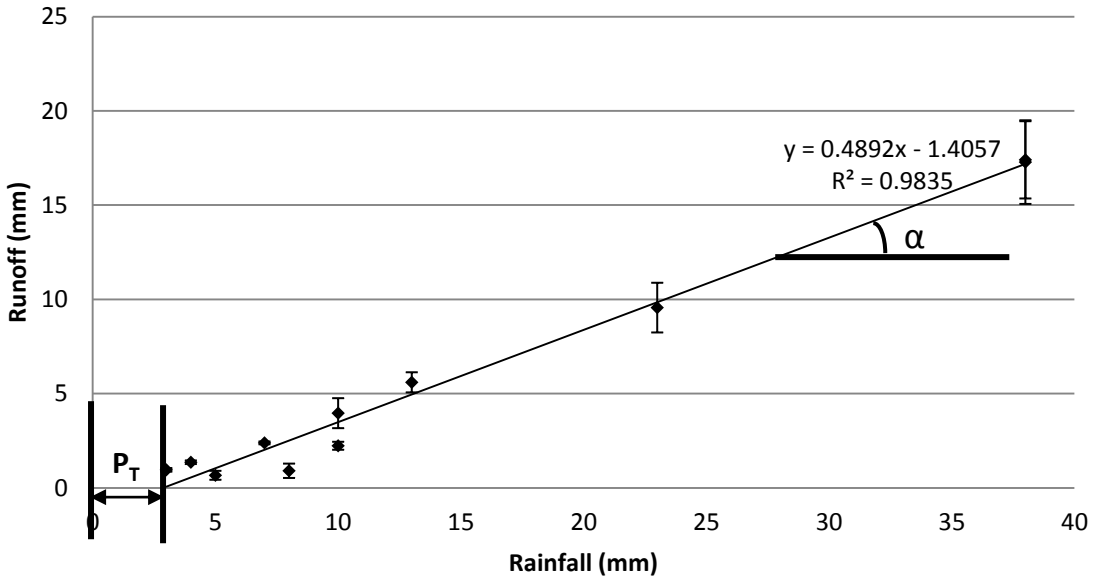

Figure 4.13 Regression analysis of the rainfall (mm) and runoff (mm) data for site GL1 (grazing land, gentle slope). The linear trend line shows the gradient, α, and the intercept on the x-axis, P_T, precipitation threshold to runoff initiation. Error bars show standard deviation (n = 3)

The slope seems to have a minor influence on alpha as can be seen from Figure 4.14, The non-parametric Kruskal-Wallis test confirmed this. For the same soil texture, grazing land has a higher alpha than cropland, probably due to compactation and low vegetation cover. The alpha is highest for grazing land rather than for cropland except for the W2 site (walka, silty clay, intermediate slope). This is probably due to its stronger water holding capacities and lower infiltration rates of this heavier soil texture, not to forget the swell shrink features of the clayey soils. During wetting the rainfall is absorbed by the soil, the cracked soil swells and impedes further infiltration.

The alpha of the U2 (loam, intermediate slope) site is high considering its lighter soil texture. This may have to do with its development on displaced basaltic material, whereas the soils on the other sites are derived from limestone. Caution must be taken when interpreting this experimental site due to the large error bars.

In Figure 4.15 the effect of slope on the precipitation threshold (P_T) is clear, especially on the cropland sites CL1, CL2 and CL3. A downward trend can be observed in the CL and GL sites (cropland and grazing land, medium soil texture). The P_T for GL1 (grazing land, gentle slope) is higher than P_T for GL2 and GL3, the slope. A steeper slope (site CL3 for example) induces faster runoff whereas a gentle slope can hold the rainfall longer before running off. According to Figure 4.14 the runoff volume is similar and not affected by slope. Roughness factors are likely to have a positively correlated relationship with P_T (mm). The W2 site (Walka, intermediate slope) is the heaviest texture and also has the lowest intercept, this is probably due to the swelling of the clay which is quickly saturated

and holds the water more effectively than the lighter textures (idem above). The grazing land sites have a lower intercept than the cropland sites with same texture, most likely due to soil compactation.

Table 4.5 The gradients, α, and the precipitation thresholds, P_T, of the eight experimental sites. Also the R^2 of the regression and the amount of data points (n) are listed.
CL: Cropland on Bahakel, GL: Grazing land on Bahakel, U: Cropland on Andelay, W: Cropland on Walka. Slope class 1: Gentle slope, 2: Middle slope, 3: Steep slope

Site	α	P_T	R^2	n
CL1	0.3793	4.29	0.8216	63
CL2	0.3693	3.23	0.8348	60
CL3	0.3974	1.44	0.9062	66
GL1	0.4892	2.87	0.9835	33
GL2	0.5171	1.87	0.8753	81
GL3	0.5099	2.16	0.8701	90
U2	0.6168	2.27	0.9788	12
W2	0.4349	0.66	0.9785	43

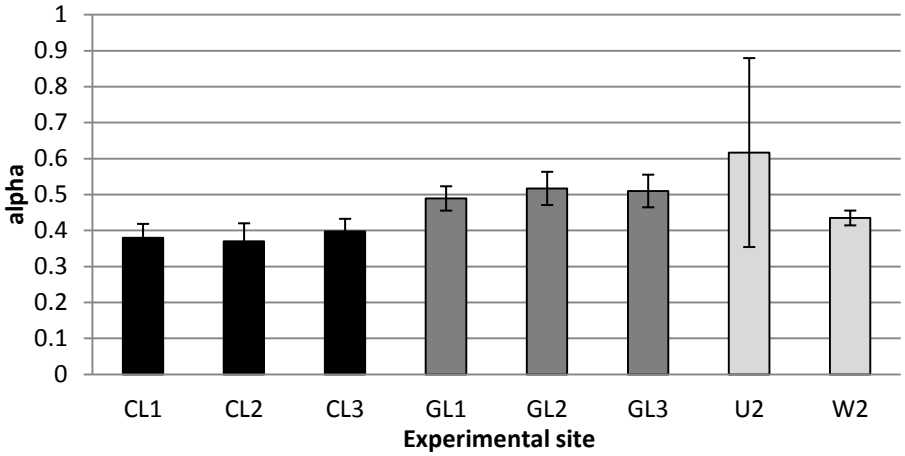

Figure 4.14 The gradients (alpha's) deduced from the regression analysis of the P/R data of the eight experimental sites.
Error bars: 95% confidence level of alpha. CL: Cropland on Bahakel, GL: Grazing land on Bahakel, U: Cropland on Andelay, W: Cropland on Walka. Slope class 1: Gentle slope, 2: Middle slope, 3: Steep slope

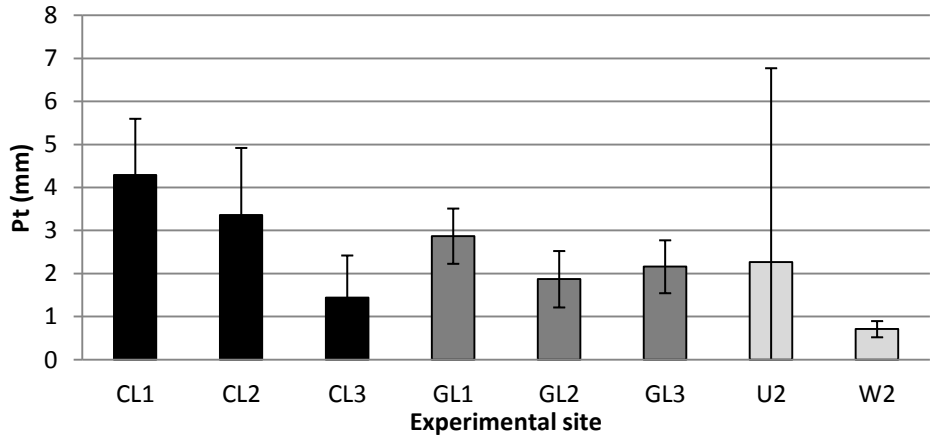

Figure 4.15 The precipitation thresholds, P_T, deduced from the regression analysis of the P/R data of the eight experimental sites.
Error bars: 95% confidence level of P_T. CL: Cropland on Bahakel, GL: Grazing land on Bahakel, U: Cropland on Andelay, W: Cropland on Walka. Slope class 1: Gentle slope, 2: Middle slope, 3: Steep slope

Now a general insight is gained in the P/R data per experimental site, the data of each site is looked at into more detail to look for any prevailing trends. First the three replicate micro-plots A, B and C for each experimental site are investigated. Then the P/R data is split into the three antecedent moisture content classes. Also the P/R data on cropland sites is divided into two groups, before and after 30% vegetation cover was reached. The rainfall-runoff relationships of these groups are explored using regression analysis. Finally, the non-parametric Kruskal-Wallis tests were used to check for significance of the possible differences.

Rainfall-Runoff relationships within replicate micro-plots

Rainfall-runoff relationships were explored per replicate micro-plot (A, B and C) within each experimental site. This was done to check if slight differences in micro-plot characteristics such as rock fragment cover, random roughness, slope and vegetation had a significant influence on the rainfall-runoff data. An example of the regression analysis for the three replicate micro-plots of the CL2 experimental site is given in Figure 4.16.

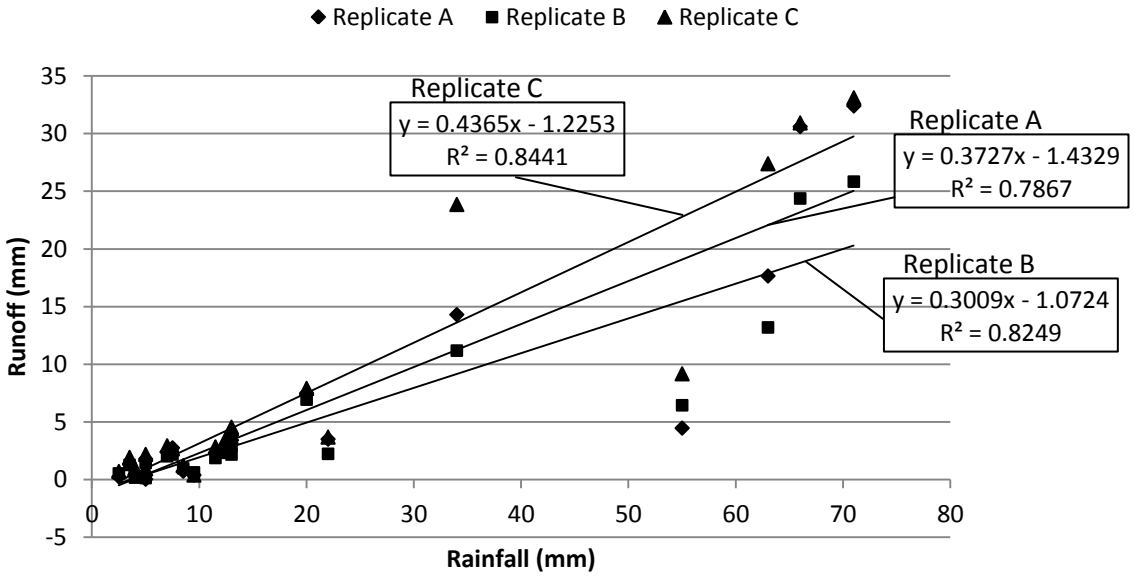

Figure 4.16 P/R data of experimental site CL2 (cropland, sandy clay loam, intermediate slope), data split into three for each micro-plot replicate (A, B and C).

The gradients, α, and the precipitation thresholds, P_T, of the three replicate micro-plots of each of the eight experimental sites are assembled in Table 4.6, Table 4.7, Figure 4.17 and Figure 4.18. In Figure 4.17 the outliers of the rainfall-runoff data for micro-plot U2A are observable as this micro-plot is very different to the two replicates. The outliers have a high influence on the alpha, but not on the precipitation threshold (P_T). There were two rainfall events that produced an exceptionally high runoff. It is not clear if this was due to an error or not.

Table 4.6 alpha values of the three replicate micro-plots within each experimental site.
CL: Cropland on Bahakel, GL: Grazing land on Bahakel, U: Cropland on Andelay, W: Cropland on Walka. Slope class 1: Gentle slope, 2: Middle slope, 3: Steep slope. A: replicate micro-plot most to the east, B: replicate middle, C: replicate most to the west

α (%)	CL1	CL2	CL3	GL1	GL2	GL3	U2	W2
A	37.55	37.27	39.62	54.84	46.48	49.87	85.73	43.42
B	39.09	30.09	37.34	43.52	52.77	46.53	48.01	43.11
C	37.14	43.65	42.26	48.41	55.89	56.57	51.3	43.95

Table 4.7 P_T values of the three replicate micro-plots within each experimental site.
CL: Cropland on Bahakel, GL: Grazing land on Bahakel, U: Cropland on Andelay, W: Cropland on Walka. Slope class 1: Gentle slope, 2: Middle slope, 3: Steep slope

P_T (mm)	CL1	CL2	CL3	GL1	GL2	GL3	U2	W2
A	4.03	3.84	2.18	3.84	1.34	2.01	2.44	0.71
B	4.78	3.56	1.89	2.33	2.15	2.42	2.32	0.67
C	4.03	2.81	0.35	2.27	2.03	2.08	1.94	0.6

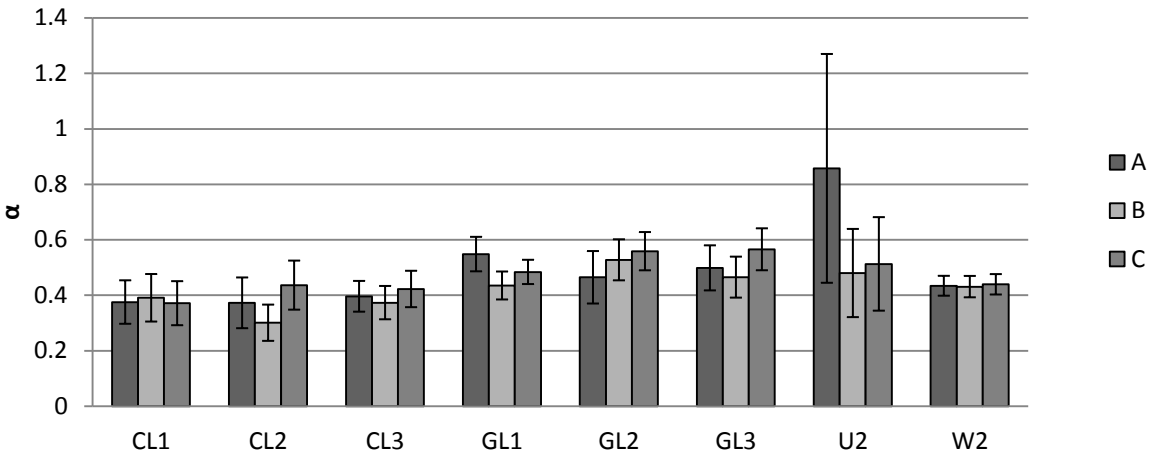

Figure 4.17 The gradients (alpha's) deduced from the regression analysis of the P/R data of the three micro-plots of the eight experimental sites.
CL: Cropland on Bahakel, GL: Grazing land on Bahakel, U: Cropland on Andelay, W: Cropland on Walka. Slope class 1: Gentle slope, 2: Middle slope, 3: Steep slope

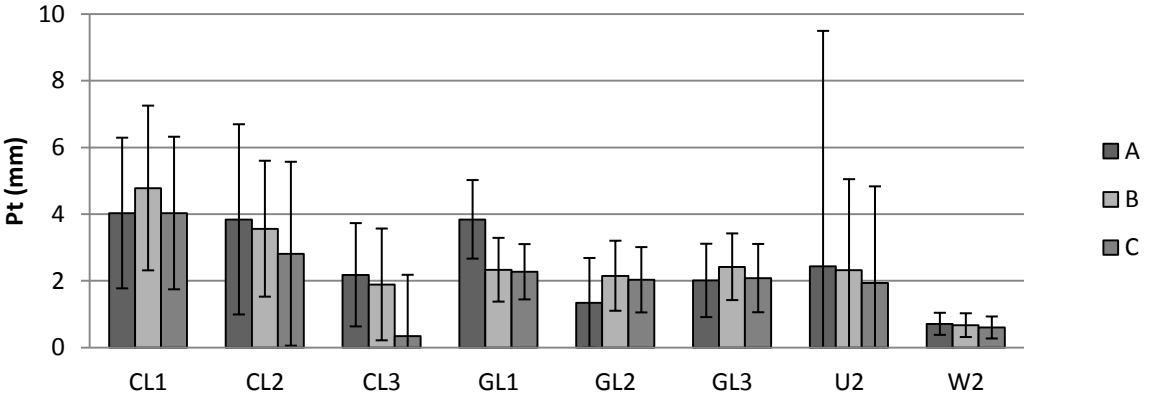

Figure 4.18 The precipitation thresholds (P_T) deduced from the regression analysis of the P/R data of the three micro-plots of the eight experimental sites.
CL: Cropland on Bahakel, GL: Grazing land on Bahakel, U: Cropland on Andelay, W: Cropland on Walka. Slope class 1: Gentle slope, 2: Middle slope, 3: Steep slope

Rainfall-Runoff relationships for different moisture condition AMC

To inspect the influence of the moisture condition of the soil on runoff generation, following course of action was followed. All rainfall-runoff events were divided into three classes according to their AMC (Antecedent moisture condition of the previous 5 days). Each group received a different symbol to graphically visualise this effect and look for trends. In Figure 4.19 an example of the regression of the rainfall-runoff data can be found for CL2 (cropland, medium texture, intermediate slope), the data has been divided into the three respective AMC classes. In Figure 4.20 a summary of all the alpha's can be found for each site. Presuming that a dry soil will absorb more rainfall and produce less runoff (and on the other hand, that a wet soil will produce more runoff) a increasing trend of the runoff response (alpha's) is expected within each site. AMC I having the lowest alpha and AMC III having the highest alpha. This is not always the case, in fact the opposite trend occurs equally often. Descheemaeker *et al*. (2008) also took AMC into account and found that it did not improve runoff predictions. The moisture will further not be taken into account as there is no clear trend. This could possibly be explained by the typical swell-shrink behaviour of the soils with high smectite clay content allowing almost no infiltration once wetted and the opposing trend of the vegetation, which can reduce runoff later in the rainy season, when the soils are more moist. Moreover Descheemaeker *et al*., 2006 investigated the impact of soil moisture condition and found that in their case it had no influence on precipitation threshold (P_T). In Figure 4.21 the P_T's are shown, these values also show opposing trends, with some negative P_T values which is not possible, possibly occurring due to AMC classes with few data points.

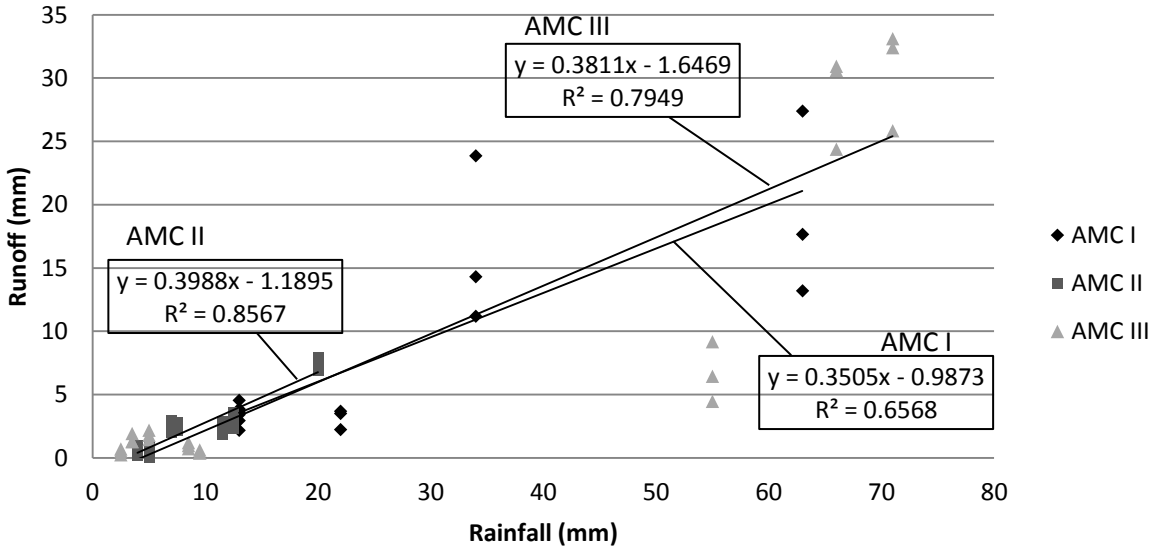

Figure 4.19 Rainfall-runoff data for CL2 (cropland, intermediate slope), each event was classed in an AMC group. The linear trend lines for each AMC group are shown.

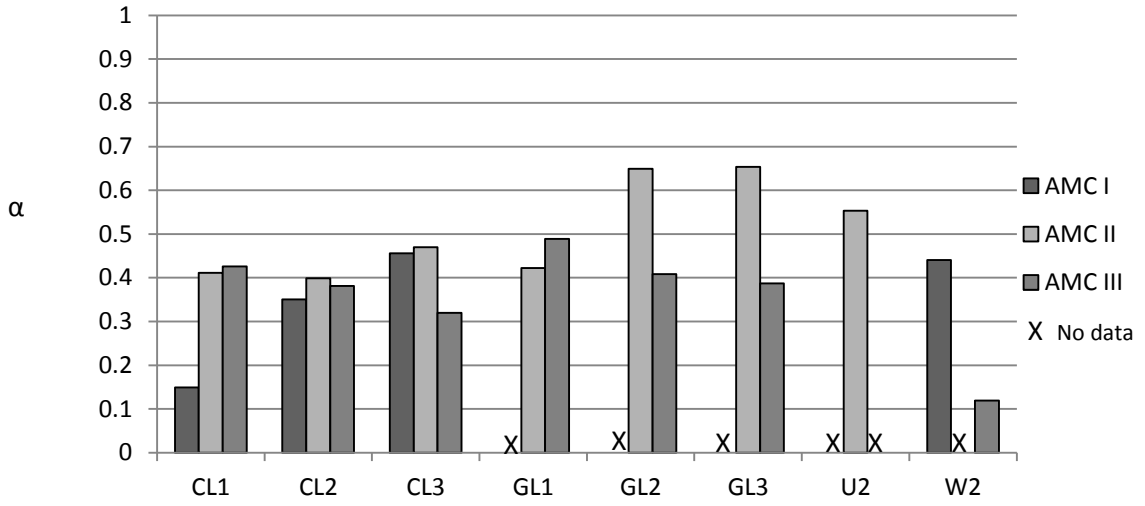

Figure 4.20 Histogram of the alpha's for each of the sites, split into three AMC classes. X marks the AMC classes where there were no rainfall-runoff events measured in that class.
CL: Cropland on Bahakel, GL: Grazing land on Bahakel, U: Cropland on Andelay, W: Cropland on Walka. Slope class 1: Gentle slope, 2: Middle slope, 3: Steep slope

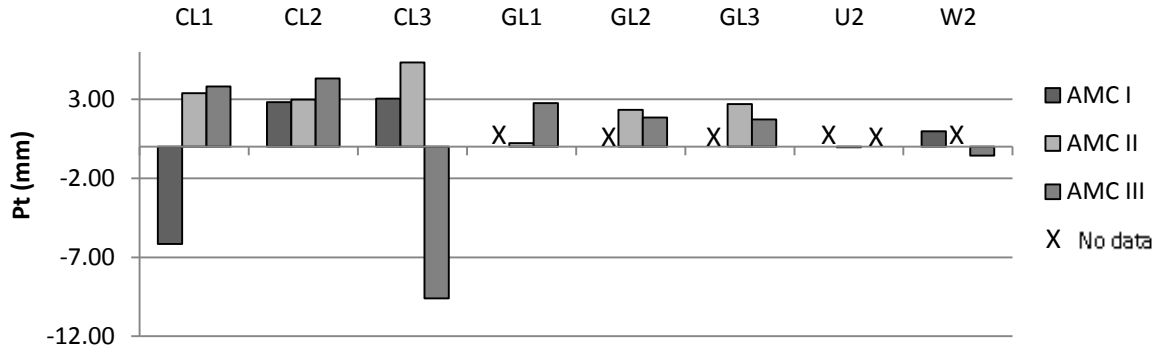

Figure 4.21 P_T's of the three AMC groups for each of the eight experimental sites.
CL: Cropland on Bahakel, GL: Grazing land on Bahakel, U: Cropland on Andelay, W: Cropland on Walka. Slope class 1: Gentle slope, 2: Middle slope, 3: Steep slope

Rainfall-Runoff relationships for different vegetation cover

The important threshold of 30% cover in conservation tillage is applied to the vegetation cover recorded on the micro-plots. The P/R data is divided into two groups: before and after reaching 30% vegetation cover. This data can be seen in Table 4.8 and Figure 4.22.

From the data it seems that a higher vegetation cover (CC) causes higher runoff. The higher CC occurs later in the rainy season when there is a higher moisture content in the soil, this is a more logical reason for the higher alpha, rather than the CC. Via the Kruskal-Wallis analysis it was shown that the two alpha's of < and > than 30% CC were not significantly different. They are not further taken into account.

A higher CC implies a higher P_T (Figure 4.23). This seems logic as the more vegetation on the micro-plot the more rainfall the vegetation can intercept, thus increasing the precipitation threshold (P_T) for runoff initiation. However, the difference was not significant.

Table 4.8 Alpha's for the five cropland sites. < 30 % CC: alpha deduced using only the rainfall-runoff data before 30% vegetation cover was reached, > 30 % CC: alpha deduced using data after vegetation cover of 30 % was reached. For grazing land no discrepancy was made in vegetation cover.

CL: Cropland on Bahakel, U: Cropland on Andelay, W: Cropland on Walka. Slope class 1: Gentle slope, 2: Middle slope, 3: Steep slope

Site	α (all data)	n	α (<30% CC)	n	α (>30% CC)	n
CL1	0.38	63	0.39	42	0.48	21
CL2	0.37	60	0.37	57	(0.53)	6
CL3	0.40	66	0.39	39	0.47	27
U2	0.62	12	/	0	0.62	12
W2	0.43	43	/	0	0.66	43

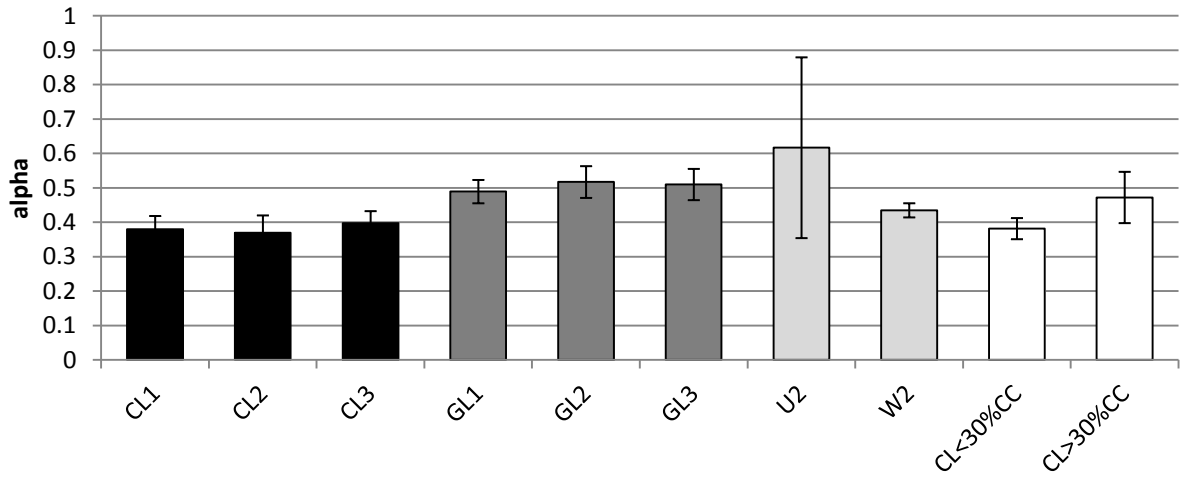

Figure 4.22 Alphas for the eight experimental sites. CL1, CL2 and CL3 data was combined and used to differentiate between < 30 % CC and > 30 % CC: alpha deduced using data resp. before and after vegetation cover of 30 % was reached.

Error bars: 95% confidence level. CL: Cropland on Bahakel, GL: Grazing land on Bahakel, U: Cropland on Andelay, W: Cropland on Walka. Slope class 1: Gentle slope, 2: Middle slope, 3: Steep slope

Table 4.9 P_T values of the eight experimental sites and the CL sites on bahakel for before and after 30% CC had been reached.

CL: Cropland on Bahakel, GL: Grazing land on Bahakel, U: Cropland on Andelay, W: Cropland on Walka. Slope class 1: Gentle slope, 2: Middle slope, 3: Steep slope

Site	CL1	CL2	CL3	GL1	GL2	GL3	U2	W2	CL<30%CC	CL>30%CC
P_T (mm)	4.29	3.36	1.44	2.87	1.87	2.16	2.27	0.71	3.21	3.61

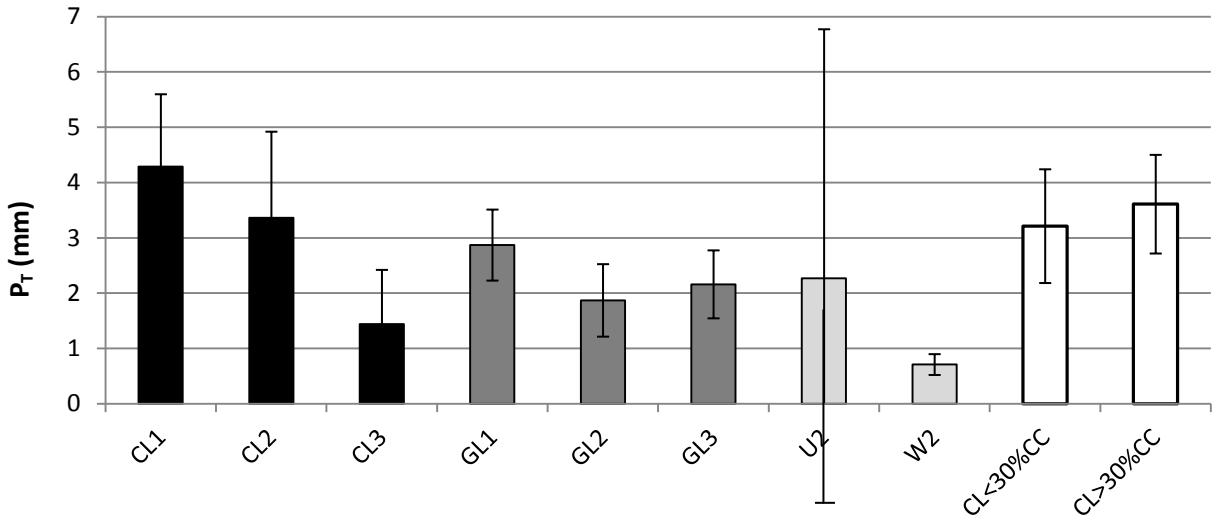

Figure 4.23 P_T (mm) for the eight sites. Deduced using P/R data when runoff > 0.5 mm, < 30 % CC: Intercept deduced using only the rainfall-runoff data before 30% vegetation cover was reached, > 30 % CC: Intercept deduced using data after vegetation cover of 30 % was reached.

For grazing land there is no discrepancy in vegetation cover. The error bars show the 95 % confidence level. CL: Cropland on Bahakel, GL: Grazing land on Bahakel, U: Cropland on Andelay, W: Cropland on Walka. Slope class 1: Gentle slope, 2: Middle slope, 3: Steep slope

4.1.3 Effect of characteristics on rainfall-runoff relationships

Some effects of the measured micro-plot characteristics on the rainfall-runoff relationships have already been identify. Most noticeable were the effect of land use on runoff response and the effect of slope on the precipitation threshold. To gain an idea of the correlations between variables and look for yet concealed correlations, a partial least squares regression analysis was performed on six variables for alpha and P_T: slope (%), clay content (%), rock fragment cover (%), random roughness (cm), vegetation cover (%) and vegetation height (%). When the PLSR analysis was performed for alpha, P_T was added as a variable and when performed for P_T, alpha was added.

Partial Least Squares Regression Analysis

The recorded characteristics of the 24 micro-plots with their corresponding alpha and P_T from previous regression analysis were the 24 observations used as input in PLSR, the observation of micro-plot U2A however was omitted due to its large deviation and low amount of P/R events that it was based on. The analysis was thus performed on 23 observations and 7 variables.

From PLSR analysis for alpha, the overall predicted RMSE of alpha is between 5.5 % and 7 % percent, this is accepted for these on-field measurements. Range of alpha [30.09 % - 56.57 %].

The output of the PLSR is shown in Table 4.10. The first two components explain 50 % of the variance of alpha, 41 % by component 1 and 9 % by component 2. This is not very high but can suffice to gain some overall insights on the influences of the variables on alpha and between variables. The loadings

of these two components are looked at into more detail to give them a meaning in relation to the variables analysed. The loadings are correlations between the components and the original variables. Component 1 describes the random roughness, veg_cover and the veg_height which can be grouped as roughness factors. Component 2 mainly describes the negative correlation of alpha with precipitation threshold and the opposing influence of slope. The loadings are plotted in Figure 4.24.

From this PLSR analysis on alpha some general conclusions can be drawn. For component 1: the roughness factors (random roughness, veg_cover and veg_height) have the same decreasing effect on alpha. More roughness lowers the runoff response. For component 2 a lower precipitation threshold indicates a higher runoff response (alpha). Also, a steeper slope induces a higher alpha according to this component. Previously it was noted that slope did not have a significant impact on the variance of alpha. This second component only explains 9 % of the variance of alpha and its effect on alpha is less significant than the that of component 1.

Table 4.10 Output of the partial least squares regression analysis on alpha, the first two components are taken into consideration.

TRAINING: % variance explained

	1 comps	2 comps	3 comps	4 comps	5 comps	6 comps	7 comps
X	35.13	58.31	67.02	90.49	95.68	97.68	100.00
alpha	40.65	50.04	63.98	66.13	68.60	69.54	69.69

Loadings:

	Comp 1	Comp 2	Comp 3	Comp 4	Comp 5	Comp 6	Comp 7
Pt		-0.971		0.135	0.214		-0.222
slope		0.600	-1.040	0.281	0.424	-0.473	0.179
clay_content		0.156		-0.868	0.122	0.273	
Rock_fragment_cover		0.168	-0.583	0.650	-0.889	0.539	-0.118
random_roughness	-0.620		0.128		-0.223	-0.469	0.704
veg_cover	-0.595	0.358	-0.195		0.234	0.625	
veg_height	-0.603	0.339				-0.116	-0.631

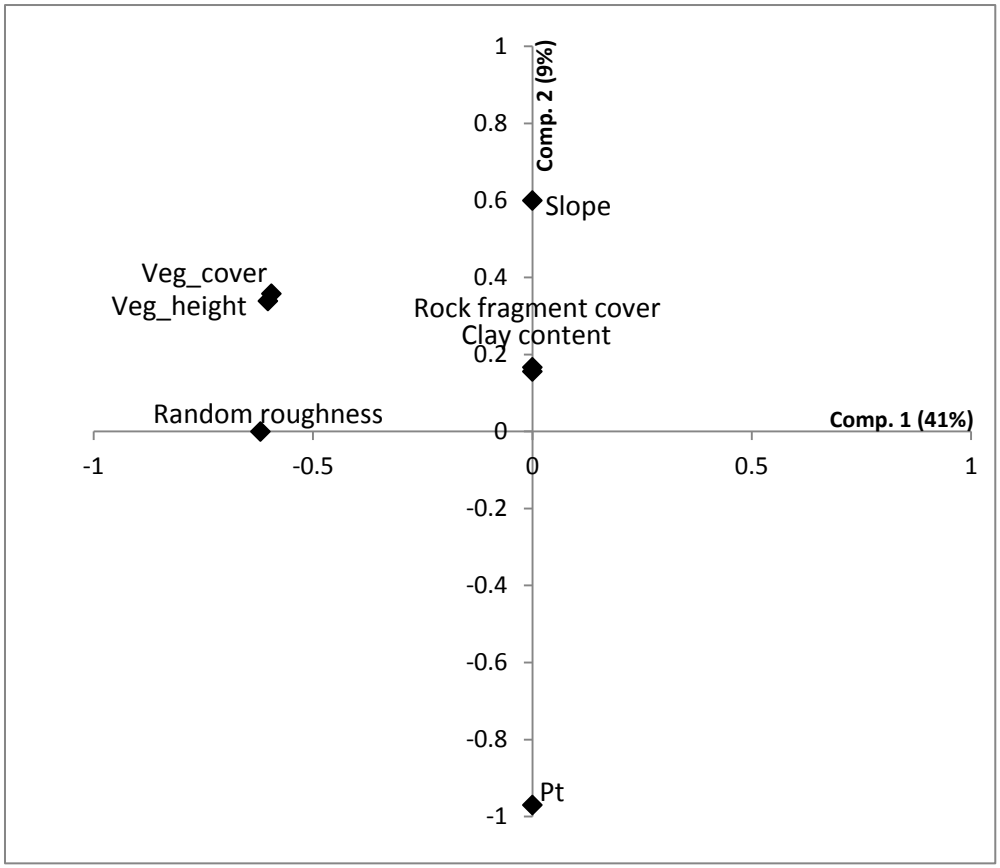

Figure 4.24 Graph of the variable contribution of Component 1 on the x-axis and component 2 on the y-axis of the partial least squares regression analysis performed for alpha.

The same analysis was performed to explain the variance of P_T (mm). The overall predicted RMSE of P_T is between 0.8 mm and 1.2 mm, which is accepted for these on-field measurements. Range of P_T [0.35 - 4.78 mm].

The output of the PLSR is shown in Table 4.11. The first two components explain 64.76 % of the variance of P_T, 57 % by component 1 and 8 % by component 2. The loadings of these two components are looked at into more detail.

The loadings are plotted in Figure 4.25. Component 1 describes the negatively correlated effect of slope on P_T. The influence of vegetation height and vegetation cover on P_T is also not negligible. Component 2 mainly describes the positive correlation of random roughness with precipitation threshold. Also the opposing influence of alpha is noticed as for previous analysis.

The general conclusions that can be drawn from this PLSR analysis on P_T are the following. For component 1: the influence of slope on precipitation threshold is large, which serves as a confirmation of the previous observations. A steeper slope lowers the precipitation threshold inducing faster runoff initiation. The influence of a higher vegetation cover and vegetation height inducing a lower precipitation threshold was not expected, this has previously been observed and

discussed. For component 2 more random roughness indicates a larger precipitation threshold. This is as expected, more random roughness allows ponding and delays runoff initiation. This second component however only explains 8 % of the variance of alpha and its effect on P_T is less significant than the that of component 1.

Using all 7 components only 75.92 % of the variance of P_T is explained. For alpha using all 7 components explained 69.69 % of the variance. This indicates that the variables measured are not the only ones with an effect on rainfall-runoff relationships. More research and measurements are necessary to account for this additional variability.

Table 4.11 Output of the partial least squares regression analysis on precipitation threshold, the first two components are taken into consideration.

TRAINING: % variance explained

	1 comps	2 comps	3 comps	4 comps	5 comps	6 comps	7 comps
X	19.86	55.08	74.53	88.64	94.83	98.44	100.00
Pt	56.78	64.76	68.90	72.88	74.80	75.68	75.92

Loadings:

	Comp 1	Comp 2	Comp 3	Comp 4	Comp 5	Comp 6	Comp 7
alpha		-0.547		-0.314	0.767	-0.542	0.194
slope	-0.740		0.784		-0.360	-0.218	0.124
clay_content	-0.168	-0.222	-0.892	0.547	-0.632	0.357	0.180
Rock_fragment_cover	-0.144	0.146	0.652	-0.882		0.449	
random_roughness	-0.100	0.591	-0.425			-0.647	0.560
veg_cover	-0.622	0.456	-0.309		0.380	0.210	0.307
veg_height	-0.534	0.455	-0.545		0.188		-0.712

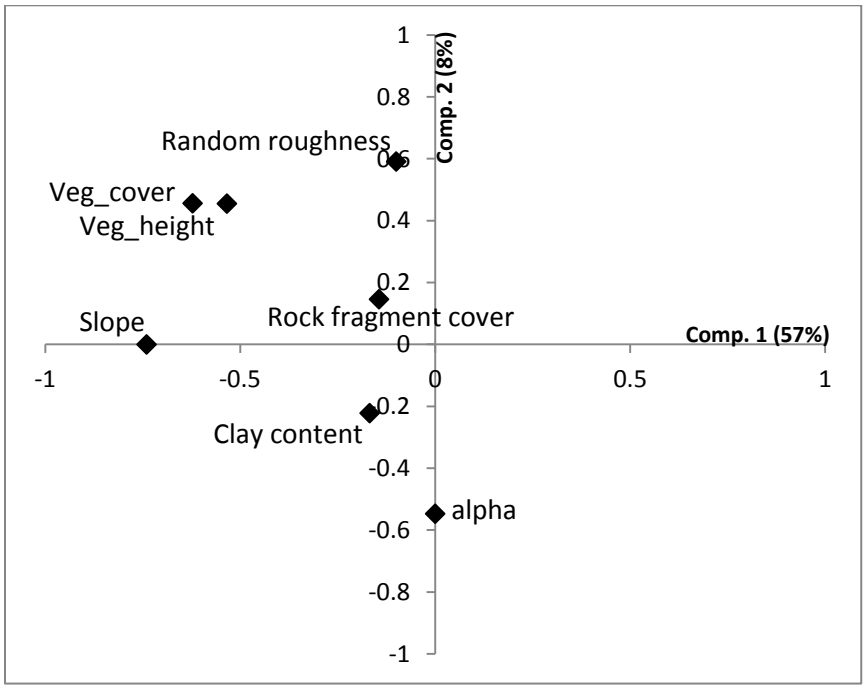

Figure 4.25 Graph of the variable contribution of Component 1 on the x-axis and component 2 on the y-axis of the partial least squares regression analysis performed for P_T.

4.1.4 Curve number derivation

Curve numbers (CN's) were derived using the P/R data of the eight experimental sites. The CN was readily calculated from the storage parameter, S, using equation (4). Each optimal S was derived using the solver Add-in in excel (2007). The starting value of S was calculated by analytically solving the quadratic equation derived from equations (1), and (3) using data from one rainfall-runoff event. The S that gave the best fit between observed and predicted values of runoff (Q) per rainfall event was obtained iteratively. This was done for both of the proposed initial abstraction ratios λ = 0.05 and λ = 0.2 to check the effect on runoff prediction.

In Figure 4.26 it can be seen that the calculation of the CN using the λ = 0.05 as proposed by Descheemaeker *et al*., 2008 gives a better fit. The root mean square error (RMSE) between the observed and the predicted runoff values is consistently lower for λ = 0.05. Lambda 0.05 was thus used in further calculations.

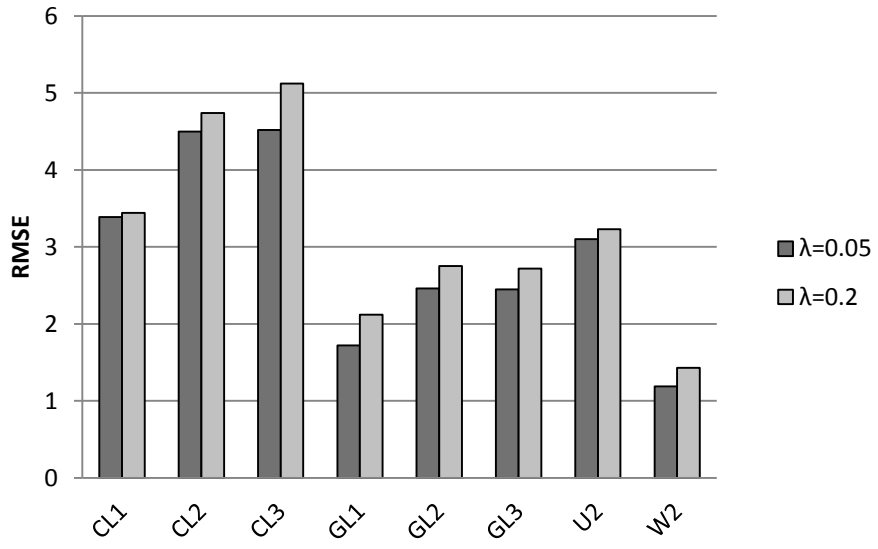

Figure 4.26 Comparison of the RMSE (root square mean error) for the calculation of the curve number of each experimental site, of the initial abstraction ratio λ = 0.05 and λ = 0.20.
CL: Cropland on Bahakel, GL: Grazing land on Bahakel, U: Cropland on Andelay, W: Cropland on Walka. Slope class 1: Gentle slope, 2: Middle slope, 3: Steep slope.

In Table 4.12 the storage parameters (S), curve numbers (CN's) and root mean squared errors between observed and predicted runoff values (RMSE) of the eight experimental sites are listed. In Figure 4.27 the CN's are presented in a histogram. The CN's don't show a high variability between different slope classes on the same land use and soil texture. This was also observed for the P/R relationships. Curve numbers of four treatments are selected for further use (Table 4.13), these four groups are CL, GL, U and W reflect two land use types and three soil textures (CL: Cropland on Bahakel, GL: Grazing land on Bahakel, U: Cropland on Andelay, W: Cropland on Walka).

Descheemaeker *et al.* (2008) derived CN's for grazing land sites based on P/R data of plots with dimensions 5 m x 2 m. Generally these sites have a high CN which is in the same order as the CN's derived from the micro-plot (1 m x 1 m) P/R data in current study. Also the values for CN derived at sub-catchment scale obtained by M.Sc student Sylvain Trigalet are similar, this will be discussed in paragraph 4.2.

Table 4.12 Storage parameter (S), Curve Number (CN) and RMSE for eight experimental sites calculated using the initial abstraction ratio, λ = 0.05.
CL: Cropland on Bahakel, GL: Grazing land on Bahakel, U: Cropland on Andelay, W: Cropland on Walka. Slope class 1: Gentle slope, 2: Middle slope, 3: Steep slope

	λ = 0.05		
	S	CN	RMSE
CL1	88.55	74.15	3.39
CL2	91.24	73.57	4.5
CL3	77.65	76.59	4.52
GL1	34.63	88	1.72
GL2	22.94	91.72	2.46
GL3	24.28	91.28	2.45
U2	14.75	94.51	3.1
W2	27.03	90.38	1.19

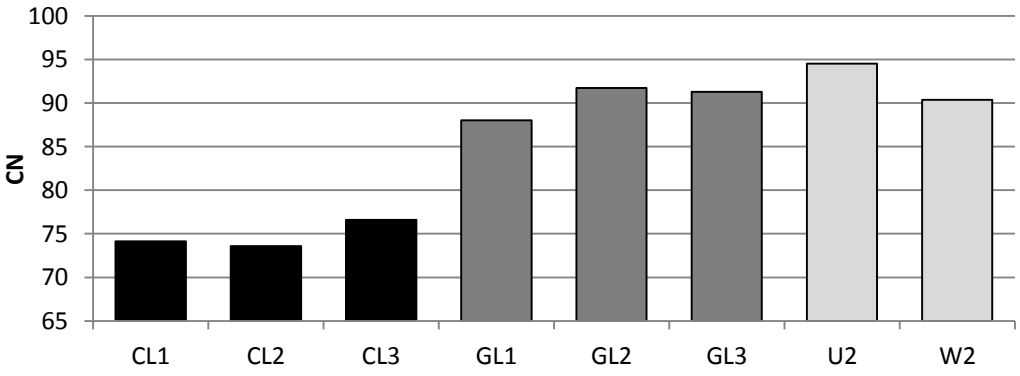

Figure 4.27 Curve Number of the treatments. Axis starting from CN = 65.
CL: Cropland on Bahakel, GL: Grazing land on Bahakel, U: Cropland on Andelay, W: Cropland on Walka. Slope class 1: Gentle slope, 2: Middle slope, 3: Steep slope

Table 4.13 Selected CN's for further use. CN's derived from micro-plot P/R data.
CL: Cropland on Bahakel, GL: Grazing land on Bahakel, U: Cropland on Andelay, W: Cropland on Walka

	λ = 0.05		
	S	CN	RMSE
CL	85.81	**74.77**	4.14
GL	27.28	**90.33**	2.21
U	14.75	**94.51**	3.10
W	27.03	**90.38**	1.19

4.2 Sub-catchment

Rainfall-runoff data of sub-catchment outlet 'MLRMT5' (runoff gauging station, Figure 3.15) is available for ten rainfall-runoff events (Table 4.14). The location of this sub-catchment within the Mayleba catchment can be seen in Figure 4.28. Runoff was predicted using the CN's derived in previous paragraph, at micro-plot level. This was done to validate the CN's. The runoff was also predicted using the CN's derived at sub-catchment level and using CN's found in literature.

Table 4.14 Rainfall-runoff data of sub-catchment MLRMT5. Ten rainfall events (P1 to P10) were registered from 11/08/11 to 01/09/11 with the corresponding runoff depths of the sub-catchment.

Rainfall event	Date (G.C.)	Rainfall (mm)	Runoff (mm) Qobs
P1	11-Aug-11	4.8	0.23
P2	11-Aug-11	6.8	0.61
P3	18-Aug-11	11.6	0.7
P4	19-Aug-11	9	0.93
P5	22-Aug-11	7.6	0.31
P6	23-Aug-11	9	1.03
P7	25-Aug-11	5.8	0.15
P8	29-Aug-11	11	1.92
P9	31-Aug-11	7.6	0.12
P10	1-Sep-11	13.6	2.98

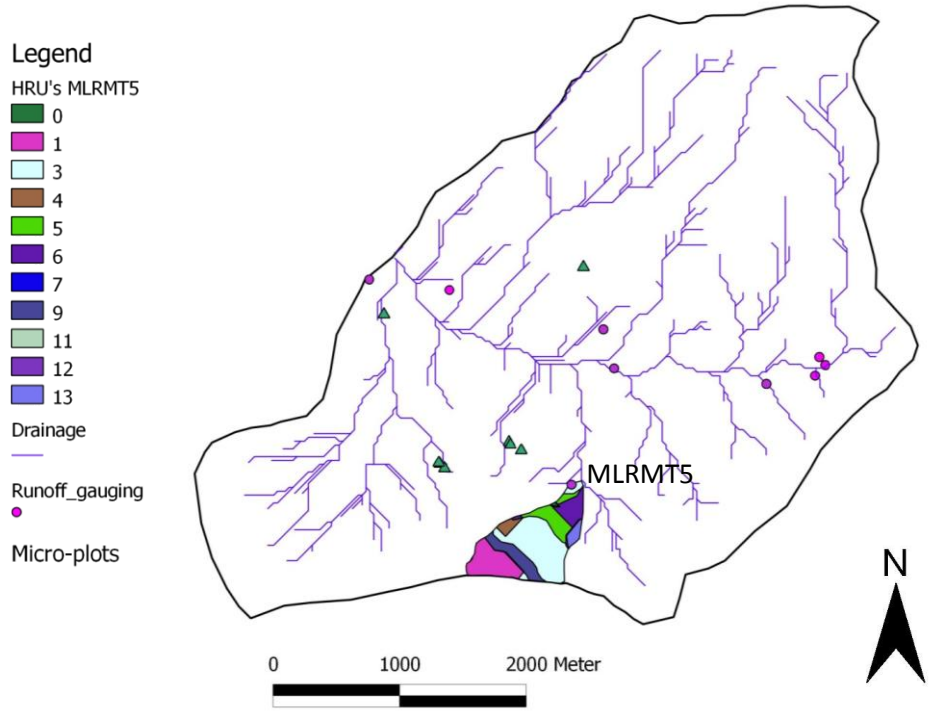

Figure 4.28 Map of Mayleba catchment with demarcation of the sub-catchment MLRMT5 and its hydrological response units (HRU's). The units are described in Table 4.15

To predict runoff using the CN's derived from P/R data obtained at micro-plot level, the sub-catchment was divided into units describing it's land use and soil texture. This was achieved by overlaying the soil texture and land use maps of Van de Wauw (2005). The curve numbers and area fractions that correspond to these units are listed in Table 4.15. For the CN's derived at sub-catchment level a distinction has been made between good and poor hydrological condition (curve number for poor hydrological condition is in parentheses). This distinction was based on observations during transect surveying.

The CN's derived at micro-plot level (Table 4.13) do not cover all units in the sub-catchment. To account for the missing values, estimates were made based on the derived CN values for cropland and grazing land. These values are underlined in Table 4.15, the derived CN's are indicated in **bold**.

For housing it was not possible to estimate a CN based on derived CN's as this land use was not investigated. A lower CN was chosen, implying a lower runoff. Although the soil is most likely to be very compact and little infiltration is expected, there are other factors of the local housing that can reduce runoff. The farmers compounds are surrounded by stone walls which can function like a SWC measure and imply lower runoff production. The roofs of houses are often made from corrugated iron and the rainfall is collected via gutters for household use, thus reducing runoff. Other roofs are often flat and vegetated or covered with straw which also intercepts rainfall.

Table 4.15 Units of the sub-catchment with corresponding curve numbers. CN for good hydrological condition not in parentheses, (CN for poor hydrological condition in parentheses). CN's derived at micro-plot level in bold, estimations underlined. CN from USDA (1986) for agricultural lands is for average runoff condition and λ = 0.2, other CN's λ = 0.05. The fraction of the total sub-catchment area described by the units is in the last column, weighted averages below the table.

Land use	Soil texture	CN derived at micro-plot level (λ = 0.05)	CN derived at sub-catchment level (λ = 0.05)	CN (USDA, '86) (λ = 0.2)	Area fraction (%)
Cropland	Heavy Clay	92.5	72 (88)	78 (80)	19.77
	Clay_SiltyClay	**90.38**	88 (92)	78 (80)	30.47
	Silty Clay Loam	**74.77**	/	71 (74)	1.16
	Loam_ClayLoam	**94.5**	84 (86)	71 (74)	15.08
Grazing land	Heavy Clay	/	74 (76)	74 (86)	0
	Clay_SiltyClay	92	90 (94)	74 (86)	24.09
	Silty Clay Loam	**90.33**	/	61 (79)	2.71
	Loam_ClayLoam	90	92 (93)	61 (79)	6.46
Housing		75	94	86	0.26
Weighted average for sub-catchment MLRMT5		91.6	84.5	76.3	∑ = 100%

The CN's from the literature (USDA, 1986) are for average runoff condition (AMC II) and λ = 0.2. These values cannot be directly compared with those derived at micro-plot and sub-catchment level using λ = 0.05. Their predictive power can be compared using the RMSE between observed and predicted values of runoff (Table 4.16) and with the Qobs-Qpred plots, which should ideally approach the 1:1 line (Figure 4.29).

The RMSE (Table 4.16) of runoff predictions using CN's derived at sub-catchment level is the lowest, this was expected as this data from sub-catchment level was part of the dataset used to calibrate these CN's. The RMSE of predictions using CN's derived at micro-plot level is ± 1.4 times higher, and the RMSE of the predictions using CN's from the literature is ± 2.8 times higher than the RMSE of runoff predictions using CN's derived at sub-catchment level.

The Qobs-Qpred plots in Figure 4.29 show the observed runoff values plotted against the predicted values using the three sets of CN's. The linear trend line equation and corresponding R^2 are shown in the graphs. The gradients should be close to 1, and the intersect close to 0, the 1:1 line is shown for easy interpretation. The intersect with the Qpred axis is always positive. This indicates that the predictions overestimate the runoff production during shallow rainfall events. Almost all data points of the Qobs-Qpred plot of prediction of runoff using CN's derived at micro-plot level are above the 1:1 line (Figure 4.29 - middle), this indicates the overestimation of runoff production.

Figure 4.29 (right) expresses the improvement of runoff predictions when using λ = 0.05 for shallow rainfall events. The constraint of using equations (1) and (3) for runoff prediction is $P > I_a$. The weighted average of the CN from literature, on this sub-catchment, is 76.3 and S = 79.37. These CN's are valid for λ = 0.2. As $I_a = \lambda S$ the equations (1) and (3) are only valid from a rainfall depth of 15.87 mm.

The difference between results from micro-plot level and sub-catchment level can be explained by the difference in area from which the CN's were derived. This is known as the scaling effect, where a lower runoff coefficient is obtained from a larger area (Van de Giesen *et al*., 2011). The CN's derived at sub-catchment level also took the soil and water conservation (SWC) measures into account whereas this was not the case for the CN's derived at micro-plot level (1 m^2). These SWC measures lower the runoff due to increased infiltration and spreading of runoff in time (Nyssen *et al*., 2010). The CN's derived from micro-plot P/R data thus lead to an overestimation of runoff.

Table 4.16 RMSE (mm) of observed and predicted runoff for the three sets of CN's used.

	CN derived at sub-catchment level	CN derived at micro-plot level	CN table (USDA, 1986) for agricultural lands
RMSE of Qpred and Qobs (mm)	0.45	0.63	1.24
Proportion of lowest RMSE	1	1.38	2.75

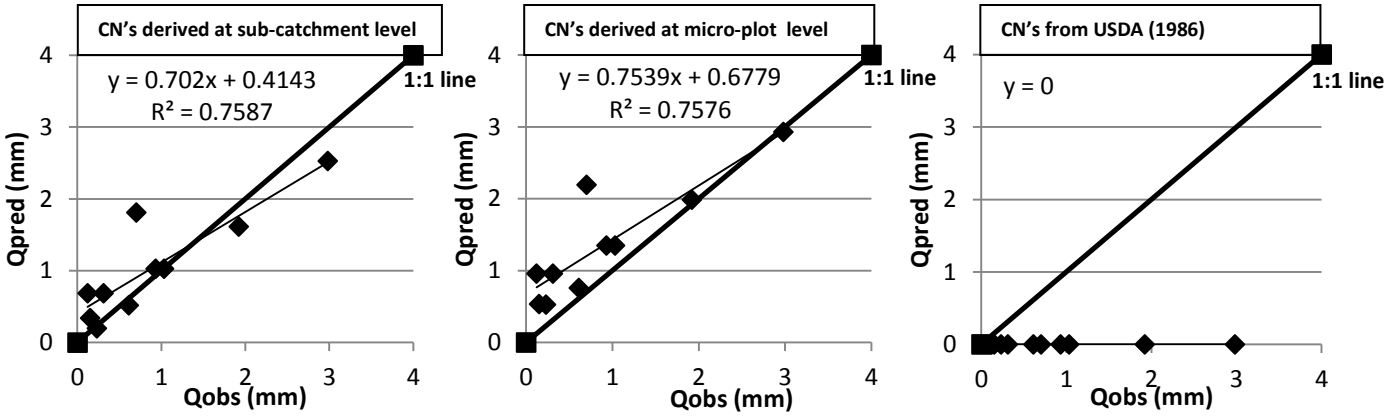

Figure 4.29 Qobs-Qpred plots of the runoff values. Left: using CN's derived at sub-catchment level (λ = 0.05), middle: using CN's derived at micro-plot level (λ = 0.05), right: using CN's found in the literature (USDA, 1986) (λ = 0.2).

4.3 Catchment

Soil Texture

The soil texture of the 16 sample points located throughout the Mayleba catchment were analysed using finger test identification and laser diffractometry methods. These soil textures are compared with the soil texture map using the sample point's location (Figure 4.30, Table 4.17). There is not much variation in the results of the soil texture using the laser diffractometry method, again almost all soil textures were measured as silty loam. This was previously discussed in paragraph 4.1.1. The correlation between the finger test identification method and the soil texture map is reasonable. A few textures determined by finger test felt more grainy than expected from the soil texture map Also, the two soil texture classes 'Heavy Clay' and 'Clay_SiltyClay' from the soil texture map are not clearly distinguished with the finger test identification method. Reference is made to paragraph 4.1.1 for more detailed elaboration.

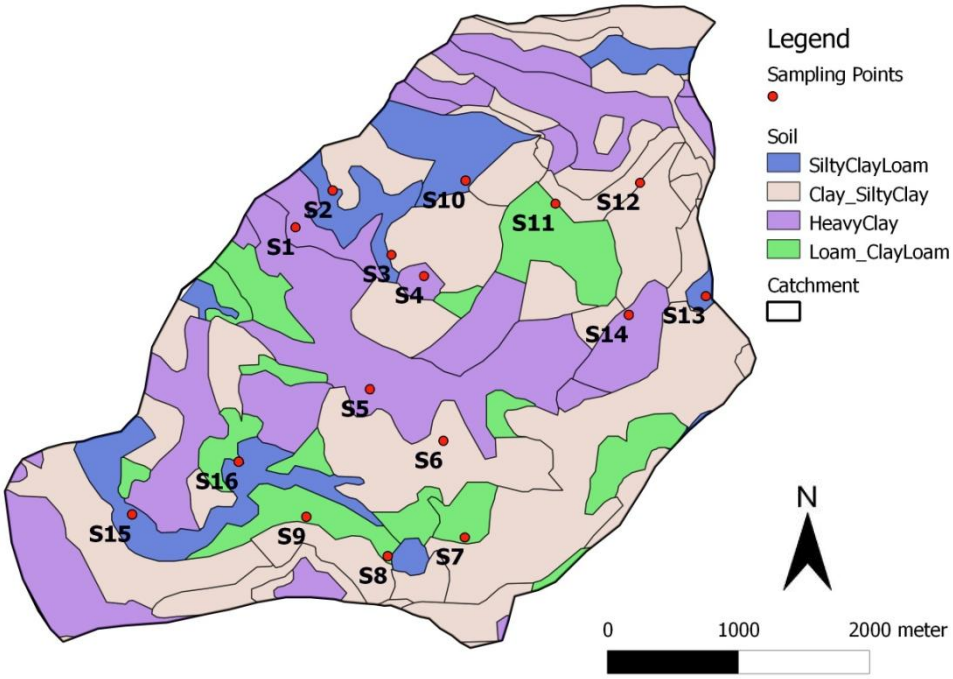

Figure 4.30 Soil texture map of Mayleba with location of the 16 sampling points

Table 4.17 Soil texture of the 16 sample points in the Mayleba catchment, determined by the coulter method, finger test identification and from the soil texture map of Van de Wauw (2005).
The textures determined by finger test identification that do not fully correspond to the soil texture map are in gray boxes are. Sample points are not ranked from 1 to 16 but are grouped per soil texture group according to the soil texture map.

Sample	Laser Diffractometry	Finger Test Identification	Soil Texture Map
S1	silty loam	Heavy Clay	Heavy Clay
S4	silty loam	Heavy Clay	Heavy Clay
S5	silty loam	Clay	Heavy Clay
S14	Loam	Clay	Heavy Clay
S3	silty loam	Clay	Clay_SiltyClay
S6	silty loam	Silty Clay	Clay_Siltyclay
S11	loam	Sandy Loam	Clay_Siltyclay
S12	silty loam	Clay	Clay_Siltyclay
S2	silty loam	Silty Clay Loam	Silty Clay Loam
S10	silty clay loam	Sandy Clay Loam	Silty Clay Loam
S13	silty loam	Silty Clay Loam	Silty Clay Loam
S15	silty loam	Silty Clay Loam	Silty Clay Loam
S7	silty loam	Loam	Loam_ClayLoam
S8	silty loam	Clay Loam	Loam_ClayLoam
S9	silty clay loam	Sandy Loam	Loam_ClayLoam
S16	silty loam	Sandy Loam	Loam_ClayLoam

Water holding capacity and bulk density

Table 4.18 shows the observed land use at each sample point and the soil texture determined using finger test identification. The saturated water content (SAT), field capacity (FC), permanent wilting point (PWP) and bulk density (BD) that were measured in the soil laboratory at Mekelle University are also in this table. The SAT, FC and PWP were measured as gravimetric moisture content (%Wt) and converted to volumetric moisture content (%Vol) using the measured bulk density in Table 4.18.

The SAT, FC, PWP and BD that were estimated using the soil water characteristic equations developed by Saxton and Rawls (2006). These estimates were based on the soil texture by finger test identification. Estimates based on the sand and clay percentages retrieved from the laser diffractometry were also calculated.

The available water was calculated as the soil moisture content at field capacity minus the soil moisture at permanent wilting point (Table 4.19). By calculating the root mean square error (RMSE) of available water between laboratory results and the estimations, the two estimations can be compared. The estimation based on soil texture using finger test identification has a much lower RMSE (1.84 %Vol) than the estimation based on texture percentages retrieved from laser diffractometry (RMSE = 22.24 %Vol). This implies a better estimation of soil texture using finger test identification, than the laser diffractometry method with no pre-treatment of the soil. However, it

must also be noted that the laboratory analysis of PWP may not be accurate. This is due to possible variations in the high pressure that was applied for the PWP analysis.

Table 4.18 Observed land use and soil texture at the 16 sample points throughout the catchment. The saturated water content (SAT), field capacity (FC), permanent wilting point (PWP) and bulk density (BD) were measured in the soil laboratory of Mekelle University. Water holding capacity (WHC) calculated as the difference of FC and PWP.

Sample point	Land use	Soil Characteristics					
		Soil Texture	SAT (%Vol)	FC (%Vol)	PWP (%Vol)	BD (g/cm³)	**Available water** (%Vol)
S1	Cropland, wheat	Heavy Clay	62.30	38.61	21.22	1.21	17.39
S2	Grazing land	Silty Clay Loam	41.76	26.10	10.02	1.26	16.08
S3	Cropland, wheat	Clay	35.61	29.40	17.76	1.27	11.64
S4	Cropland, wheat	Heavy Clay	52.86	47.88	34.69	1.36	13.19
S5	Cropland, wheat	Clay	40.92	33.25	20.14	1.14	13.11
S6	Cropland, wheat	Silty Clay	43.85	29.05	14.24	1.34	14.81
S7	Cropland, wheat	Loam	56.89	29.26	18.81	1.22	10.45
S8	Cropland, wheat	Clay Loam	44.13	27.26	16.19	1.39	11.07
S9	Grazing land	Sandy Loam	41.86	27.91	15.34	1.47	12.56
S10	Cropland, barley	Sandy Clay Loam	58.62	31.52	19.91	1.11	11.61
S11	Cropland, lentil	Sandy Loam	39.34	12.90	8.77	1.33	4.13
S12	Cropland, lentil	Clay	60.16	27.75	13.11	1.13	14.64
S13	Grazing land, very compact	Silty Clay Loam	60.48	27.92	16.67	1.50	11.25
S14	Cropland, hamfets	Clay	44.90	20.46	13.35	1.08	7.11
S15	Cropland, wheat and grass	Silty Clay Loam	69.92	31.60	15.48	1.12	16.11
S16	Grazing land, very stony	Sandy Loam	74.42	missing	14.71	1.19	/

Table 4.19 Available water of the 16 sample points throughout the Mayleba catchment, measured from laboratory results (lab), estimation based on soil texture by finger test identification (finger test) and estimation based on soil texture by laser diffractometry (laser diffr.). RMSE between lab results and estimations are at the bottom of the table.

Sample point	**Available water (lab) (%Vol)**	**Available water (finger test) (%Vol)**	**Available water (laser diffr.) (%Vol)**
S1	17.39	11.00	19.30
S2	16.08	16.90	19.50
S3	11.64	12.10	18.60
S4	13.19	11.00	18.80
S5	13.11	12.10	17.20
S6	14.81	13.80	20.70
S7	10.45	14.10	19.50
S8	11.07	13.70	19.70
S9	12.56	9.80	17.20
S10	11.61	10.00	18.00
S11	4.13	9.80	12.60
S12	14.64	12.10	17.90
S13	11.25	16.90	17.20
S14	7.11	12.10	15.90
S15	16.11	16.90	19.20
S16	/	9.80	19.40
RMSE (%Vol)		**1.84**	**22.24**

Due to compactation, the bulk density measured in the soil laboratory of Mekelle University is expected to be higher than the estimated bulk density when the land use type is grazing land. Sample points S2, S9, S13 and S16 are located on grazing land. S2 and S9 have a higher BD on field, especially the BD of S9 is much higher. The high degree of compactation for S9 was noticed in the field when taking samples. The laboratory measurements of BD for S16 were lower than estimated. However, S16 was a severely compacted soil and core sampling was difficult. The lower BD measured can be explained by the high stoniness of the soil influencing the BD measurement. On reflection it might have been necessary to correct the bulk densities for stones. Although this was not done, it can be mentioned that stones were highly avoided when taking samples. For cropland sites this was not a difficulty whereas for grazing land sites the soils were often extremely compact and contained many rock fragments.

Condition of SWC measures and hydrological condition

Observations of the condition of soil and water conservation (SWC) measures and the hydrological condition (good, average and poor) of the Mayleba catchment were used to make maps to visualise these conditions spatially. Observations were recorded by M.Sc student Sylvain Trigalet, in August 2011. In Figure 4.31 and Figure 4.32 the SWC conditions and hydrologic conditions are spatially presented. Both maps were made using Kriging and application of pseudocolours for interpretation. These conditions are linked spatially. Along the North of the central drainage line most areas are found with good SWC condition and good hydrological condition. This implies the positive impact of SWC measures on hydrological condition.

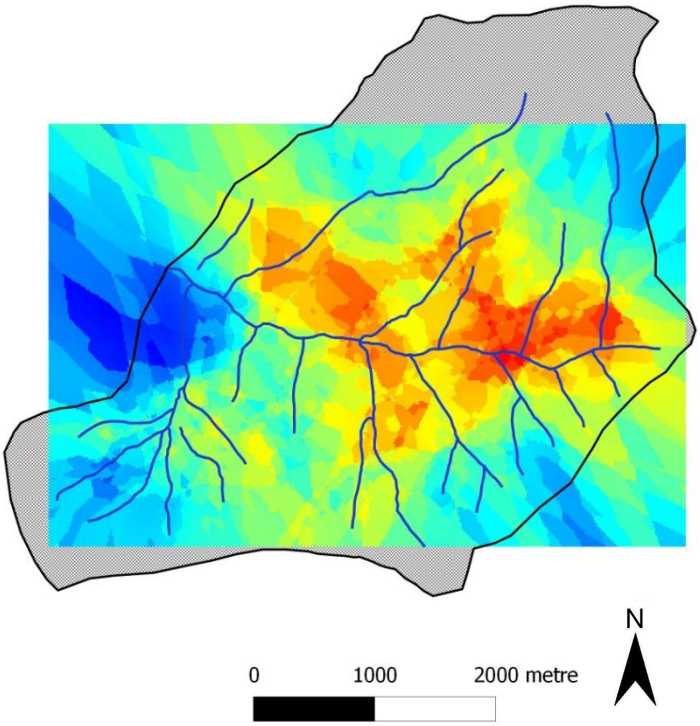

Figure 4.31 Condition of the soil and water conservation (SWC) measures in the Mayleba catchment, more red colours indicate good conditions, from yellow over green to blue colours indicate worse conditions or absence of SWC. In the gray areas no conditions were recorded.

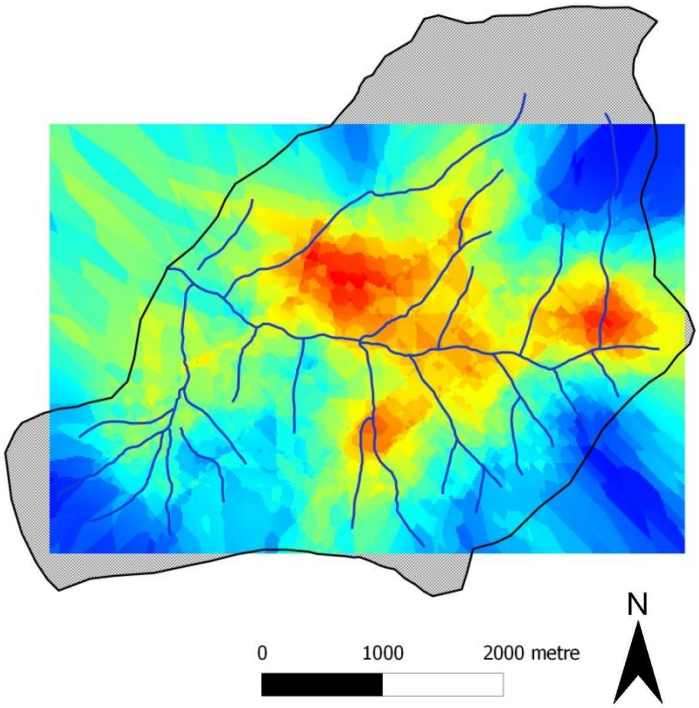

Figure 4.32 Hydrological condition of the Mayleba catchment, more red colours indicate good conditions, from yellow over green to blue colours indicate worse conditions. In the gray areas no conditions were recorded.

Upscaling - towards a generalisation

The specific objectives of this research have been explored:

- Investigation of the influence of land use, soil texture and slope on the rainfall-runoff (P/R) relationships.
- Derivation of curve numbers based on the rainfall-runoff data at micro-plot level (1 m²).
- Verification of the derived curve numbers at sub-catchment level (0.4 km²).

By combining the available and recorded data at catchment, sub-catchment and micro-plot level an attempt towards a generalisation of the hydrological characteristics of the catchment is the next challenge. This is motivated by the overall objectives:

- To understand the hydrological behaviour of small catchments (5 - 20 km²), this to improve the design and spatial implementation of water harvesting systems and soil and water conservation measures.
- To come to realistic estimates of water supply, this in order to apply water resource planning more accurately and avoid oversized reservoirs.

To steer this study in the direction of these overall objectives, the Mayleba catchment was looked at in its whole. Using the soil map (Figure 2.7), soil texture map (Figure 4.30), land use map (Figure 2.8), geological and geomorphologic map (Figure 2.6) and the two previous maps of SWC condition and hydrological condition (Figure 4.31, Figure 4.32), some general trends could be observed.

On areas with better SWC condition a better hydrological condition is observed, this is mainly along the North side of the central drainage line. In these lower landscape areas, soil texture is heavier and soils have more vertic properties. These areas correspond to vertic clay flows and displaced basaltic material according to the geomorphologic map. Combined, these characteristics provide adequate circumstances for agriculture which is confirmed by the land use map.

On the other hand, areas with worse SWC condition and bad hydrological condition can be observed in the South-West of the catchment. Soil textures are lighter and Leptosols and Regosols are often occurring on the steeper slopes, Cambisols on the flatter slopes. The parent material here is limestone. These areas are more often used for grazing land, housing and some cropland.

On sub-catchments consisting mainly of poor SWC and hydrological conditions, compacted soil and high percentage of grazing land, a high runoff response is expected (Table 4.5, Figure 4.14). These sub-catchments can be used for implementation of small reservoirs at the outlet for water harvesting.

If the SWC and hydrological condition is extremely poor and a bad situation of degradation is observed, then the implementation of exclosures can be considered. Due to the regeneration of vegetation, troublesome excessive runoff can be significantly reduced when compared to runoff production on grazing land (Descheemaeker *et al*., 2006).

Final reflections

In general, the CN's derived at micro-plot level are high, which implies a high runoff generation. This is surprising as the micro-dams often remain unfilled. Is this inconsistency due to oversized dams, or are the CN's erroneous?

When using CN's derived from micro-plot level (1 m^2) the scaling effects lead to overestimations of runoff. Also the influence of SWC measures was not taken into account. However, the effects of SWC measures on runoff production were intrinsically taken into account in the CN's derived at sub-catchment level, which were also high. Moreover, Descheemaeker *et al*. (2008) found high CN's for grazing land in this area.

When considering oversized micro-dams, the overestimation of runoff production also leads to overestimations of design discharge. This results in micro-dams with too large dimensions. Extrapolation of runoff production over larger areas can also cause overestimations due to certain characteristics in the catchment that account for runoff losses, such as the influence of SWC measures, river losses and evaporation. Also, during dry years, when lower rainfall depths are reached than the dependable rainfall used in the design, the micro-dams will collect less runoff.

For water harvesting, a high runoff coefficient is desirable, but a high runoff can cause problems in the catchment due to the erosion prone hill slopes. This problem of land degradation is reduced due to soil and water conservation measures applied in the catchment and decreases the micro-dam sedimentation. These SWC measures however result in a decrease of runoff and thus lower water harvesting potential of reservoirs.

More research is necessary to gain a better understanding of these effects on small catchments. Quantitative and qualitative knowledge can help improve the design and allow more careful spatial implementation of water harvesting systems and soil and water conservation measures.

Part III

5 CONCLUSION & SCOPE FOR FURTHER RESEARCH

5.1 Conclusion

To summarize the intermezzo conclusions of the previous paragraph the hypotheses are recalled.

Hypothesis A: Variations of rainfall-runoff relationships within replicate micro-plots (1 m²) occur due to minor differences in characteristics such as random roughness, stoniness and slope.

From the results it was clear that the replicate micro-plots did not respond identically to rainfall. Due to the amount of both static and dynamic characteristics of the micro-plots, the variation could not unambiguously be explained. When the micro-plots were investigated individually the differences between replicates were not significant (Figure 4.17, Figure 4.18). This in fact proves that they suffice as good replicates. For further calculations replicates were grouped and average values were taken (n = 3) to smooth out variations. Error bars were used for assuredness of results.

More generally, the effect of several micro-plot characteristics on the rainfall-runoff relationships, between experimental sites, could be observed and clarified (see next hypothesis).

Hypothesis B: Slope and soil texture have a larger effect on the rainfall-runoff relationships than the antecedent moisture content (AMC).

The most pronounced influences on the two descriptors of the rainfall-runoff relationships are recalled.

Influences on runoff response, alpha:
Variations of alpha were mainly caused by differences in *land use*. A higher degree of soil compactation on grazing land increased the runoff response significantly. The effect of *soil texture* was lower than the influence of land use. Limestone derived soils with a higher clay content showed higher alphas. On the experimental site with soil derived from displaced basaltic material a higher alpha was recorded than on the limestone derived soils, even though it had a slightly lighter soil texture. This possibly indicates the important influence of *parent material* on rainfall-runoff relationships. The number of observations on this experimental site was very low and should be investigated in more detail before drawing conclusions. Contrary to expectations the *slope* merely influenced the runoff response (Figure 4.14). Also, no clear trend was found on the influence of *AMC* (Figure 4.20). The *soil roughness factors* showed an inverse proportional influence on runoff response.

Influences on precipitation threshold P_T:

The slope had the largest impact on precipitation threshold (Figure 4.15). Steeper slopes reduced P_T and induced faster runoff initiation. Soil texture only slightly influenced the P_T, a higher clay content induced a faster runoff initiation. Contrary to expectations a higher vegetation cover reduced P_T, but not significantly (Figure 4.23). Assumptions were made to try and explain this, such as the higher moisture content in soils when vegetation cover is higher and the swell shrink properties of the soils. Again, no clear trend is observed due to AMC on P_T.

Hypothesis C: Curve numbers, deduced from P/R data of micro-plots (1 m²), applied to a sub-catchment (0.4 km²) give an overestimation of runoff.

Application of curve numbers derived from micro-plots indeed gave an overestimation of runoff when applied to a larger area (Figure 4.29 - middle). This effect is known as the scaling effect (Van de Giesen *et al*., 2011). Another factor that most likely increased the overestimation is the fact that SWC measures were not taken into account in these CN's derived at micro-plot level. SWC measures increase infiltration and spread runoff in time (Nyssen *et al*., 2010). However, the derived curve numbers correlated well with those found by Descheemaeker *et al*. (2008) on plots with dimensions 5 m x 2 m, and with those found by M.Sc student Sylvain Trigalet at sub-catchment scale, both studies conducted in the Dogu'a Tembien district of Tigray.

Overall conclusion

It is very complex to simultaneously take many possible explanatory variables of rainfall-runoff relationships into account at once. Static and dynamic variables can induce opposing influences, changing throughout the season. These combined effects, measured on-field, however give a view on the real life circumstances. Overall, the land use seems most important, where runoff is significantly increased on compacted grazing land as opposed to cropland (Figure 4.14).

The derived CN's are plausible and call for further exploration. Quantifying the water harvesting potential of small catchments requires more research to further investigate explanatory variables at micro-plot level, but also variables that occur over larger areas. These include the soil and water conservation measures and river losses. This leads to the design of more optimal reservoir dimensions due to more accurate estimates of runoff.

5.2 Scope for further research

Areas for improvement

The instantaneous rainfall-runoff measurements were not successful. Depending on the goal of these measurements, using rainfall simulators can provide constant rainfall intensities. This can be of interest to e.g. record the effect of rainfall intensity on the rainfall-runoff relationships for different treatments. In view of recording final infiltration rates other methods such as the double ring infiltrometer can be used. Also, to improve accuracy of instantaneous runoff measurements, volumetric discharge can be recorded rather than runoff depth in a runoff collector.

For quantitative soil textural analysis it is important to remove carbonates and organic matter, as well as to disperse the soil adequately for correct classification of particles during analysis.

Follow-up

Expansion and improvement of the data series over several years can help gain insights of climatologic variability and is necessary to attain more reliable data and provide more decisive conclusions for future management. Also the influence of parent material on rainfall-runoff relationships seems interesting to further investigate as in this study remarkable features were noticed for the experimental site on displaced basaltic material. Due to the few measurements and large standard deviation no conclusions could be drawn.

New idea's

The latest images of Google earth for the Mayleba catchment date from 28/06/11. Towards Mekelle the images are even more recent: 12/07/11. This is interesting due to their improved quality, trenches and stone bunds are easily observed and distinguished from each other. This can be used for mapping the SWC structures. Also the experimental sites of PhD student Gebeyehu Taye are visible to large detail.

When the influences on runoff production are quantified for a large amount of explanatory variables such as land use, soil texture, slope, vegetation cover and SWC measures, then it could be possible to make a model where these explanatory variables are used as input (mapping tools) and runoff depth at a defined point can be simulated for a certain rainfall depth. Simulating the effect of addition of SWC structures or a change in land use can be of interest for future water resource planning and land management. This could be combined with the WaTEM/SEDEM model for soil erosion and sediment delivery (Van Oost *et al*., 2000; Van Rompaey *et al*., 2001).

BIBLIOGRAPHY

Asmelash, T., Dejenie, T., Declerck, S., Nyssen, J., Van der Gucht, K., Risch, S., Rousseaux, S., De Wit, J., Mulugeta, A., Haregeweyn, N., Gebrekidan, A., Poesen, J., Deckers, J., Vyverman, W., De Meester, L., **2007**. Ecological Atlas of reservoirs in Tigray, Northern Ethiopia. Tigray Livelihood Papers No 4. VLIR-Mekelle University, IUC Programme, 83 pp.

Beuselinck, L., Govers, G., Poesen, J., Degraer, G. and Froyen, L., **1998**. Grain-size analysis by laser diffractometry: comparison with the sieve-pipette method. Catena 32, 193-208

Bosellini, A., Russo, A., Fantozzi, P.L., Getaneh, Assefa, Solomon, Tadesse, **1997**. The Mesozoic succession of the Mekele outlier (Tigre Province, Ethiopia). Memorie di Scienze Geologiche 49, 95–116

CIA – The World Factbook **2012** [online]. Available on https://www.cia.gov/library/publications/the-world-factbook/geos/et.html. [Date of access: 02/04/2012]

Conway, D., Schipper, E.L.F., **2011**. Adaptation to climate change in Africa: Challenges and opportunities identified from Ethiopia. Global Environmental Change, 21 (1), 227‑237

Corbeels, M., Abebe, S., Mitiku, H., **2000**. Farmers' knowledge of soil fertility and local management strategies in Tigray, Ethiopia. Managing Africa's Soils No. 10

Critchley, W., Siegert, K., Chapman, C., **1991**. A Manual for the Design and Construction of Water Harvesting Schemes for Plant Production. Food and Agriculture organisation of the United Nations, Rome, Italy

CSA – Central Statistics Agency of Ethiopia, **2007** [online]. Available on http://www.csa.gov.et/ [Date of access: 04/04/2012]

De Wit, J., **2003**. Stuwmeren in Tigray (Noord-Ethiopie): Kenmerken, Sedimentatie En Sedimentbronnen. M.Sc Thesis, Faculty of Geography, K.U.Leuven, Leuven

DeltaLINK (version 2.6, 2011) software package from Delta T devices©

Descheemaeker, K., Nyssen, J., Poesen, J., Raes, D., Mitiku Haile, Muys, B., Deckers, J., **2006**. Runoff processes on slopes with restored vegetation: a case study from the semi-arid Tigray highlands, Ethiopia. Journal of Hydrology, 331, 219–241

Descheemaeker, K., Poesen, J., Borselli, L., Nyssen, J., Raes, D., Mitiku Haile, Muys, B., Deckers, J., **2008**. Runoff curve numbers for steep hillslopes with natural vegetation in semi-arid tropical highlands, northern Ethiopia. Hydrological processes, 22, 4097-4105

Descheemaeker, K., Raes, D., Nyssen, J., Poesen, J., Mitiku Haile & Deckers, J. **2009**. Changes in water flows and water productivity upon vegetation regeneration on degraded hillslopes in northern Ethiopia: a water balance modelling exercise. Rangeland Journal 31(2), 237-259

Edwards, S, Gebre Egziabher, T. and Araya, H., **2011**. Success and challenges in ecological agriculture: experience from Tigray, Ethiopia. Climate change and Food system Resilience. Food and Agriculture organisation of the United Nations, Rome, Italy, 231-294

FAO, **2006**. Guidelines for soil description. Fourth edition. Food and Agriculture organisation of the United Nations, Rome, Italy, 96 pp.

FAO, **2010**. CLIMPAG | DATA and MAPS | New_LocClim: Local Climate Estimator [online]. Available on http://www.fao.org/nr/climpag/pub/en3_051002_en.asp [Date of access: 08/04/2012]

Fekadu Bekele, **1997**. Ethiopian Use of ENSO Information in Its Seasonal Forecasts. Ethiopian National Metrological Services Agency, Addis Ababa, Ethiopia [online]. Available on http://ccb.colorado.edu/ijas/ijasno2/bekele.html, [Date of access: 06/04/2012]

García Moreno, R., Díaz Álvarez, M.C., Tarquis Alonso, A., Barrington, S., Saa Requejo, A., **2008**. Tillage and soil type effects on soil surface roughness at semiarid climatic conditions. Soil & Tillage research 98, 35-44

Gebreyohannes, G., Nyssen, J., Poesen, J., Bauer, H., Merckx, R., Mitiku, H. Deckers, J., **2012**. Land reclamation using reservoir sediments in Tigray, Northern. Soil use and Management 28, 113-119

Govers, G., Van Orshoven, J., 2011. Cursus tekst Geographican Information Systems, ION62A

Hagos Fitsum, Pender J. and Nega Gebreselassie. **2002**. Land degradation and strategies for sustainable land management in the Ethiopian highlands: Tigray Region. (Second edition). Socio-economics and Policy Research Working Paper 25. ILRI (International Livestock Research Institute), Nairobi, Kenya. 80 pp.

Hawkins, R.H., Woodward, D.E., Hjelmfelt, A.T., Van Mullem, J.A., Quan, Q.D., **2002**. Runoff curve number method: examination of the initial abstraction ratio. In Hydrologic Modeling for the 21st Century. Second Federal Interagency Hydrologic Modeling Conference. Las Vegas, Nevada, USA.

Hawkins, R.H., Ward, T.J., Woodward, D.E., Van Mullem, J.A., **2010**. Continuing evolution of Rainfall-Runoff and the curve number precedent. 2nd Joint Federal Interagency Conference, Las Vegas, Nevada, USA.

Helland, K., Berntsen, H. E., Borgen, O.S., Martens, H., **1991**. Recursive algorithm for partial least squares regression Chemometrics and Intelligent Laboratory Systems, 14, 129-137

IMWI, **2007**. Water for Food, Water for Life: A Comprehensive Assessment of Water Management in Agriculture. Earthscan, London, UK & International Water Management Institute (IWMI), Colombo, USA. 688 pp.

Ismail, S.M., Ozawa, K., **2007**. Improvement of crop yield, soil moisture distribution and water use efficiency in sandy soils by clay application, Applied Clay Science 37: 81–89

Karcher, D.E., Richardson, M.D., **2005**. Batch analysis of digital images to evaluate turfgrass characteristics. Crop Science 45, 1536-1539

Lal, R., **1997**. Residue management, conservation tillage and soil restoration for mitigating greenhouse effect by CO,-enrichment. Soil and Tillage research 43: 87-108

Loizeau, J.L., Arbouille, D., Santiago, S., Vernet, J.-P., **1994**. Evaluation of a wide range laser diffraction grain-size analyser for use with sediments. Sedimentology 41, 353–361

n.n., 2004. Determination of particle size distribution in mineral soil material. Laboratorium voor bodem en water, FBIW, K.U.Leuven.

Nyssen, J., Poesen, J., Mitiku Haile, Moeyersons, J. and Deckers, J. **2000**. Tillage erosion on slopes with soil conservation structures in the Ethiopian highlands. Soil and Tillage Research 57, 115-127

Nyssen, J., Moeyersons, J., Poesen, J., Deckers, J. and Mitiku Haile, **2003**. The environmental significance of the remobilisation of ancient mass movements in the Atbara-Tekeze headwaters, Northern Ethiopia. Geomorphology 49 (3-4): 303-322

Nyssen, J., Poesen, J., Moeyersons, J., Deckers, J., Mitiku Haile, Lang A., **2004a**. Human impact on the environment in the Ethiopian and Eritrean Highlands – a state of the art. Earth Science Reviews, 64/3-4, 273-320

Nyssen, J., Veyret-Picot, M., Poesen, J., Moeyersons, J., Mitiku Haile, Deckers, J., Govers G., **2004b**. The effectiveness of loose rock check dams for gully control in Tigray, northern Ethiopia. Soil Use and Management 20, 55-64

Nyssen, J., Vandenreyken, H., Poesen, J., Moeyersons, J., Deckers, J., Mitiku Haile, Salles, C., Govers, G., **2005**. Rainfall erosivity and variability in the Northern Ethiopian Highlands. Journal of Hydrology 311, 172-187

Nyssen J., Descheemaeker, K., Nigussie Haregeweyn, Mitiku Haile, Deckers, J., Poesen, J., **2007a**. Lessons learnt from 10 years research on soil erosion and soil and water conservation in Tigray. Tigray Livelihood Papers No. 7, Mekelle: Zala-Daget Project, Mekelle University, K.U.Leuven, Relief Society of Tigray, Africamuseum and Tigray Bureau of Agriculture and Rural Development, 53 pp.

Nyssen, J., Poesen, J., Gebremichael, D., Vancampenhout, K., D'aes M., Yihdego, G., Govers, G., Leirs, H., Moeyersons, J., Naudts, J., Haregeweyn, N., Haile M., Deckers, J. **2007b**. Interdisciplinary on-site evaluation of Stone bunds to control soil erosion on cropland in northern Ethiopia. Soil and Tillage Research 94, 151-163

Nyssen, J., Clymans, W., Descheemaeker, K., Poesen, J., Vandecasteele, I., Vanmaercke, M., Amanuel Zenebe, Van Camp, M., Mitiku Haile, Nigussie Haregeweyn, Moeyersons, J., Martens, K., Tesfamichael Gebreyohannes, Deckers, J., Walraevens, K., **2010**. Impact of soil and water conservation on catchment hydrological response - a case in north Ethiopia. Hydrological Processes, 24(13), 1880-1895

Poesen, J., Torri, D. and Bunte, K., **1994**. Effects of rock fragments on soil erosion by water at different spatial scales: a review. Catena 23, 141-166

Poesen, J., van Wesemael, B., Bunte, K. and Solé Benet, A. **1998**. Variation of rock fragment cover and size along semiarid hillslopes: a case-study from southeast Spain. Geomorphology 23, 323-335

Quantum GIS (Q-GIS) version 1.5.0-Tethys, **2008**. Built against code revision 13923M

R version 2.14.2, **2012**. The R Foundation for Statistical Computing

Raes, D., Wilems, P., and Gbaguidi, F., **2006**. RAINBOW – A software package to compute frequency analysis and perform testing of homogeneity on hydrometeorological data sets.

Saxton, K.E., Rawls, W.J., **2006**. Soil Water Characteristic Estimates by Texture and Organic Matter for Hydrologic Solutions. Soil Science Society of America Journal 70, 1569–1578

SPSS 16.0, **2007**. SPSS for windows, release 16.0. SPSS Inc.

Sorbie F., van Wesemael B., Teka D., Poesen J., Deckers J., **2012**. Hydrological characterisation of the Mayleba catchment for evaluation of water harvesting potential in an irrigation reservoir Tigray, Ethiopia. Day of young soil scientists, 22 February, 2012, Brussels, Belgium

UN-Water, **2007**. Coping with water scarcity - Challenge for the twenty-first century [online]. FAO, Land and Water Development Department, Rome, Italy. Available at: http://www.fao.org/nr/water/docs/escarcity.pdf [Date of access: 06/04/2012]

USDA-SCS (U.S. Department of Agriculture-Soil Conservation Service), **1972**. SCS National Engineering Handbook, Section 4, Hydrology. Chapter 10, Estimation of Direct Runoff From Storm Rainfall. U.S. Department of Agriculture, Soil Conservation Service, Washington, D.C., pp. 10.1-10.24

USDA-NRCS (United States Department of Agriculture - Natural Resources Conservation Service), **1986**. Urban Hydrology for Small Watersheds, Technical Release-55, second edition, 164 pp.

USDA (United States Department of Agriculture) Soil Survey Staff, **2003**. Keys to soil taxonomy. Ninth edition. Washington, DC, Natural Resources Conservation Service, USDA, 322 pp.

Van de Wauw, J., **2005**. Soil-landscape relationships in the basalt-dominated highlands of Tigray, Ethiopia. Unpublished Msc Thesis. K.U.Leuven, 127 pp.

Van de Wauw, J., Baert G., Moeyersons J., Nyssen J., De Geyndt K., Nurhussen T., Amanuel Z., Poesen J., Deckers J., **2008**. Soil-landscape relationships in the basalt dominated highlands of Tigray, Ethiopia. Catena 75 (1), 117-127

Van de Giesen, N., Stomph, T.J., Ajayi, A.E., Bagayoko, F., **2011**. Scale effects in Hortonian surface runoff on agricultural slopes in West Africa: Field data and models. Agriculture, Ecosystems and Environment 142, 95-101

van Wesemael, B., Poesen, J., De Figueiredo, T., Govers, G., **1996.** Surface roughness evolution of soils containing rock fragments. Earth surface processes and landforms 21, 399-411

van Wesemael, B., Poesen, J., Kosmas, C., Danalatos, N.G. and Nachtergaele, J. **2002**. The impact of rock fragments on soil degradation and water conservation. In Geeson, N.A., Brandt, C.J. and Thornes, J.B. (eds.). Mediterranean Desertification: A mosaic of Processes and Responses. John Wiley, Chichester, U.K., 131-145 pp.

Van Oost, K., Govers, G., Desmet, P.J., **2000**. Evaluating the effects of changes in landscape structure on soil erosion by water and tillage. Landscape Ecology 15, 577-589.

Van Rompaey, A., Verstraeten, G., Van Oost, K., Govers, G., Poesen, J., **2001**. Modelling mean annual sediment yield using a distributed approach. Earth Surface Processes and Landforms 26 (11), 1221-1236

Vancampenhout, K., Nyssen, J., Gebremichael, D., Deckers, J., Poesen, J., Mitiku Haile and Moeyersons, J., **2006**. Stone bunds for soil conservation in the northern Ethiopian highlands: impacts on soil fertility and crop yield. Soil and Tillage Research 90, 1-15

Verachtert, E., Smets, T., Langhans, C., **2011**. Handleiding practicum geomorfologische processen. Afdeling Geografie, K.U.Leuven, 58 pp.

World Atlas, 2012. Map of Ethiopia – Ethiopia Map, Ethiopia information – World Atlas, [online]. Available on http://www.worldatlas.com/webimage/countrys/africa/et.htm [Date of access: 02/04/2012]

NEDERLANDSE SAMENVATTING

In de hooglanden van Ethiopië werden tijdens het voornaamste regenseizoen van 2011 de neerslag-afvoer relaties onderzocht op 24 micro-plots van 1 m². Deze studie werd uitgevoerd om het hydrologische karakter van kleine stroomgebeiden (5 – 20 km²) beter te begrijpen en om een meer realistische begroting te bekomen van het wateropvangpotentieel.

De micro-plots werden verdeeld over acht experimentele sites binnen het Mayleba stroomgebied (17 km²), elke site bestond uit drie replica micro-plots. Zowel akkerland als graasland werden beschouwd, evenals drie bodemtextuurklassen en drie hellingsklassen. Een aantal kenmerken van de individuele micro-plots werden opgenomen: de stenigheid, de bodemruwheid, de vegetatiebedekking, de vegetatiehoogte, de bodemtextuur en de helling. De invloed van deze kenmerken werd nagegaan op de afvoerproductie.

Om het effect van voorgaande kenmerken op de neerslag-afvoer relaties te beschrijven werden de afvoerrespons, α, en de neerslag drempelwaarde, P_T, gedefinieerd. Het landgebruik en de bodemruwheid hadden de grootste impact op de afvoer respons, terwijl deze niet echt werd beïnvloed door de helling. De helling had echter wel een grote impact op de neerslag drempelwaarde, die ook beïnvloed werd door de bodemruwheid.

'Curve numbers' (CN) werden afgeleid uit de bekomen data van de micro-plots om de afvoer te voorspellen. Deze werden vervolgens toegepast op een sub-stroomgebied binnen het Mayleba stroomgebied ter verificatie. Op een grotere oppervlakte gaf deze toepassing een overschatting van de afvoer. Deze schattingen waren echter nauwkeuriger dan wanneer men de 'curve numbers' uit de literatuur gebruikte. Dit wijst op het voordeel van het bepalen van gebiedspecifieke 'curve numbers' voor verdere toepassingen.

Realistische schattingen van het wateropvangpotentieel dragen bij tot het verbeteren van de planning der watervoorraden om overmaatse reservoirs te voorkomen en de lokale bevolking te voorzien van water tijdens droge periodes.

Trefwoorden: Noord-Ethiopië, hooglanden, semi-aried, waterwinning, irrigatie reservoirs, neerslag-afvoer relaties, curve numbers, afvoer reactie, neerslag drempelwaarde

Appendix

Contents of CD-ROM[3]

The data set used and analysis performed for the elaboration of this thesis can be found on the CD-ROM.

MICRO-PLOTS

Gereral characteristics:

- Coordinates (Adindan UTM zone 37N)
- Dimensions, area calculations, gutter areas, slope
- Rock fragment cover: point-method, transect-method and visual estimate
- Vegetation height, random roughness
- Photographs

Rainfall-runoff data per 3 min for rainfall events between 27/07/11 and 23/09/11:

- Volume-depth relationship for runoff in collector
- Regression analysis (with α's and P_T's)
- Daily rainfall measurements for the eight experimental sites
- Rainfall data W2 site, weather station dam
- Data raingage walka weather station intensity

Moisture data (theta probes - open with DeltaLINK software package from Delta T devices©).

Photographs used for vegetation cover analysis with SigmaScan Pro©

Texture laser diffractometry (KULeuven)

Texture finger test identification

SUB-CATCHMENT

Rainfall-runoff data of sub-catchment MLRMT5

Boundary of sub-catchment MLRMT5

Hydrological Response Units of MLRMT5

Runoff calculations using 3 sets of CN's

[3] Inexhaustive list

CATCHMENT

Soil characteristics measured in Mekelle University and from Soil water characteristics calculator

- Saturated water content,
- Field capacity
- Permanent wilting point
- Bulk density

Texture by finger test identification

Texture measured with laser diffractometry at KULeuven

SWC condition and Hydrological condition along transects

OTHER

PDF version of this Master thesis

Read-me file with explanatory file of data set

Solver Add-in explanation for iterative CN derivation

Shape files and raster files of the Mayleba catchment

R Script for PLSR

For copyright reasons this CD-ROM is available upon request:

Prof. Dr. B. van Wesemael
Georges Lemaître Centre for Earth and Climate Research
Earth and Life Institute
Université Catholique de Louvain
email: bas.vanwesemael@uclouvain.be

Prof. Dr. Ir. J.A. Deckers
Department of Earth and Environmental Sciences
Soil- and Water engineering division
Catholic University of Leuven
email: seppe.deckers@ees.kuleuven.be

Information Chart

Summary of the micro-plot characteristics

	Land use	Slope	Replicate	Site code	Micro-plot code	Soil texture	Slope (%)	Rock fragment cover (%)
To see effect of slope & to see effect of land use	Cropland	1	A	CL1	CL1A	Silty clay loam	6.1	14
			B		CL1B	Silty clay loam	4.4	6
			C		CL1C	Silty clay loam	4.4	11
		2	A	CL2	CL2A	sand clay loam	12.8	29
			B		CL2B	sand clay loam	14.9	26
			C		CL2C	sand clay loam	13.2	24
		3	A	CL3	CL3A	sand clay loam	17.6	43
			B		CL3B	sand clay loam	21.7	34
			C		CL3C	sand clay loam	17.6	37
	Grazing land	1	A	GL1	GL1A	silt clay loam	5.7	22
			B		GL1B	silt clay loam	7.9	34
			C		GL1C	silt clay loam	6.1	18
		2	A	GL2	GL2A	silt clay loam	13.2	34
			B		GL2B	silt clay loam	13.2	20
			C		GL2C	silt clay loam	12.3	27
		3	A	GL3	GL3A	sand clay loam	22.2	24
			B		GL3B	sand clay loam	16.3	28
			C		GL3C	sand clay loam	15.8	35
To see effect of soil texture	Cropland	2	A	U2	U2A	loam	8.7	28
			B		U2B	loam	8.7	36
			C		U2C	loam	13.2	34
		2	A	W2	W2A	Silty clay	14.9	8
			B		W2B	Silty clay	7.9	7
			C		W2C	Silty clay	14.9	6

Clarification of abbreviations: Each micro-plot has a code with structure **XYZ. X**: Type of land use and soil texture (CL: Cropland on **Bahakel**, GL: Grazing land on **Bahakel**, U: Cropland on **Andelay**, W: Cropland on **Walka**). **Y**: Slope classes (1: Gentle slope 0% - 8%, 2: Middle slope 8% - 15%, 3: Steep slope >15%). **Z**: Distinction between the 3 replicates (A: Most to the east, B: Middle plot, C: Most to the west)

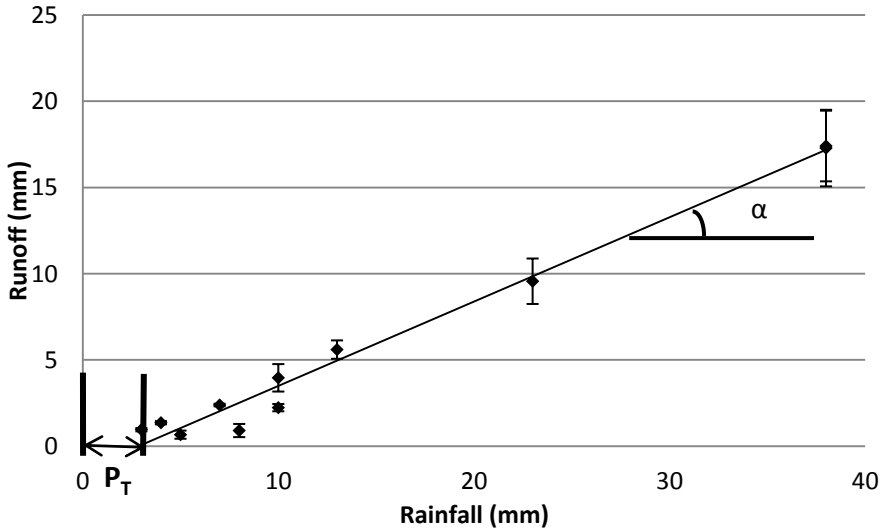

Alpha is the runoff response: degree of runoff depth increase with increasing rainfall depth.

P_T is the precipitation threshold: depth of rainfall prior to runoff initiation.

Illustration of the regression analysis of rainfall (mm) and runoff (mm) data. The linear trend line of the rainfall-runoff data points shows the gradient: α, and the intercept on the x-axis: P_T.


water
harvesting
runoff
micro-plots
reservoirs
Ethiopia
highlands
Northern
slope
relationships
influence
precipitation
response
three
P/R
roughness
numbers
potential
impact
threshold
km
estimates
significant
curve-numbers
random
characteristics
cover
Rainfall-runoff
vegetation
soil
curve
PT
texture
behaviour
conducted
defined
predict
improve
study
dry
develop
indicates
prevent
use
advantage
area-specific
catchments
periods
realistic
Cropland
larger
level
consisting
irrigation
distributed
rainy
grazing
Keywords
literature
overestimation
hydrological
replicate
experimental
data
semi-arid
within
site
whereas
resource
Realistic
provide
area
describe
application
help
fragment
accurate
local
production
understanding
come
classes
gave
account
land
Land
Curve-numbers
using
catchment
season
small
investigated
much
sites
applied
verification
individual
influenced
However
sub-catchment
order
Several
textures
Mayleba
derived
height
applications
rainfall-runoff
main
well
determining
measured
observed
population
greater
however
assessed
oversized
threshold.Rainfall-runoff
estimations
taken
planning
rock
recorded